On three levels of complexity in mathematical modelling of population dynamics

Dissertation
zur Erlangung des Grades
eines Doktors der Naturwissenschaften (Dr. rer. nat.)

Michael Sieber

Fachbereich Mathematik/Informatik
Universität Osnabrück

August 2011

Preface

Mathematical modelling as a tool in the study of population dynamics has a long and diverse history, spanning at least three centuries. Although a multitude of models has been put forward and many challenging problems have been solved, the endeavour to explain and formulate general principles underlying the dynamics of populations in space and time is far from over. The pros and cons of particular models and concepts are still subject of lively debates, which makes population dynamics a wide-open field for researchers interested in mathematical modelling.

This thesis attempts to provide new insight into some population-dynamical problems and also proposes a new perspective on certain models of ecological communities. The specific research questions have been classified according to the level of modelling complexity on which they are situated and the organization of this thesis as outlined below intends to reflect this classification.

Chapter 1. Introduction. In this chapter basic terminology of mathematical modelling of population dynamics is introduced. A *population* is defined as a group of individuals living in the same place and basic models of population growth are presented. Ecological communities are introduced as a family of interacting populations. The chapter closes by stating the specific research questions that are discussed in the subsequent chapters.

Chapter 2. Predator–prey cycles and the Hydra Effect. This chapter has been published as a paper in the *Journal of Mathematical Biology* (Sieber and Hilker, 2011a). It investigates the paradoxical *Hydra Effect*, the increase of mean population size as a response to an increase in mortality rate, in a class of simple predator–prey models. The main result is that a Hydra Effect occurs if and only if the system dynamics are oscillatory, which has interesting implications for the theory of optimal harvesting and biocontrol of invasive species.

Chapter 3. Transformation of intraguild predation community modules. This chapter is a slightly modified version of a paper previously published in the *Journal of Animal Ecology* (Sieber and Hilker, 2011b). Discussed here are how coordinate transformations change the structure of *intraguild predation* food webs, establishing a close connection of

certain cases of intraguild predation to simpler community modules such as exploitative competition and food chains. These results and possible generalizations of them could have wide-ranging implications for the question of how structural properties of food webs determine population-dynamical properties such as ecological stability and persistence.

Chapter 4. The impact of environmental fluctuations on travelling waves and chaos. The introductory section of this chapter on reaction-diffusion equations is a shortened version of a text that has been published in the book *Modelling complex ecological dynamics*, see Sieber and Malchow (2011). The main part is based on two papers previously published in the *Proceedings of the Royal Society A* (Sieber et al., 2010) and the *European Physical Journal Special Topics* (Sieber and Malchow, 2010). Presented are numerical investigations of how random environmental fluctuations affect the spatiotemporal dynamics of oscillatory reaction-diffusion models, such as classical predator–prey and simple $\lambda - \omega$ systems. These results in particular question whether travelling waves arising from these models can explain similar spatiotemporal waves found in natural populations.

Acknowledgements

I am very grateful to my supervisor Horst Malchow for helping me on my way into the scientific world. He provided the encouraging and open atmosphere that made collaborating with him and pursuing my own scientific ideas a wonderful endeavour.

I am also deeply indebted to Frank Hilker, Sergei Petrovskii and Ezio Venturino for interesting discussions, fruitful collaborations and generous hospitality.

To all of my friends and colleagues at the University of Osnabrück I am very thankful for the warm and stimulating atmosphere they created and, maybe above all, for having a good time together.

Finally, I would like to thank my family for their support and faith in me.

Contents

1 Introduction

The green Westerberg campus of the University of Osnabrück where this thesis was written is home to a great number of rabbits. Even without systematically counting them on a regular basis it is clear that the number of rabbits on campus shows considerable variation over time. It is also apparent that the rabbits favor certain lush areas over more concreted parts of the campus, which adds a spatial dimension to the population dynamics of rabbits. In the case of this rabbit population much of the apparent variation in population numbers can be explained by some obvious environmental factors, such as the course of the seasons and the fact that rabbits need hiding places and thrive mainly on grass, not concrete. But there are also more involved factors such as predation by birds and cats and infectious diseases which have a great impact on the number of rabbits. The temporal and spatial variation found in this particular population on Westerberg campus is in fact a feature of virtually every natural population and the question of "how and why population numbers change in time and space" is the central problem of population dynamics (Turchin, 2003, p. 3).

Mathematical models have been used extensively to address this question and many modelling approaches have been taken. However, differential equations remain probably the most popular tool to solve population dynamical problems. This thesis tackles three specific problems arising in population dynamics which are situated on different levels of model complexity, ranging from investigating the properties and bifurcations of particular solutions to predator–prey models (Chapter 2) over the study of structural properties of food web models (Chapter 3) to addressing the impact of external environmental processes on spatiotemporal population dynamics (Chapter 4). In order to set the stage for this endeavour this first chapter mainly follows the Postulates of population dynamics proposed by Turchin (2003) to give a short general introduction into mathematical modelling of population dynamics, leading to a short overview of the specific research questions that are discussed in this thesis.

1.1 Basic models of population growth

Before giving a brief derivation of basic models of population growth we first need to specify what this *population* is that is growing. The two main ingredients of the population concept have already been hinted at in the example of the rabbits on Westerberg campus. Firstly, we have been concerned only with rabbits, meaning we are dealing with individuals of the same species. Secondly, the rabbits have occupied a well defined area, the University campus, which gives the population a spatial identity. These two concepts are embraced in the definition of population "as a group of individuals of the same species that live together in an area of sufficient size to permit normal dispersal and/or migration behavior and in which numerical changes are largely determined by birth and death" (Berryman, 2002). In particular this means that emigration from or immigration into the population should be negligible. Apparently this does not apply to the rabbits of Westerberg campus, which following this definition should better be denoted a *local population* for which emigration and immigration from other local populations plays a significant role.

Note, that although this definition refers to a particular area occupied by the population most of this thesis focuses on nonspatial aspects of population dynamics, implicitly assuming that within the boundaries of its habitat the population is well mixed and evenly distributed. However, spatial dynamics will play a role in Chapter 4.

Employing the abovementioned definition implies that population size can only change as a result of individuals producing offspring or dying for whatever reason, which is *Postulate 1* in Turchin (2003). If we denote by N the non-negative population density, an informal equation for this rate of change in population density reads

$$\frac{\mathrm{d}N}{\mathrm{d}t} = \text{“births - deaths”}. \tag{1.1}$$

To give the right hand side of this equation a meaning we need to put the birth and death processes in more rigorous terms. Therefore, let us first consider the growth of a single isolated population, in which case we only have to deal with processes that are intrinsic to this population and not with those that are due to interactions with other populations.

To begin with it is important to always keep in mind that all population mechanisms are ultimately "a result of what happens to individuals", which is *Postulate 2* of Turchin (2003). However, to keep things as simple as possible, we make the assumption that all these individuals are identical or in other words, that our population is *unstructured*. Each individual in the population will have a certain number of offspring produced in a fixed time interval and have a certain life expectancy, giving rise to a per capita birth rate $b \geq 0$

and per capita mortality rate $d \geq 0$, respectively. Because of our unstructured population assumption we can simply integrate these rates over the whole population N to obtain the absolute number of births $B = bN$ and deaths $D = dN$ occuring during a fixed time interval. This leads us to the basic but very important exponential growth model:

$$\frac{\mathrm{d}N}{\mathrm{d}t} = B - D = bN - dN = (b-d)N. \tag{1.2}$$

This simple model has a long history (Malthus, 1798) and it predicts a growing population if the per capita birth rate b exceeds the mortality rate d, the opposite case leads to a decline in population numbers.

Despite its simplicity the exponential growth model is sometimes raised to the level of a law, the *exponential law* of population growth. The exponential law can be thought of "as the null state in which any population would be if no forces (= environmental changes) were acting on it" and as such it is a direct analogue of Newton's *law of inertia* for the undisturbed movement of a body (Turchin, 2003). According to (1.2) for $b > d$ this null state of population dynamics corresponds to unbounded population growth. However, this null state can usually only be observed at sufficiently low population densities and in favorable environments and it will never prevail for extended periods of time.

Eventually every natural population will confront limits imposed by the environment, leading to competitive interactions among members of the population (Smith and Smith, 2006). This *intraspecific competition* for space and other resources which is mediated by the environment regulates the size of the population and the existence of an upper density bound is *Postulate 3* in Turchin (2003). It has to be accounted for in more realistic models of population growth and hence we consider a simple extension of the exponential model.

We make the reasonable assumption that organisms require resources to produce offspring and shrinking resources due to increased demand at high population densities will result in a lower rate of reproduction. Thus, we can incorporate the limiting effect of high population densities into the basic model (1.2) by making the per capita birth rate b decrease with population density. Assuming for simplicity a linear relationship between population density and per capita birth rate $b = b_0 - cN$ yields

$$\frac{\mathrm{d}N}{\mathrm{d}t} = [(b_0 - cN) - d]\, N = (b_0 - d)N - cN^2. \tag{1.3}$$

Here $b_0 \geq 0$ is the ideal per capita birth rate realized only at very low population densities ($N \approx 0$) and the parameter $c > 0$ represents the decrease in birth rate as population density increases. The growth model given by (1.3) is the well known *logistic growth model*

first studied by Verhulst (1838) and rediscovered by Pearl and Reed (1920). Regardless of the initial population size the model (1.3) predicts that population density will eventually approach the value $K = (b_0 - d)/c$ if $b_0 > d$, otherwise the population goes extinct. The value K is commonly referred to as the *carrying capacity* of the population and it serves as the required upper density bound. In the classical formulation (1.3) of logistic growth this value is implicitly determined by demographic parameters of individual members of the population, but the logistic growth model is most often used in the form

$$\frac{\mathrm{d}N}{\mathrm{d}t} = rN\left(1 - \frac{N}{K}\right) \tag{1.4}$$

with intrinsic growth rate $r = b_0 - d$ and independent explicit carrying capacity K.

It was also Pearl (1926) who was one of the first to conduct controlled experiments with the explicit purpose to test the logistic model using a complex multi-cellular organism and he found the population growth of the fruit-fly *Drosophila melanogaster* in good agreement with theoretical predictions. However, this early synthesis of experimental and theoretical results should not deceive from the fact that the logistic model is purely phenomenological with limited mechanistic underpinning. This becomes most evident in the second formulation (1.4), since this case may lead to unreasonable predictions about population growth, especially in the case of negative per capita growth rates. Namely, if $r < 0$ but $K > 0$ and at the same time the population density happens to be above the carrying capacity for some reason, which is perfectly possible in natural or laboratory scenarios, equation (1.4) predicts unbounded population growth since $dN/dt > 0$ for all $N > K$, which makes no sense at all. Nevertheless in this thesis mostly the common formulation (1.4) of logistic growth is used, but all presented results do not crucially depend on this form and could also be obtained with model (1.3).

Exponential growth (1.2) and logistic growth in the form (1.3) or (1.4) are two of the most commonly used growth models. Further extensions and complications of these models are possible, but almost all unstructured models of population growth of a single population have the following general form:

$$\frac{\mathrm{d}N}{\mathrm{d}t} = f(N)N\,. \tag{1.5}$$

The properties of the per capita growth rate as described by the function f completely determine the dynamics of population growth which, since (1.5) does not explicitly depend on time, can only fall into two categories. Either the population grows unbounded as in the case of the exponential law with positive per capita growth rate or the population size

approaches some equilibrium value. For more complicated population dynamics we need to take into account that in nature we will only very rarely encounter an isolated population. Rather, almost every population will be part of a larger ecosystem or community of interacting populations.

1.2 Models of ecological communities

The exponential growth model (1.2) and in particular its logistic extension (1.3) are all about interactions within the same population. While these basic single population models have a long history and still spur lively debates about their usefulness and different formulations (Fulda, 1981; Slobodkin, 2001), the study of population dynamics only gets really interesting once individuals of different populations are allowed to interact with each other. Note, that this again stresses the fact that population dynamics is a result of processes on the individual level. However, since the simplifying approach we have taken does not account for the individual, but aggregates them into unstructured populations, we will usually speak of interactions between populations rather than individuals. Keeping this in mind, the interactions of two different populations can be grouped into three major classes according to their respective effects on the populations.

We have already mentioned intraspecific competition as an interaction of individuals within the same population, but more generally one speaks of *competition* between two populations if the interaction has a negative effect on both populations. A classical example is competition for resources where two populations consume the same resource, thereby lowering the amount of nutrient available to the other one. This type of interaction does not necessarily require a direct encounter of two individuals entailing an actual fight over some resource, since competition is often indirectly mediated simply by the diminished amount of resources available to either competitor.

In contrast to this, *mutualism* is an interaction where two populations are better off together than if they were isolated from each other. Many mutualistic relationships involve the mutual allocation and transfer of nutrients, as in the relationship of *Rhizobium* bacteria and certain plant species such as beans. The nitrogen-fixing *Rhizobium* infects the roots of the plant and provides fixed nitrogen to it, receiving carbon and other resources in return (Smith and Smith, 2006).

Maybe the most prominent interaction of two populations is *predation*, where the encounter of two individuals has negative, usually fatal, consequences for one of them since it serves as food for the other one. Classical examples for such consumer–resource in-

teractions are predator–prey relationships and grazing on plants by herbivores, but more generally also parasitism falls into this category (Holt and Dobson, 2006). In the following all of these types of consumer–resource or host–parasite relations will be subsumed under the term *trophic interaction*.

When several populations interact via any of the abovementioned ways they form an ecological community, and most larger natural communities contain examples from all of these relationships. Some populations may even engage in all of the different interaction types at the same time with several different other populations of the community. In any case the representation of an ecological community with n interacting species in a mathematical model usually requires a system of at least n differential equations, one dynamical variable N_i for each population. If we simply take n copies of the general equation (1.5) for the growth of a single population and assume that the per-capita growth rate f may now depend on all of the other populations in the community, then a very general model for an ecological community of n populations can be written as

$$\begin{aligned} \frac{\mathrm{d}N_1}{\mathrm{d}t} &= f_1(\mathbf{N})\,N_1 \\ &\vdots \\ \frac{\mathrm{d}N_n}{\mathrm{d}t} &= f_n(\mathbf{N})\,N_n \end{aligned} \tag{1.6}$$

Here $\mathbf{N} = (N_1, ..., N_n)$ is the vector of population densities and for biological species it is reasonable to assume that $N_i \geq 0$ for all i.

Given a particular ecological community, or just a general type of community, the central task in mathematical modelling of population dynamics now usually splits into two major challenges which are tackled by different tools and techniques. The first challenge is to specify the per capita growth rate for each population by identifying the key mechanisms that affect population growth. The goal is to derive a completely mechanistic formulation of f_i, which in addition to natural birth and death events as described in the previous section must now also account for the process rates of all existing trophic interactions between the different populations.

As has been pointed out above, population growth is ultimately an individual-based process, so this first modelling task requires a detailed understanding of the properties of individuals and how they interact. As such this first step emphasizes the biological side of mathematical biology and since all conclusions and insights depend on the particular form of the model, this is a crucial step. However, this first task is not in the focus of this thesis.

Rather, this thesis is devoted to the second challenge in mathematical modelling, which arises once a reasonable model has been formulated, namely to investigate as thoroughly as possible the dynamical behavior of the model. Since this investigation is done mainly with mathematical tools one could say that in contrast to the more biological first challenge this second step puts the mathematics into mathematical modelling. In general there are several levels of complexity to this second challenge and on each level different questions are asked and different tools are used. The next section gives a brief explanation of the different levels of complexity and the specific questions that are studied in the subsequent chapters of this thesis.

1.3 Research questions on three levels of complexity

In general the *complexity* of a system denotes the multitude of elements and interactions between them and the collective dynamics which the system as a whole exhibits, which usually embraces the notion that the dynamical properties of the system can not be inferred from its individual elements. This notion will be made somewhat more precise in the following introduction of three different levels of complexity in the modelling of population dynamics.

1.3.1 First level: The dynamics of the model

The major problem when dealing with a system such as (1.6) concerns the dynamical behavior of solutions to this equation and how these dynamics change under variation of one or more parameters. The question of "what one may expect to occur in the dynamics with a given number of parameters allowed to vary" is the realm of classical dynamical systems and bifurcation theory (Kuznetsov, 1995). The answers to this and more specific questions concerning the dynamical properties of a population model are directly relevant for practical purposes, such as ecosystems management or conservation efforts.

However, the investigation of systems such as (1.6) is inherently difficult and in general a complete understanding of the global behavior of solutions and their possible bifurcations under parameter variation is impossible. Although we have a completely deterministic description of every individual part of our population model, the dynamics generated by it can be utterly complicated and unpredictable, even for very simple systems. Note, that on this level we can often completely forget about where our model comes from, since the tools provided by dynamical systems theory are naturally oblivious to the population-dynamical background of our system. As such the possibly very complicated dynamical behavior

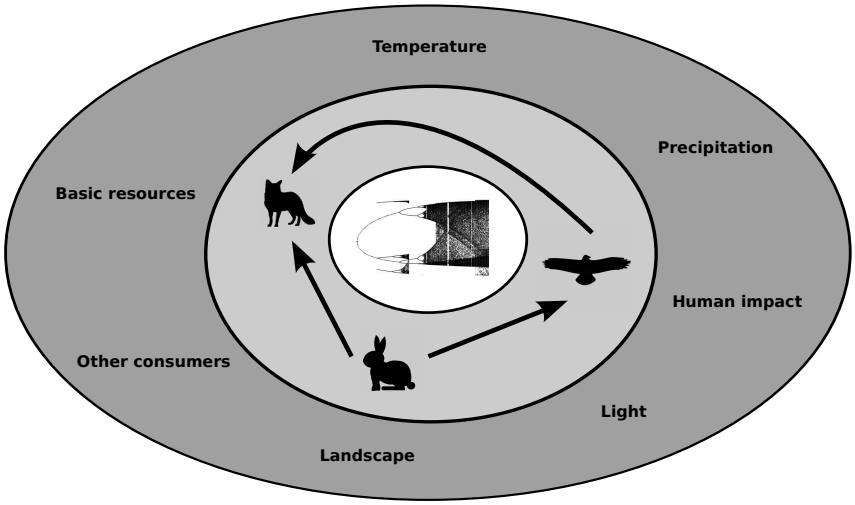

Figure 1.1: The three levels of complexity.

of system (1.6) forms a self-contained first or lowest level of complexity of mathematical modelling of population dynamics, symbolized by the bifurcation diagram at the centre of Figure 1.1.

It has already been mentioned that in the one-dimensional single population growth models the long term dynamics will always approach an equilibrium, if they are bounded at all. One may now ask how this particular equilibrium value depends on the system parameters and whether there is more than one feasible equilibrium and if so, which one is approached depending on initial population sizes. Due to their relative simplicity equilibria are usually also the first type of solutions analyzed for ecological communities comprising of more than one population, but here also more complicated dynamics may arise. The most prominent example are perhaps the periodic rise and fall of population densities found in many consumer–resource systems. The observation of these population cycles in natural populations motivated a lot of the pioneering work in theoretical ecology and they remain an active area of research (Kendall et al., 1999).

Classical predator–prey models naturally give rise to such population cycles and one of the important properties of these cycles is the mean population density measured over many cycles. In contrast to the actual population size, which typically shows significant periodic changes over time and thus depends on a particular point in time, the mean density is a suitable measure to assess the long term effects of changes in parameter values. In their pioneering work Lotka (1925) and Volterra (1926) found that in the predator–prey model now bearing their name, the mean population size over one population cycle actually

coincides with the unique positive equilibrium of the system. This immediate relationship is due to the simple linear structure of the Lotka-Volterra model and it does not hold for nonlinear models, for which analytical results concerning mean population densities are rare.

This lack of rigorous results and a recent review by Abrams (2009) motivates the following question on the population-dynamical level, which is discussed in Chapter 2: When does higher predator mortality lead to higher mean predator population densities in simple predator–prey models? This question refers to the somewhat paradoxical situation that higher mortality, which is clearly disadvantageous on an individual-based level, may actually yield a positive outcome on the population level by increasing mean population size. That many classical predator–prey models in fact predict this counterintuitive behavior is the conclusion of the main result presented in Chapter 2.

1.3.2 Second level: The community structure implied by the model

A key principle in systems theory is that *structure determines behavior*. Here the structure of a system is the complex web of interlinkages between different elements, where two elements are linked when a change of the state of one element directly influences the state of the other. In ecological scenarios the elements of the system are the populations of an ecological community and the interlinkages are trophic interactions such as predation or parasitism. Note, that this notion of ecological complexity comes closest to the general definition given above, and by stating which populations and processes are relevant for our community we explicitly draw a line between the community and the surrounding environment. Thus, the ecological community is the second self-contained level of complexity of population dynamics, represented by the schematic food web in the middle ring of Figure 1.1.

The complex web of trophic interactions between populations is usually called a *food web* and the "structure determines behavior" principle seems to imply that the structure and complexity of a given food web somehow entails the population dynamics of the involved populations, at least qualitatively. And indeed in community ecology this principle lies at the heart of the so-called *diversity-stability debate* about whether there is a negative or positive relationship between food web complexity and ecological stability (McCann, 2000). One view is that structurally more complex food webs with many species and a high degree of connectance tend to be more stable than simpler webs (MacArthur, 1955; Elton, 1958), a view that was challenged later (Gardner and Ashby, 1970; May, 1973).

While we do not want to participate in this ongoing debate, it is clear that both sides agree

on the premise that the structure and complexity of a food web has profound implications for the dynamics and stability properties of the ecological community. In other words, we should expect similar food webs to be of similar ecological stability, or vice versa that food webs with different degrees of complexity also differ in their dynamical properties. This of course leaves much room for interpretation, in particular with regard to the meaning of "similar" in this context.

One approach to tackle this problem is to recognize that the structure of a food web should somehow be reflected in the structure of the corresponding mathematical model, which gives a more rigorous meaning to "similar food web structure". On the other hand in the realm of mathematical models such as (1.6) we are in the lucky position to be able to rigorously state when two given models are equivalent, meaning that they possess exactly the same dynamics and thus the same stability properties. The charm of this approach now is the observation that two dynamically equivalent models need not necessarily possess the same community structure. While strictly speaking this is not an invalidation of the structure determines behavior principle, it nevertheless questions the importance of food web structure for population dynamics and persistence. In the worst case many different food web structures with varying degrees of complexity could lead to the same dynamical behavior, making the analysis of structural properties of food webs somewhat arbitrary and implying that food web complexity alone is not an adequate indicator for ecological stability.

While the described approach still lacks some rigorous definitions Chapter 3 presents some first results based on a simple case of dynamical equivalence, which arises when a model is transformed into another but equivalent model via a coordinate transformation. This study is motivated by the observation that coordinate transformations in general do not preserve the community structure as represented by a model, but under certain circumstances may in fact lead to a model which resembles a completely different type of community. This is shown specifically for a community structure known as intraguild predation which contains three trophic links, but which under certain conditions may be reduced to a community with only two links.

1.3.3 Third level: What is not in the model

Just as natural populations are almost always part of a larger ecological community these communities are themselves placed in the larger arena of the environment. Here they are influenced by a multitude of interacting processes, not all of which are well understood and many even remain unknown. This forms the third level of complexity in population dynam-

ics, as shown in the outer ring in Figure 1.1. Strictly speaking, the fact that populations and ecological communities are not isolated systems but interact with the environment would require "making the per capita rate of population change a function of all sorts of things" (Turchin, 2003) in order to represent the influence of environmental processes:

$$\frac{\mathrm{d}N_i}{\mathrm{d}t} = f_i(\mathbf{N}, \text{“all sorts of things”})\, N_i \,. \tag{1.7}$$

Probably most of these environmental processes would justify the use of a dedicated mathematical model of their own if we wanted to assess their impact on our population as accurately as possible. Clearly, in general it will be unfeasible to do so because of the sheer complexity of most natural biotic and abiotic processes. Even a single and apparently simple variable such as temperature, which can have a tremendous impact on birth and mortality rates, demands a full climate simulation model if we wanted to include an adequate representation of temperature dynamics in our model.

If there are only a few environmental variables that we need to include in our model one way out of the predicament of necessary detail and too much complexity, is to represent these processes by typical time series rather than fully-fledged dynamical variables. This can be done by making one or more parameters explicitly depend on time, and in such non-autonomous models temperature for example could be represented by a simple time-periodic function reflecting the interannual variation of mean temperature. However, this requires that the typical behavior of the variable in question is known to some extent and of course it only covers processes for which we already know that they have an influence on the system.

In the case of many environmental processes, some of which may remain obscure or very purely understood and which show a considerable amount of variation on the relevant timescales, it might be more appropriate to treat the entirety of these superimposed fluctuations as some random external forcing. The statistical properties of this environmental noise depend largely on the setting of the ecological community (Vasseur and Yodzis, 2004), but regardless of the particular form of noise this approach ultimately leads to stochastic models. Such models often come in the form of stochastic differential equations which have a long history in physics, but which have also received considerable amount of attention in ecological applications (see Section 4.2 and references therein).

The introduction of noise into a deterministic model can have manifold consequences, ranging from merely blurring the deterministic trajectories to significant regime shifts in system dynamics. This latter case is especially interesting because it naturally questions

conclusions drawn from the deterministic model. In Chapter 4 we specifically address the question how robust certain spatiotemporal patterns such as periodic travelling waves are with respect to environmental fluctuations.

2 Predator–prey cycles and the Hydra Effect

2.1 The Hydra Effect

In a recent review Abrams (2009) discusses the counterintuitive increase of a species population size in response to an increase in its mortality rate. This phenomenon has been termed "Hydra Effect" by Abrams and Matsuda (2005), after the nine-headed beast from Greek mythology that would grow two more heads for each that was cut off. Effects that qualify as Hydra Effects had already been described by Ricker (1954) and, without necessarily calling them Hydra Effects, they have been shown to occur in discrete-time (Sinha and Parthasarathy, 1996; Schreiber, 2003; Hilker and Westerhoff, 2006; Seno, 2008; Zipkin et al., 2009; Liz, 2010) and continuous-time models (Abrams et al., 2003; Matsuda and Abrams, 2004) as well as in delay differential equations (Terry and Gourley, 2010); see also Abrams (2009) for more references. As has been pointed out by Abrams (2009), empirical evidence for Hydra Effects is rare and this poses the question whether this is due to a lack of appropriate observations or due to shortcomings of the underlying theoretical models. This question is complicated by the fact that analytical results concerning the Hydra Effect are also rare and mainly heuristic explanations have been given to define and explain Hydra Effects in ecological terms. Abrams (2009) names, for example, altered population cycles, consumer mortality leading to more prudent resource exploitation and temporal separation of mortality and density-dependent processes as possible mechanisms leading to Hydra Effects. These explanations are illustrated by numerical simulations, focusing on a few well-known models. While this already shows that Hydra Effects are not an uncommon phenomenon in ecological models, we propose to rigorously define the term "Hydra Effect". This allows to formalize the understanding of the term and to derive analytical results. This is the purpose of this paper, where we will address the phenomenon of the Hydra Effect in a series of continuous-time models.

Our main analytical results are (i) that Hydra Effects are typical for Gause-type predator–prey models and (ii) that they occur whenever an unstable coexistence equilibrium exists. Our results also imply that increasing predator mean densities occur necessarily right be-

fore a further increase in predator mortality may drive the population to extinction, thereby giving a false impression of the healthiness and sustainability of the population.

This chapter is organized as follows. The next section introduces a general population model and some basic notation. The third section recalls some well-known results regarding mean values of solutions to differential equations and it gives a rigorous definition of the Hydra Effect. The fourth section contains the main result that Hydra Effects are a typical feature of Gause-type predator–prey models. This is illustrated by a suite of some of the most commonly used examples. The fifth section discusses Hydra Effects in a three-species model. Finally, the last section discusses the implications of the results and identifies avenues for future research.

2.2 Population models and mortality rates

We adopt the basic assumption that the population dynamics of an ecological community of n species can be modeled by the parameter-dependent differential equation

$$\dot{Y} = f(Y, m)\,, \tag{2.1}$$

with $f : D \subseteq \mathbf{R}^n \to \mathbf{R}^n$ and $\dot{Y} = \frac{\mathrm{d}Y}{\mathrm{d}t}$. The domain D of the vectorfield f is assumed to be an open subset of $\mathbf{R}^n$ and will be referred to as the phase space of system (2.1). The biologically reasonable subset of the phase space is $D_{\geq 0} = D \cap \mathbf{R}^n_{\geq 0}$, where $\mathbf{R}_{\geq 0}$ denotes the non-negative real numbers. Correspondingly, the strictly positive real numbers are denoted $\mathbf{R}_{>0}$. A solution Y is given by a real–valued function $Y(t, \xi, m)$ satisfying (2.1), which depends on the initial condition $\xi \in D$ and the parameter m. The components $Y = (y_1, \ldots, y_n)$ of a solution correspond to the population densities of the n respective species, and the i–th component of $f = (f_1, \ldots, f_n)$ describes the growth and interaction of the i–th species. We make the following assumptions concerning the vectorfield f. First, f is assumed to be sufficiently smooth, being at least C^1 in Y and m on the open set $D \times \mathbf{R}_{>0}$. Second, since (2.1) is supposed to describe the population dynamics of biological species, we require that all components of $Y(t, \xi)$ with $\xi \in D_{\geq 0}$ remain non-negative for all times. Third, we assume that all solutions eventually enter and remain in a compact absorbing set $K \subset D_{\geq 0}$, e.g. the population densities of all species are ultimately bounded. These assumptions ensure the uniqueness and existence of solutions starting in $D_{\geq 0}$ for all forward times. Note that throughout this paper by an equilibrium or stationary solution we mean a point satisfying $f(\xi) = 0$ and by a cycle we mean a periodic solution with $Y(t) = Y(t + T)$ for all t and

some period $T > 0$ so that $Y(t) \neq Y(t+\tau)$ for $0 < \tau < T$.

While we make no assumptions about the particular form of the functions f_i, for the sake of clarity we deliberately restrict our analysis to systems where the growth and interaction rate of at least one species can be written as

$$f_i(Y, m) = g_i(Y) - m y_i,$$

where g_i and f_j, $j \neq i$ do not depend on m. The parameter $m > 0$ will be denoted as per-capita *mortality rate* of species i. Note that mortality rate in the sense of this assumption may not only include the natural mortality rate of a species, but also processes such as harvesting, culling or other forms of removal.

For many ecological systems, it is important to understand how the population size of a focal species responds to an increase in its mortality rate. When the population dynamics approach an equilibrium, this amounts to solving an algebraic problem. However, when there are nonequilibrium dynamics, the problem becomes much more difficult since one has to assess the mean population size, where ideally the average is taken over a long time interval to avoid the influence of transient effects.

2.3 Definition of mean population density and the Hydra Effect

As indicated in the previous section, we are often interested in the long-term behavior of solutions to (2.1) and in particular the mean abundance of a population. The following definition of the average size of a population is the one implicitly used in all previous studies that have addressed the Hydra Effect.

Definition 2.1. Let $\phi : M \times \mathbf{R}_{>0} \to \mathbf{R}^n$ be the *mean value map*

$$\phi(\xi, m) = \lim_{t\to\infty} \frac{1}{t} \int_0^t Y(s, \xi, m)\, \mathrm{d}s,$$

where $M \subseteq D$ is the subset of initial conditions for which the limit on the right-hand side exists. The map assigns to a point $\xi \in M$ and a mortality rate the *asymptotic mean value* of the parameter-dependent solution $Y(t, \xi, m)$ through this point. Integration of the solution Y is componentwise as usual and $\phi_i(\xi, m)$ is the asymptotic mean value of the i–th species. If either the initial condition or the mortality rate is fixed, we will frequently simplify notation to $\phi(m)$ or $\phi(\xi)$, respectively.

Note that in general M will be a proper subset of the phase space D. For example, consider

a model of nontransitive competition, in which three species coexist via cyclic domination—an ecological variant of the rock-scissors-paper game (May and Leonard, 1975). For this model Gaunersdorfer (1992) has shown that asymptotic mean values do not exist for large regions of the phase space. This result is related to the formation of a heteroclinic cycle connecting three equilibrium points and the exponentially lengthening periods of time a solution approaching this cycle spends in the vicinity of each of these equilibria.

Nevertheless, the existence of the asymptotic mean value is ensured in the situations we are mainly concerned with. Therefore, let us first recall the notion of the stable set of a solution.

Definition 2.2. The *stable set* $A(Y)$ of a solution $Y(t,\xi)$ is the set of all points which get attracted to Y for large times:

$$A(Y) = \{\eta \in D \,|\, \exists\, t_0 \geq 0 : Y(t_0,\xi) = \xi_0 \text{ and } \lim_{t\to\infty} \|X(t,\eta) - Y(t,\xi_0)\| = 0\}\,.$$

Since we are only interested in positive solutions, a solution $Y(t,\xi)$ is called *globally stable* if it attracts all strictly positive initial conditions.

The following result now implies that the mean value map, if it is well defined, is in fact constant on the stable set of a solution.

Proposition 2.3. *Let $Y(t,\xi)$ be a solution of (2.1) and let $\phi(\xi)$ exist. Then $\phi(\eta) = \phi(\xi)$ for all $\eta \in A(Y)$.*

Proof. Let $\phi(\xi) = L$. We first observe that this mean value is of course the same for all points on the solution $Y(t,\xi)$. Namely, with $Y(t_0,\xi) = \xi_0$ for some $t_0 > 0$ a reparametrization of time yields

$$\begin{aligned}\phi(\xi) &= \lim_{t\to\infty} \frac{1}{t}\int_0^t Y(s,\xi)\,\mathrm{d}s = \lim_{t\to\infty} \frac{1}{t}\left[\int_0^{t_0} Y(s,\xi)\,\mathrm{d}s + \int_{t_0}^t Y(s,\xi)\,\mathrm{d}s\right] \\ &= \lim_{t\to\infty} \frac{1}{t}\int_{t_0}^t Y(s,\xi)\,\mathrm{d}s = \lim_{t\to\infty} \frac{1}{t}\int_0^t Y(s,\xi_0)\,\mathrm{d}s = \phi(\xi_0)\,.\end{aligned}$$

Now assume that a different solution $X(t,\eta)$ with $\eta \in A(Y)$ exists. Then there is a ξ_0 so that $\lim_{t\to\infty}\|X(t,\eta) - Y(t,\xi_0)\| = 0$, which implies $\lim_{t\to\infty}[x_i(t,\eta) - y_i(t,\xi_0)] = 0$ for each coordinate $i = 1,\ldots,n$. Now define $F_i(t) = \displaystyle\int_0^t [x_i(s,\eta) - y_i(s,\xi_0)]\,\mathrm{d}s$ and $G(t) = t$. Then $\lim_{t\to\infty} G(t) = \infty$ and using L'Hôpital's rule we obtain:

$$\lim_{t\to\infty} \frac{F_i(t)}{G(t)} = \lim_{t\to\infty} \frac{F_i'(t)}{G'(t)} = \lim_{t\to\infty} [x_i(t,\eta) - y_i(t,\xi_0)] = 0\,.$$

Now, since $\phi_i(\xi_0) = \lim_{t\to\infty} \frac{1}{t} \int_0^t y_i(s, \xi_0)\,\mathrm{d}s = L_i$ and

$$\lim_{t\to\infty} \frac{F_i(t)}{G(t)} = \lim_{t\to\infty} \left[\frac{1}{t} \int_0^t x_i(s, \eta)\,\mathrm{d}s - \frac{1}{t} \int_0^t y_i(s, \xi_0)\,\mathrm{d}s \right] = 0\,,$$

this implies $\phi_i(\eta) = \phi_i(\xi_0) = L_i$. □

Before proceeding, let us turn to two important special cases in which we need not consider infinite time intervals to obtain the asymptotic mean value. In the case of a stationary solution the mean value is of course the equilibrium value itself and thus equilibria of (2.1) are fixed points of the mean value map. And for periodic solutions the asymptotic mean value can obviously be obtained from a single period. This is summarized in the following proposition.

Proposition 2.4. *Let $Y(t, \xi)$ be a solution of (2.1).*

(i) If ξ is an equilibrium, then $\phi(\xi) = \xi$.

(ii) If Y is a cycle with period T, then $\phi(\xi) = \frac{1}{T} \int_0^T Y(s, \xi)\,\mathrm{d}s$.

During the following analysis we will be mainly concerned with these two special cases for which asymptotic mean values surely exist. However, in a more general setting ergodic theory tells us when these long time averages are well defined (Eckmann and Ruelle, 1985).

Now that we have recalled some basic properties of the mean value map $\phi(\xi, m)$, we can study how the mean population density of a species changes with respect to its mortality rate. Intuitively, in an ecological scenario one would expect a species mean population density to decrease if its mortality increases for some reason. The apparently paradoxical situation, where the mean population density of a species increases in response to an increasing mortality rate, has been termed the Hydra Effect.

Definition 2.5. Species i is said to experience a *Hydra Effect*, if there exist an initial condition $\xi \in D_{\geq 0}$ and mortality rates $m_1 < m_2$ so that $\phi_i(\xi, m_1) < \phi_i(\xi, m_2)$. The Hydra Effect is *smooth* if $\phi_i(\xi, m)$ is continuous on $[m_1, m_2]$, otherwise it is *non-smooth*.

Note that this definition distinguishes two qualitatively different types of Hydra Effects. Smooth Hydra Effects occur when an attractor of system (2.1) smoothly changes its position or shape in phase space in response to a change in the mortality rate. The simplest example of a smooth Hydra Effect would be given by a stable equilibrium $E^* = (y_1^*, \ldots, y_n^*)$ of system (2.1), for which $\partial y_i^* / \partial m > 0$ holds with m being the mortality rate of the i–th species.

This form of a smooth Hydra Effect may occur in stage-structured models which introduce a temporal separation between mortality and density-dependent growth, a scenario discussed by Abrams (2009) for a model describing the dynamics of juvenile and mature subpopulations. The most prominent examples of Hydra Effects are however associated with smooth changes in the amplitude of population cycles (Abrams, 2009), which will be discussed in sec. 2.4 for Gause-type predator–prey models.

On the other hand, non-smooth Hydra Effects are characterized by discontinuous changes in a species mean population density. There are essentially two scenarios, which can lead to non-smooth Hydra Effects. The first scenario arises when attractors suddenly appear or vanish due to global bifurcations. A striking form of a non-smooth Hydra Effect due to this scenario may occur when strictly positive attracting solutions to equation (2.1) do not exist for low mortality rates, but emerge suddenly via a global bifurcation. This is a typical scenario when the growth of a prey species is subject to a strong Allee effect, cf. sec. 2.4. The second scenario which may lead to non-smooth Hydra Effects is associated with multiple coexisting attractors, where the boundaries of the respective basins of attraction shift in response to changes in a species mortality rate. The long-term behavior of a solution starting at a particular initial condition ξ may then undergo a discontinuous change when ξ switches from one basin of attraction to another. Non-smooth Hydra Effects due to this second scenario in a two-stage model by Schreiber and Rudolf (2008) have been referred to as "very large magnitude Hydra Effects" by Abrams (2009). Although non-smooth Hydra Effects may appear as especially striking since the associated jump in species mean density occurs suddenly and without warning, this term is somewhat misleading since non-smooth Hydra Effects need not be of large magnitude at all, cf. sec. 2.5.

2.4 The Hydra Effect in models of purely prey-dependent predator growth

An important class of predator–prey equations is obtained by assuming that the per-capita growth rate of each predator does not depend on its own density. These systems will be called *pure predator systems* in the following, in analogy to "pure resource–consumer systems" where the per-capita growth rates of all species are independent of their own respective density (Turchin, 2003, p. 34). In the following we will consider mainly two- or three-dimensional systems and we write $Y = (x, y, z)$ for the components of respective solutions. Consequently, ϕ_x denotes the asymptotic mean density of species x.

Gause-type models

In this section we will show that the predator typically experiences a Hydra Effect in a class of standard predator–prey models. We obtain this class of models by assuming that prey per-capita growth g and the predation term ρ are functions only of the prey density. These assumptions lead to the general model (Gause, 1934)

$$\dot{x} = g(x)\,x - \rho(x)\,y, \tag{2.2}$$

$$\dot{y} = \varepsilon\,\rho(x)\,y - m\,y, \tag{2.3}$$

for the prey density x and the predator density y. Here, $\varepsilon\,\rho$ denotes the numerical response of the predator, which accounts for the limited conversion efficiency ε. The parameter m is the predator's mortality rate. These general equations have been used over decades as a cornerstone of theoretical predator–prey ecology (May, 1976; Yodzis, 1989; Turchin, 2003). A significant feature of eqns. (2.2–2.3) is that predator growth is purely prey dependent. In ecological terms this means that predator individuals are assumed not to interact with each other, but only indirectly through the consumption of the prey. From now on we will consider system (2.2–2.3) with the following assumptions (A)–(C).

(A) There exists $0 < K$ such that $(x-K)\,g(x) < 0$ for $x \geq 0$, $x \neq K$.

(B) $\rho(0) = 0$ and $\rho'(x) > 0$ for $x > 0$.

Assumption (A) basically introduces a self-limitation of the prey population, with positive per-capita prey growth for all prey densities below a certain carrying capacity K and negative per-capita growth if prey density exceeds this value. This excludes a strong Allee effect, which we are going to study in section 2.4. Assumption (B) states that predator consumption is a strictly increasing function of prey density. This includes the linear functional response of Lotka–Volterra type as well as functional responses with a saturation effect (e.g., Holling-type II and III), but not type IV functional responses. Both assumptions (A) and (B) are consistent with standard predator–prey theory and they have clear biological interpretations. Note that under assumptions (A) and (B) all solutions of system (2.2–2.3) starting in the positive quadrant are ultimately bounded (Bauer, 1979) and eventually remain in a compact subset of the phase space. As an important consequence of (A) and (B) we have that whenever $x^* > 0$ exists so that $\varepsilon\,\rho(x^*) = m$, it is unique. With the non-trivial part of the prey nullcline

$$\nu(x) = x\,\frac{g(x)}{\rho(x)},$$

this gives rise to the unique positive equilibrium $E^* = (x^*, \nu(x^*))$ of eqns. (2.2–2.3), which exists for $0 < x^* < K$. The function ν will simply be denoted the *prey nullcline* from now on, neglecting the trivial part $x = 0$.

The Hydra Effect is defined in terms of the mortality rate m, and due to the purely prey-dependent predator y there is a close connection between m and the location of the equilibrium E^*. The predation term ρ is a strictly increasing function of x, and thus for fixed ε the equation $\dot{y} = 0$ implies a strictly increasing map $x^*(m) = \rho^{-1}(m/\varepsilon)$, mapping a mortality rate to a prey density. Here, ρ^{-1} denotes the inverse of ρ. Setting $\nu(m) = \nu \circ x^* = \nu(x^*(m))$, we can consider the set of equilibria $E^*(m) = (x^*(m), \nu(m))$ as a smooth curve in phase space parameterized by the mortality rate m. The equilibrium $E^*(m)$ exists for all $m \in]0, m_+[$, where $x^*(m_+) = K$ and we know that $E^*(m) \to (K, 0)$ as $m \to m_+$.

It is a standard result of graphical predator–prey theory that the equilibrium E^* is locally asymptotically stable whenever $\nu'(x) < 0$ is fulfilled, i.e. whenever the prey nullcline has negative slope (Rosenzweig and MacArthur, 1963). If on the other hand E^* is unstable, the Poincaré–Bendixson theorem implies that there is at least one cycle surrounding E^*. To rule out the existence of cycles in the case when E^* is locally asymptotically stable we additionally need the following assumption:

(C) $(x - x^*)\,(\psi(x) - \psi(x^*)) > 0$ for $0 < x < K, x \neq x^*$,

where $\psi(x) = -\nu''(x)\,\rho(x)^2/\rho'(x)$. This additional assumption allows the application of Dulac's classical theorem for the nonexistence of closed orbits to system (2.2–2.3). Liu (2005) has used this approach to show that the Gause-type model (2.2–2.3) has no cycles if and only if the unique equilibrium E^* is located on a downslope of the prey nullcline $\nu(x)$. As a corollary this extends the local asymptotic stability of E^* to global stability.

Corollary 2.6. *Under assumptions (A) – (C), the equilibrium E^* is globally stable if and only if $\nu'(x^*) \leq 0$.*

While assumption (C) has no straightforward biological interpretation, we note that it is fulfilled for many of the usual choices for the prey growth term g and predation rate ρ found in the literature. Cor. 2.6 immediately implies as a necessary condition for the occurrence of a Hydra Effect that the coexistence equilibrium E^* has to be unstable.

Proposition 2.7. *If $\nu'(x) \leq 0$ for all $0 < x < K$, then under assumptions (A) – (C) a Hydra Effect of the predator population does not occur.*

As a first very simple application we consider the following well-known example.

Example 2.8. A Hydra Effect does not occur in the Lotka–Volterra predator–prey model with logistic prey growth (Volterra, 1931) and linear functional response

$$g(x) = g_1(x) = r\left(1 - \frac{x}{K}\right),$$
$$\rho(x) = \rho_1(x) = ax.$$

The prey nullcline

$$\nu(x) = \frac{r}{a}\left(1 - \frac{x}{K}\right)$$

is linear with negative slope $-r/(aK)$ and the unique equilibrium is always globally stable. Thus, $\phi_y(m) = \nu(m)$ decreases linearly for increasing mortality rate m.

Therefore, in terms of predator mean density, the interesting parts of the prey nullcline are the intervals for which it has a positive slope and the corresponding equilibrium is unstable. As mentioned, in this case the equilibrium is surrounded by at least one cycle which lies in the strip $0 < x < K$ and $0 < y < \infty$.

The following proposition relates the predator mean density to the prey nullcline $\nu(x)$. It will allow us to give an upper bound for ϕ_y, which can subsequently be used to derive a sufficient condition for the occurrence of a Hydra Effect in the predator population.

Lemma 2.9. *For any solution $Y(t, \xi)$ of (2.2–2.3) starting at strictly positive initial conditions the mean predator density is given by*

$$\phi_y(\xi) = \frac{1}{T}\int_0^T \nu(x)\,\mathrm{d}\tau,$$

where either x is the prey component of a stationary solution or it is cyclic with period T. This implies

$$\min\{\nu(x(t)) \,|\, t \in [0, T]\} \leq \phi_y(\xi, m) \leq \max\{\nu(x(t)) \,|\, t \in [0, T]\},$$

with equalities if and only if x is stationary.

Proof. First observe that using (2.2), we can write the predator component of any solution as

$$y = x\frac{g(x)}{\rho(x)} - \frac{\dot{x}}{\rho(x)} = \nu(x) - \frac{\dot{x}}{\rho(x)}.$$

The Poincaré–Bendixson theorem tells us that the solution $Y(t, \xi)$ will either approach the unique equilibrium $E^* = (x^*, y^*)$ or a cycle C surrounding E^*. This implies $\xi \in A(E^*)$ or

$\xi \in A(C)$ and by Prop. 2.3 it suffices to consider the mean value of the equilibrium E^* or the cycle C, respectively. If it approaches E^* the result is immediate, since by Prop. 2.4.(i) the mean value is $\phi_y(\xi) = y^* = \nu(x^*)$. Now assume that Y approaches a cycle $C = (x, y)$ with period T. Applying Prop. 2.4.(ii) for the mean value of cycles yields

$$\phi_y(\xi) = \frac{1}{T}\int_0^T y\,\mathrm{d}\tau = \frac{1}{T}\int_0^T \nu(x)\,\mathrm{d}\tau - \frac{1}{T}\int_0^T \frac{\dot{x}}{\rho(x)}\,\mathrm{d}\tau$$

and using integration by substitution for the rightmost integral we obtain

$$\phi_y(\xi) = \frac{1}{T}\int_0^T \nu(x)\,\mathrm{d}\tau - \int_{x(0)}^{x(T)} \frac{1}{\rho(s)}\,\mathrm{d}s\,.$$

Now, since C is a cycle with $x(0) = x(T)$ the last integral vanishes, giving the result. The lower and upper bounds follow immediately. □

The simple result that the mean predator density can be expressed in terms of the prey nullcline immediately implies our main result, which states that the necessary condition $\nu'(x) > 0$ is in fact sufficient for the occurrence of a Hydra Effect in the general model (2.2–2.3).

Theorem 2.10. *Under assumptions (A)–(C), a Hydra Effect of the predator y occurs if and only if there exists a* $0 < x < K$ *so that* $\nu'(x) > 0$.

Proof. First note that assumption (A) implies $\nu'(K) < 0$, that is, the prey nullcline crosses the prey axis from above at $x = K$. Now let $\nu'(x) > 0$ for some $0 < x < K$. Thus $\nu(x)$ has at least one local maximum at some point $x_0 < K$ with $x_0 = x^*(m_0)$. Then, due to Cor. 2.6 we have $\phi_y(\xi, m_0) = \nu(x_0)$ for all $\xi \in \mathbf{R}_{>0}$. Now assume that this is the only extremum of the prey nullcline ν. Then the result follows from Lem. 2.9, since $\phi_y(\xi, m) < \nu(x_0) = \phi_y(m_0)$ for all $\xi \in \mathbf{R}_{>0}$ and all $m < m_0$. If on the other hand there is more than one local extremum of the prey nullcline, without loss of generality we can assume that there is a minimum at x_1 and a maximum at $x_2 > x_1$, so that $\nu'(x) > 0$ for $x_1 < x < x_2$. With $x_1 = x^*(m_1)$ and $x_2 = x^*(m_2)$ this implies $\phi_y(m_1) = \nu(x_1) < \nu(x_2) = \phi_y(m_2)$. □

Thus, although the equilibrium is never actually attained in the case $\nu'(x) > 0$ our result implies that an increase in predator equilibrium density is nevertheless a necessary and sufficient condition for the occurrence of a Hydra Effect in the predator population. Accordingly, the remark by Abrams (2009, p. 436) concerning a special case of system (2.2–2.3)

that "the average predator population size need not change in the same direction as the equilibrium" should not be taken to imply that the mean predator abundance does not follow an increase in its equilibrium abundance at all, since it has to do so at least for a certain range of mortality rates.

Note that Th. 2.10 is essentially an indirect result in the sense that it is not necessary to know how exactly solutions are affected by changes in the mortality rate, i.e. how the amplitude of a cycle changes when the mortality rate is increased.

Examples and the quantification of the magnitude of a Hydra Effect

Probably the simplest models which fulfill the requirement of Th. 2.10 and which thus allow for a Hydra Effect to occur are those where the prey nullcline is given by a quadratic polynomial. A very important representative of this type of model is the focus of the next example.

Example 2.11. Consider a model with logistic prey growth $g(x) = g_1(x)$ and hyperbolic or Holling type II predation term

$$\rho(x) = \rho_2(x) = \frac{ax}{h+x}.$$

This well-known model (Rosenzweig and MacArthur, 1963) has been a cornerstone of predator–prey ecology over the last decades. The prey nullcline of this model is given by the quadratic polynomial

$$\nu(x) = \frac{r}{a}\left(1-\frac{x}{K}\right)(h+x).$$

This nullcline has a unique maximum at prey density $x_0 = \frac{1}{2}(K-h)$, that is $\nu'(x_0) = 0$, and the equilibrium E^* is globally stable for $x^*(m) \geq x_0$. A supercritical Hopf bifurcation occurs at $x^*(m_0) = x_0$ (Kuznetsov, 1995, p. 93) and for $x^*(m) < x_0$ the equilibrium is unstable, surrounded by a unique stable limit cycle which attracts all solutions except for E^* (Liou and Cheng, 1988). Theorem 2.10 tells us that a Hydra Effect occurs in the Rosenzweig–MacArthur model, and we can in fact quantify the magnitude of the Hydra Effect for this example. If the predator mortality rate is increased from 0 to the Hopf-bifurcation value m_0, the corresponding increase in mean predator density is at least

$$\nu(x_0) - \nu(0) = \frac{r}{a}\left(h + \frac{(K-h)^2}{4K}\right) - \frac{rh}{a} = \frac{r(K-h)^2}{4Ka}.$$

This is the difference between the maximum value of the prey nullcline and the value at its intersection with the predator axis at $x = 0$. To see this, let $m < m_0$ and T be the period of the unique asymptotically stable cycle Y. Using Lem. 2.9, we can bound the mean predator density of this limit cycle from above in terms of the mean prey density by

$$\begin{aligned}\phi_y(m) = \frac{1}{T}\int_0^T \nu(x)\,\mathrm{d}\tau &= -\frac{r}{aK}\frac{1}{T}\int_0^T x^2\,\mathrm{d}\tau + \frac{r}{a}\left[\left(1-\frac{h}{K}\right)\phi_x(m)+h\right] \\ &< \frac{r}{a}\left[\left(1-\frac{h}{K}\right)\phi_x(m)+h\right].\end{aligned}$$

Note that a similar estimate can in fact be made for every model with a quadratic prey nullcline. Since $\nu(0) = \frac{rh}{a}$, it remains to show that $\phi_x(m) \to 0$ for $m \to 0$. Therefore observe that the mean intrinsic growth of the predator along the periodic orbit vanishes

$$\frac{1}{T}\int_0^T [\varepsilon\,\rho(x) - m]\,\mathrm{d}\tau = \frac{1}{T}\int_0^T \frac{\dot{y}}{y}\,\mathrm{d}\tau = \frac{1}{T}\left[\log(y(T)) - \log(y(0))\right] = 0$$

and we obtain

$$\frac{1}{T}\int_0^T \rho(x)\,\mathrm{d}\tau = \frac{m}{\varepsilon}.$$

This simply reflects that the average numerical response of the predator along the periodic orbit exactly outweighs its losses due to mortality during one cycle. Thus

$$\frac{1}{T}\int_0^T \rho(x)\,\mathrm{d}\tau \to 0 \quad \text{for } m \to 0,$$

where T in general depends on m. Clearly, any cycle will attain a maximum prey value $x_+ > x^*$ during one cycle. The claim follows immediately if $x_+ \to 0$ for $m \to 0$, since $\phi_x(m) < x_+$ always holds. Now assume that x_+ does not tend to zero for vanishing predator mortality m. Consider $\ell(x) = c\,x$ with $c = \rho(x_+)/x_+ > 0$. Then $\ell(x_+) = \rho(x_+)$ and $\ell(x) \le \rho(x)$ on $0 \le x \le x_+$, since ρ is concave downwards. Therefore

$$\frac{1}{T}\int_0^T \rho(x)\,\mathrm{d}\tau \ge \frac{1}{T}\int_0^T \ell(x)\,\mathrm{d}\tau = c\,\phi_x(m),$$

and by comparison $\phi_x(m) \to 0$ for $m \to 0$. This result shows that low predator mortality rates are in any case not beneficial for the prey species.

In conclusion, we have seen that for a vanishing predator mortality rate the mean predator density tends to some value smaller than $\nu(0)$. Thus, if m is increased from 0 to the bifurcation value m_0 for which x^* intersects the prey nullcline at its maximum, the mean predator

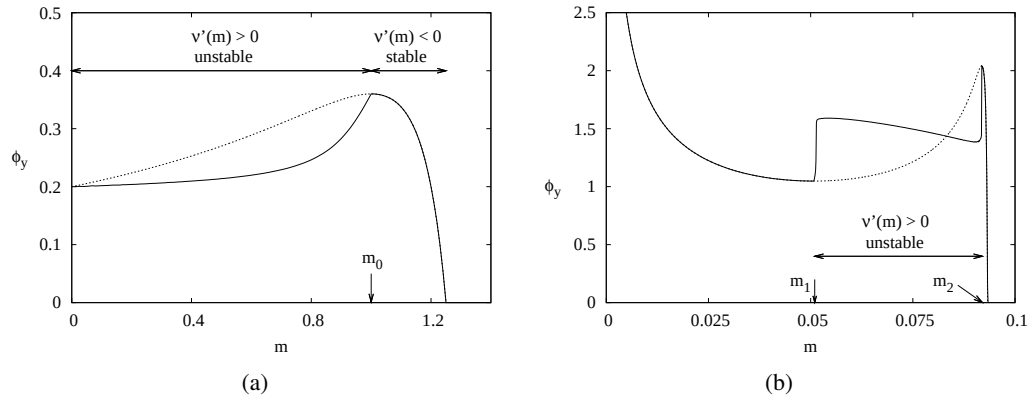

Figure 2.1: Mean predator population density (solid line) vs. predator mortality for (a) the model with a type II functional response (Ex. 2.11) and (b) the model with a type III functional response (Ex. 2.14). Predator density at the unique equilibrium (dashed line) coincides with the mean value when the equilibrium is stable and differs from the mean value when it is unstable. The arrows indicate the location of Hopf bifurcation points.

density has to increase at least from $\nu(0)$ to $\nu(x_0)$. A numerical simulation is shown in Figure 2.1a. For m very small the mean predator density ϕ_y is very close to $\nu(0)$ and it increases over the whole range of mortality rates for which the unique equilibrium is unstable. Once the unique equilibrium becomes stable at m_0 via the Hopf bifurcation, the predator mean density conincides with $\nu(x^*)$ and it decreases until the predator goes extinct.

Remark 2.12. In the special case of slow predator and fast prey dynamics, the mean predator abundance in the cyclic regime has been derived to be $\phi_y(m) = \nu(0) = rh/a$ by Dercole et al. (2006). This value is independent of the predator mortality rate and it only holds for the singular limit cycle obtained from slow–fast dynamics. Thus, in the slow–fast special case we have $\phi_y(m) = rh/a$ for $m < m_0$ and $\phi_y(m) = \nu(m)$ for $m \geq m_0$. This implies a discontinuous or "sharp increase" (Dercole et al., 2006, Appendix A4) in mean predator abundance when the system moves from the cyclic to the stationary regime via an increase in predator mortality rate. This corresponds to a non-smooth Hydra Effect in our terminology and the increase at the Hopf bifurcation point is exactly the value derived in the previous example, namely the difference $\nu(m_0) - \nu(0)$.

Remark 2.13. The previous example also has interesting implications for the theory of harvesting. Consider that the predator population in the previous example has a natural mortality rate $\bar{m}$ and is harvested with constant effort q. Then the combined mortality rate

of the predator is $m = \bar{m} + q$ and the long-term mean yield is $H = q\,\phi_y(m)$. Now, first, the existence of a Hydra Effect implies that the mean yield H depends nonlinearily on the harvesting effort q, since ϕ_y increases with q. Second, it implies that if the harvested predator population is in the cyclic regime, e.g. $m < m_0$, the harvesting effort should always be increased in order to increase the mean yield since the mean predator density ϕ_y is maximized at $m = m_0$. It also complements previous work on harvesting in the Rosenzweig–MacArthur model and in tritrophic food chains (de Feo and Rinaldi, 1997; Gragnani et al., 1998). In particular, Gragnani et al. (1998) state simple operating rules for the nutrient supply of a harvested population in order to maximize the mean yield, which can be reformulated in the context of the Hydra Effect in the following way: If a harvested predator experiences a Hydra Effect and the underlying predator–prey system is cyclic, then increase the harvesting effort.

In Ex. 2.11 numerical simulations indicate that the mean predator density $\phi_y(m)$ is strictly increasing on the whole interval of mortality rates for which $v'(m) > 0$ is fulfilled. However, as has already been observed in numerical simulations by Abrams (2009), in some cases the overall trend of increasing mean predator density may be reversed by significant intermediate intervals of decreasing predator mean densities. At this point it is important to note that Th. 2.10 essentially only states that $\phi_y(m)$ has to increase *somewhere* on the interval of mortality rates for which $v'(m) > 0$ is fulfilled and that it has to do so at least in the vicinity of a maximum of the prey nullcline. The next example illustrates the case of alternating intervals of increasing and decreasing predator mean densities.

Example 2.14. Let $g(x) = g_1(x)$ be of the logistic type again and let the predation term be of Holling type III

$$\rho(x) = \rho_3(x) = \frac{a x^2}{h + x^2}\,.$$

This model has been analyzed by Yodzis (1989). The prey nullcline $v(m)$ has two extremal points, a minimum at some mortality rate m_1 and a maximum at some $m_2 > m_1$. A numerical example for this model is shown in Figure 2.1b. As expected, intervals of increasing predator mean density occur, when the unique equilibrium is unstable and surrounded by a limit cycle. There are two distinct jumps in mean population density close to the two Hopf bifurcations occurring at the two mortality rates $m_1 < m_2$. Shortly after the second Hopf bifurcation at m_2, a sudden collapse of the predator population occurs for a relatively small further increase of the mortality rate.

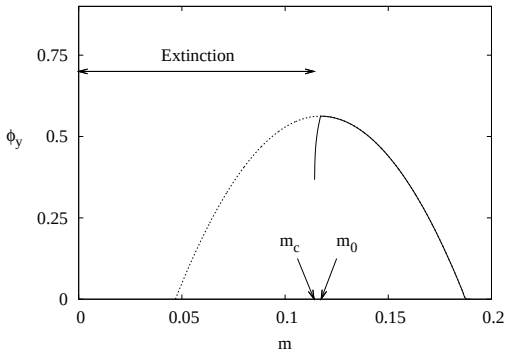

Figure 2.2: Predator mean (solid line) and equilibrium density (dashed line) vs. predator mortality for the model in example 2.15. m_c refers to the global bifurcation in which a limit cycle appears. m_0 denotes the parameter value where the limit cycle disappears in a Hopf bifurcation.

Allee effects and non-smooth Hydra Effects

Species with a strong Allee effect are especially prone to cause a Hydra Effect in purely prey-dependent predator populations. The presence of a strong Allee effect means that small populations below a critical minimal viable population size (Allee threshold) go extinct. This can be caused, e.g., by a shortage in mating partners and fertilization opportunities at low densities, inbreeding or reductions in the effectiveness of group activities such as anti-predator defense or social care (Allee, 1931; Courchamp et al., 2008). Here, a predator with a low mortality rate may suppress the prey population below its Allee threshold, thereby causing the extinction of both species. Translating this scenario into a system of differential equations, this implies that at sufficiently low predator mortality rates attracting strictly positive solutions do not exist but may emerge only at higher mortality rates, thereby giving rise to a non-smooth Hydra Effect.

For a simple general setting with an Allee effect, consider the basic framework given by system (2.2–2.3). We drop assumption (C) and extend assumption (A) slightly by assuming that there is an Allee threshold $0 < K_- < K$, such that $g(x) < 0$ for $0 < x < K_-$ and $g(x) > 0$ for $K_- < x < K$. This assumption corresponds to a strong Allee effect of the prey population, with negative growth rates at low prey densities. This implies $\nu(m) < 0$ for $0 < m < m_-$ and $\nu(m) > 0$ for $m_- < m < m_+$. Thus, for the mean predator density we have $\phi_y(m) = 0$ for all $0 < m \leq m_-$, since no strictly positive solutions exist at all. On the other hand, strictly positive attractive solutions may exist for $m_- < m < m_+$ and indeed they surely exist whenever $\nu'(m) < 0$ is fulfilled, since in this case the unique equilibrium E^* is locally stable. And since the prey nullcline crosses the prey axis from above at $x = K$, it has negative slope at least in a neighborhood of K, which implies $\phi_y(m) > 0 = \phi_y(m_-)$ for some $m_- < m < m_+$.

Example 2.15. Consider a model with the following growth and predation terms (Conway

and Smoller, 1986; Bazykin, 1998; Wang et al., 2011)

$$g(x) = g_4(x) = r\,(1-x)\,(x-K_-)\,,$$
$$\rho(x) = \rho_4(x) = a\,x\,.$$

The predation term is of simple Lotka–Volterra form, while the growth term implies an Allee effect with carrying capacity $K = 1$ and Allee threshold $0 < K_- < 1$. The system possesses a unique positive equilibrium E^* which exists for $m_- = \varepsilon\,a\,K_- < m < \varepsilon\,a = m_+$. A numerical simulation of the change of the predator mean density in response to its mortality rate is presented in Figure 2.2. The behavior of the mean value ϕ_y reflects that below some bifurcation value $m_c > m_-$ no strictly positive solutions exist, this is the extinction region in Figure 2.2. There is a sudden increase in predator mean density at m_c, where a strictly positive limit cycle arises via a global bifurcation (van Voorn et al., 2007). At the Hopf bifurcation value m_0 the mean value coincides with the equilibrium E^* which is stable for all $m > m_0$. For a further increasing predator mortality the mean density follows the downslope of the prey nullcline until the predator goes extinct again.

2.5 Hydra Effect in a three-dimensional model

The general two-species model (2.2–2.3) gives rise to a unique equilibrium, whose stability is easily determined. This was exploited to derive elementary conditions for the occurrence of a Hydra Effect of the predator population. In contrast to this, the situation becomes considerably more complicated if there is more than one pure consumer of the prey x. The problems arise mainly due to the fact that in contrast to the two-dimensional case (2.2–2.3), such systems do not allow for stable coexistence at a unique equilibrium of all species. Nevertheless, coexistence of all species is possible in the form of strictly positive nonstationary solutions. The existence of such solutions for certain systems of two pure predators and one prey has been proved by McGehee and Armstrong (1977), which has been extended by Zicarelli (1975) to the case of an arbitrary number of predators coexisting on one prey species. For an illustrative example, we will focus on one particular system, which has been proposed by Armstrong and McGehee (1980).

Example 2.16. The pure coupled resource–consumer equations for a Lotka–Volterra-type

predator y, a Holling-type II predator z and the shared logistically growing prey x read

$$\dot{x} = \left[r\left(1 - \frac{x}{K}\right) - a_1 y - \frac{a_2 z}{h+x} \right] x, \tag{2.4}$$

$$\dot{y} = [\varepsilon_1 a_1 x - m_y] y, \tag{2.5}$$

$$\dot{z} = \left[\varepsilon_2 \frac{a_2 x}{h+x} - m_z \right] z. \tag{2.6}$$

Note that the predator–prey subsystems on the invariant planes $(x, y, 0)$ and $(x, 0, z)$ are of Gause-type. A Hydra Effect never occurs in the Lotka–Volterra subsystem (x, y), but a Hydra Effect always occurs in the (x, z) Rosenzweig–MacArthur subsystem, cf. examples 2.8 and 2.11, respectively. Due to the lack of strictly positive stationary solutions however, these results cannot be easily extended to the full two-predator and one-prey system. In the full three-dimensional system, complicated periodic and chaotic solutions may be observed, as well as coexisting alternative attractors (Abrams et al., 2003; Sieber and Hilker, 2011b).

Let $E_y^* = \left(x_y^*, y^*, 0\right)$ and $E_z^* = \left(x_z^*, 0, z^*\right)$ denote the semi-trivial equilibria in the $(x, y, 0)$ and $(x, 0, z)$ predator–prey subsystems, respectively. A necessary condition for the existence of strictly positive solutions is $x_z^* < x_y^*$, since otherwise the semi-trivial equilibrium E_y^* becomes globally stable. Assume now that a strictly positive solution exists and that it is periodic with period T. In this case, by integrating (2.5) from 0 to T we immediately obtain the mean prey density along this periodic orbit as

$$\phi_x(m_y) = \frac{m_y}{\varepsilon_1 a_1} = x_y^*.$$

The Lotka–Volterra predator y completely determines the mean prey density in the full three-dimensional predator–prey system, regardless of the biological and ecological parameters of the Holling predator z. In fact, this is of course the case with any Lotka–Volterra predator in any purely prey-dependent predator–prey system with arbitrary many predators. The presence of a single Lotka–Volterra predator in an ecological model community determines the mean amount of prey at any time and it also implies the well-known result that two or more linear predators cannot coexist on a single shared prey (McGehee and Armstrong, 1977).

So while we cannot expect to derive an analytical expression for the mean predator densities of system (2.4–2.6), we exactly know how much prey there is on average. This can be used to derive upper bounds for both predator mean densities. In a similar fashion as in the

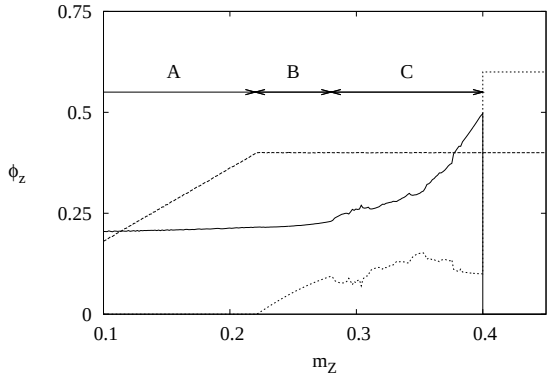

Figure 2.3: Mean population densities (prey x: dashed; linear predator y: dotted; nonlinear predator z: solid) vs. predator z mortality m_z for model (2.4–2.6). A: Cyclic coexistence of x and z. B: Cyclic coexistence of all three species. C: Alternative cyclic and chaotic attractive solutions. Parameters: $r = 1, K = 1, a_1 = 1, a_2 = 0.5, h = 0.1, m_y = 0.4, \varepsilon_1 = \varepsilon_2 = 1$.

two-dimensional Gause-type model we obtain from (2.4)

$$\phi_y < r - \frac{\phi_x(m_y)}{K} = r - \frac{m_y}{\varepsilon_1 a_1 K},$$
$$\phi_z < \frac{r}{a_2}\left[\left(1 - \frac{h}{K}\right)\phi_x(m_y) + h\right] = \frac{r}{a_2}\left[\left(1 - \frac{h}{K}\right)\frac{m_y}{\varepsilon_1 a_1} + h\right].$$

Apparently, an increase in the prey carrying capacity K seems beneficial for the whole ecological community, since it increases the upper bounds for both predator mean densities. However, in the case of unlimited carrying capacity $K \to \infty$, the upper bounds for both predators approach finite values. As one would expect, the mortality rate m_y adversely affects the upper bound for the mean value of predator y on the one hand and increases the upper bound for ϕ_z on the other hand. The mortality rate m_z however does not change the upper bounds at all, again reflecting the dominance of the linear predator. Also, the first inequality gives another necessary condition for the existence of strictly positive solutions. The mean value of predator y can only be positive, if $x^* < rK$, giving the complete necessary condition $x_z^* < x_y^* < rK$ for strictly positive solutions. For a further analysis of the predator mean densities, we now turn to numerical simulations.

In Figure 2.3 a numerical approximation of the population mean densities for varying predator z mortality m_z is shown for model (2.4–2.6). Note that varying m_z only affects the stationary point x_z^* in the (x, z) subsystem, while x_y^* remains constant. If a small amount of predator y is introduced into the system, it is clearly not able to establish unless a critical mortality rate m_- is exceeded. This is region A in Figure 2.3. After establishment of predator y, in region B we observe cyclic coexistence of all three species and the corresponding mean prey density remains fixed at $\phi_x(m_z) = x_y^*$ as expected. Clearly, in this region an increasing predator z mortality m_z is beneficial for the first predator y, reflected by

Model	Reference	Biological mechanism	Hydra effect
Ex. 2.8	Volterra (1931)	linear functional response	no
Ex. 2.11	Rosenzweig and MacArthur (1963)	type II functional response	yes
Ex. 2.14	Yodzis (1989)	type III functional response	yes
Ex. 2.15	Bazykin (1998)	prey with strong Allee effect	yes, non-smooth
Ex. 2.16	Armstrong and McGehee (1980)	two predators (linear/nonlinear)	yes, smooth and non-smooth

Table 2.1: Hydra effects occur in various nonlinear standard predator–prey models

an increasing predator mean value $\phi_y(m_z)$.

In region C, at least two alternative attractors may coexist, both of which may be periodic or chaotic (Sieber and Hilker, 2011b). Both predator mean densities show a more irregular behavior in this region with several small magnitude non-smooth Hydra Effects occurring when the fixed initial condition switches from one basin of attraction to another or when one of the attractors vanishes in a boundary crisis.

Over the whole range of mortality rates, however, the predator z mean density $\phi_z(m_z)$ clearly shows a Hydra Effect, which is even more pronounced after predator y has established in the system, leading to a doubling in its initial value until the mortality rate m_z reaches a critical value. This critical value of m_z is given by

$$m_z = \frac{\varepsilon_2 a_2 m_y}{\varepsilon_1 a_1 h + m_y} \;\Leftrightarrow\; x_y^* = x_z^*. \tag{2.7}$$

If m_z is increased over this critical value, a sudden extinction of the predator z population can be observed. This extinction can easily be understood in terms of stability of the boundary equilibria, since the stationary solution E_y^* in the (x, y) subsystem becomes globally stable for $x_y^* < x_z^*$. However, from a biological viewpoint, this sharp threshold phenomenon is an interesting effect and even more so, since the increasing predator mean density right before the catastrophic crash gives the impression of a healthy population.

2.6 Discussion

The analytical and numerical results above show that Hydra Effects are a typical feature of Gause-type predator–prey systems, whenever the model allows for an unstable non-trivial equilibrium. Table 2.1 summarizes the results from the examples that have been discussed in the text.

The examples have also shown that one can distinguish between two qualitatively dif-

ferent types of Hydra Effects. A smooth Hydra Effect is due to a smooth change in the shape of an attractor, like changes in the amplitude of a limit cycle as in examples 2.11 and 2.14. A non-smooth Hydra Effect, by contrast, is associated with an abrupt change in the long-term behavior of a solution starting at a particular initial condition. This change can either be due to a global bifurcation as in Ex. 2.15, where a strictly positive attractive solution arises suddenly at a certain mortality rate. Alternatively, the long-term behavior of a solution might change abruptly because changing the mortality rate alters the shape of the basins of attraction of coexisting attractors and the initial condition switches from one basin of attraction to another one as in Ex. 2.16.

The Hydra Effect is closely associated with the imminent collapse of the respective species for which the Hydra Effect is observed. This is due to the fact that an increase in predator mean density has to occur right before maximal predator population sizes are reached, after which a further increase of the mortality rate necessarily leads to a decline in population size. The population collapse is most pronounced and unexpected in the case of two predators coexisting on one shared prey species (Ex. 2.16), where there is a distinct critical mortality rate at which the sudden collapse of the seemingly healthy predator population occurs. In the case of just one predator, the imminent extinction of the predator is indicated by a continuous but nevertheless very rapid decline in mean population density in response to further increasing mortality rate (cf. Figure 2.1). This has the implication that the observation of mean population densities alone may lead to false assumptions regarding the persistence of a population. In fact, catastrophic crashes are inherently present in models with purely prey-dependent predators. This is especially of concern when the predator population is harvested, see Remark 2.13.

The general Gause-type model (2.2–2.3) is a cornerstone of predator–prey ecology. It has been used in various specific forms and the results presented here show that Hydra Effects are typically present in all of these variants, except for the simplest Lotka–Volterra models. It is therefore striking that direct evidence for the existence of Hydra Effects in natural populations is rare. This lack of empirical evidence has partly been attributed to the lack of appropriate observations (Abrams, 2009). Another cause for the apparent discrepancy at least between the predator–prey models investigated here and empirical data, however, might be attributed to shortcomings of the general model (2.2–2.3).

A prominent peculiarity of the model is that the intrinsic growth rate of the predator does not depend on its own density. This feature greatly simplifies the analysis of the model, but given that "[i]n real life, we never expect to encounter *pure* resource–consumer systems" (Turchin, 2003, p. 36), it is certainly worthwhile to address the problem of Hydra Effects

in non-pure resource–consumer systems. An obvious way to make the predator growth rate dependent on its own density is to add a quadratic closure term reflecting intraspecific competition to the predator equation (2.3), thereby implicitly introducing an upper density bound for the predator population. A corresponding variant (Bazykin, 1998, p. 67) of the Rosenzweig–MacArthur model (cf. Ex. 2.11) is inherently more stable (Turchin, 2003, p. 98) and thus the parameter range for which a Hydra Effect might occur is greatly reduced. In addition to quadratic closure, there are other biologically meaningful mechanisms which make the predator growth rate dependent on its own density, such as ratio-dependent predation (Abrams and Ginzburg, 2000) and predator interference (Beddington, 1975; DeAngelis et al., 1975). While the relative importance of these factors is usually difficult to measure in real populations, it is an interesting question for future research whether they may resolve at least in part the apparently paradoxical phenomenon of Hydra Effects in predator–prey models.

3 Transformation of intraguild predation community modules

3.1 Community modules and intraguild predation

One approach to investigate the manifold forms of ecological communities with often thousands of interacting species is to identify, in the unmanageable structure of the larger system, a few general patterns of species interaction. Then, by looking at the dynamics that arise from those community modules (Holt, 1997), the structure and population dynamics of the whole community may be addressed. Three-species modules which have gained a lot of attention among ecologists include tri-trophic food chains, apparent competition, and exploitative competition. All of these modules assume that two of the three species involved do not directly interact with each other. By contrast, the community module of intraguild predation (IGP) includes direct interaction of all three species.

In its simplest form, an intraguild predator (IG predator) grazes on an intraguild prey (IG prey), while both share a common prey or basal resource. IGP contains the beformentioned simpler modules as special cases, when either one of the three interactions can be neglected. The theoretical framework of IGP has been laid out in the work of Polis et al. (1989) and Holt and Polis (1997). IGP has attracted a lot of attention from ecologists and is believed to be a very common scenario in natural populations (Arim and Marquet, 2004). Theoretical studies show that the occurrence of IGP may have important implications for the persistence of food webs and biodiversity; for a comprehensive review, see the special feature on IGP in *Ecology*, vol. 88 (11).

While the original concept of IGP focuses on interactions between predators and their prey, more recently it has been recognized that the basic structure of IGP arises naturally in several subdisciplines of ecology. In particular, similarities between host–parasitoid and host–pathogen interactions with classical IGP have been highlighted (Borer et al., 2007). Parasites are recognized as major players in the functioning of ecosystems (Lefèvre et al., 2009) and they have subsequentely been incorporated into food webs on the trophic level

above their hosts (Hochberg et al., 1990; Raffel et al., 2008). In a similar way, the field of eco-epidemiology has integrated host–pathogen epidemiology with community ecology (Anderson and May, 1986; Holt and Dobson, 2006; Holt and Roy, 2007). As such, on the community level, parasites and pathogens have been found to play a role analogous to classical predators.

Thus, even though predators, parasites and pathogens differ substantially in terms of body size, generation times, durability and intimacy of the interaction with their resource, a unification of host–parasite and prey–predator interactions within the IGP framework may provide useful insights across the borders of ecological subdisciplines. This paper shows that parasitism does not only fit into the IGP framework, but that it may suggest a different and rather unexpected perspective on the underlying community structure. Technically, this change of perspective corresponds to a transformation of variables, a powerful tool routinely used across all scientific disciplines. Physics for example is abound in problems which may appear intractable in one coordinate system, but which get dramatically simplified by an appropriate coordinate transformation. Similar changes in the frame of reference have also lead to fresh insights into problems in ecology and evolution, such as replacing absolute values by time-averaged values to explain the coexistence of species in variable environments (Levin, 1979) or looking at gene numbers rather than gene frequencies (Holt and Gomulkiewicz, 1997).

Using this approach we will first show that after an appropriate transformation of variables particular cases of IGP are structurally similar to 'simpler' community modules. We will then demonstrate that this structural similarity also translates into remarkably similar community dynamics. These similarities can be effectively exploited to bridge gaps in our current understanding of food webs, as suggested already by Holt and Polis (1997).

3.2 Transformation of intraguild predation

In this section, we show how a intraguild predation module can be transformed into simpler module structures. The only condition concerns indiscriminate predation (see below for a definiton). The model considered here is deliberately very general. This highlights that the transformation of IGP into other food web modules is not restricted to certain functional responses and growth functions. The next sections will introduce a more specific example illustrating the benefits of the module transformation.

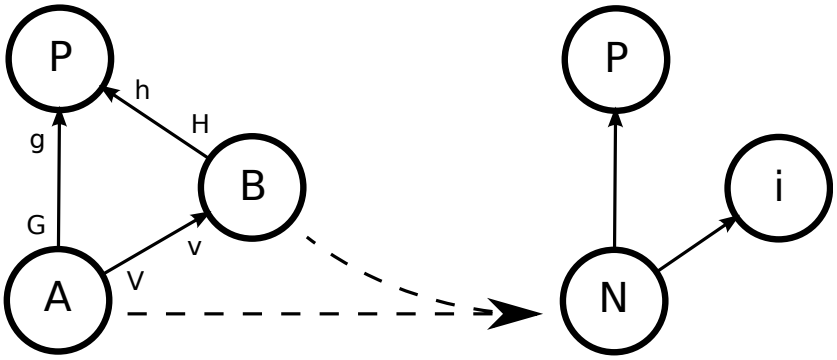

Figure 3.1: Transfer diagram for IGP (left) and exploitative competition (right). An IGP module is equivalent to exploitative competition when the two prey species A and B are similar from the IG predator's (P) point of view; see the main text.

A general model of intraguild predation

We begin with an IGP module consisting of a basal prey A, an IG prey B, and an IG predator P (Figure 3.1). A, B, and P are assumed to represent the total biomass of each species. Interactions between the species lead to the conversion of biomass, which is illustrated by the arrows in Figure 3.1. In general, there is no one-to-one correspondence between the outflow of resource biomass and the subsequent increase of consumer biomass. To account for the conversion efficiency, the flow of biomass is often split into a functional response of the resource and the corresponding numerical response of the consumer. In Figure 3.1, an upper (lower) case letter at the tail of an arrow corresponds to the biomass flow associated with the functional (numerical) response, respectively.

The IGP community is then described by the following set of differential equations

$$\frac{\mathrm{d}A}{\mathrm{d}t} = \underbrace{r(A,B)}_{\text{production}} \quad \underbrace{-V(A,B)}_{\text{consumption by } B} \quad \underbrace{-G(A,B,P),}_{\text{consumption by } P} \tag{3.1}$$

$$\frac{\mathrm{d}B}{\mathrm{d}t} = \underbrace{v(A,B)}_{\text{conversion of } A} \quad \underbrace{-H(A,B,P)}_{\text{consumption by } P} \quad \underbrace{-n(B),}_{\text{natural mortality}} \tag{3.2}$$

$$\frac{\mathrm{d}P}{\mathrm{d}t} = \underbrace{g(A,B,P)}_{\text{conversion of } A} \quad \underbrace{+h(A,B,P)}_{\text{conversion of } B} \quad \underbrace{-m(P),}_{\text{natural mortality}} \tag{3.3}$$

where $V(A,B)$ and $v(A,B)$ denote the biomass flow from species A to B; $G(A,B,P)$ and $g(A,B,P)$ the biomass flow from A to P; and $H(A,B,P)$ and $h(A,B,P)$ the biomass flow from B to P. There are three more demographic processes. First, there is an inflow r of biomass into the community, corresponding to intrinsic growth of the basal prey A. We

assume that this growth may, in general, also depend on the IG prey. For example, the IG prey might be lowering the reproductive success of the basal prey through competition for essential resources, a scenario which arises naturally in eco-epidemiology. A model where this is the case will be discussed in the next section. The two other processes not describing direct interaction of two species are natural mortality of the IG prey, $n(B)$, and IG predator, $m(P)$.

Indiscriminate predation

Having thus formalized the description of an IGP community in very general terms, we now consider some scenarios where there is little or no distinction between the IG prey and basal prey from the IG predator's point of view. Such scenarios, for example, arise naturally in eco-epidemiology, when a predator P grazes upon a prey population which is affected by an infectious disease. The disease splits the otherwise homogeneous prey population into a susceptible portion A and an infected portion B. Since both groups are subject to predation by P, the susceptibles A may be considered as a basal resource for the infecteds B and the IG predator P. Another example concerns host–parasitoid systems, where two different parasitoids depend on the same host species A and a parasitoid is able to outcompete the other one within the host (Holt and Hochberg, 1998; Raffel et al., 2008). The underlying assumption is that the hyperparasitoid does not or is not able to distinguish between healthy hosts A and already parasitized hosts B. A similar scenario is related to hyperinfections, where one pathogen is able to infect healthy and already diseased hosts and becomes the solely transmitted pathogen. In the latter two examples, P denotes the portion of hosts which are infested by the hyperparasitoid or infected by the hyperinfectious agent, respectively.

Last but not least, 'classical' IGP communities with little or no distinction between basal prey and IG prey may also arise in predator–prey ecology. For example, the wolf spider species *Pardosa milvina* and *Hogna helluo* both ordinarily prey on crickets and they also readily consume smaller individuals of the other species. While the relative strength of these predatory interactions in natural situations is not fully known, at least under laboratory conditions *Pardosa* appeared to make no difference between its basal cricket prey and small juvenile *Hogna* intraguild prey (Rypstra and Samu, 2005).

Let us now put into more rigorous terms the assumption that the IG predator does not or cannot distinguish between IG prey and basal prey. This means, first, that the IG predator's attack rate is the same for both prey species. That is, the ratio of the consumption rates of B

and A equals the ratio of abundances B and A:

$$\frac{H(A,B,P)}{G(A,B,P)} = \frac{B}{A}. \tag{3.4}$$

Second, the total flow of biomass to the IG predator and its conversion from the two prey species depend only on the sum of the two prey species:

$$g(A,B,P) + h(A,B,P) = f(A+B,P), \tag{3.5a}$$
$$G(A,B,P) + H(A,B,P) = F(A+B,P). \tag{3.5b}$$

In other words, the numerical and functional responses can be subsumed when we lump together the two prey species A and B. Equations (3.4–3.5) express that the IG predator does not distinguish between IG and basal prey, and that the latter two are energetically equivalent. We will refer to these properties as *indiscriminate predation*. Obviously, they do not hold in general. In particular, they are not fulfilled for predators with a preference for certain prey, or for manipulative parasites that make their host easier to catch.

The transformed model

For many communities such as those described earlier, we may safely assume indiscriminate predation. In this case, we can sum up both groups A and B and deal with the total prey biomass $N = A + B$. Since we still want to keep track of the distinct groups that make up the total prey population N we introduce the prey ratio $i = B/A$ of IG prey B to basal prey A, assuming $A > 0$. The IG predator variable is not modified and the original prey quantities can be obtained as $A = N/(1+i)$ and $B = Ni/(1+i)$.

Now, how does the general model look like from this perspective? As the new variables N and i essentially correspond to a change of coordinates, Equations (3.1–3.3) can be transformed accordingly. More rigorously, we transform the model according to the map

$$\begin{pmatrix} A \\ B \\ P \end{pmatrix} \longmapsto \begin{pmatrix} A+B \\ B/A \\ P \end{pmatrix} = \begin{pmatrix} N \\ i \\ P \end{pmatrix}.$$

With the assumption of indiscriminate predation, the transformed system (3.6–3.8) is then obtained as follows. The differential equation for the predator P is easiest to determine, as we keep this state variable. We simply have to subsume $A + B = N$ in the original equation (3.3) to obtain (3.8) below. The differential equation for the total prey population

$N = A + B$ is obtained by

$$\frac{\mathrm{d}N}{\mathrm{d}t} = \frac{\mathrm{d}A}{\mathrm{d}t} + \frac{\mathrm{d}B}{\mathrm{d}t}.$$

Here the predation terms can be subsumed by using the identity $A + B = N$. The growth term applies only to the susceptible prey $A = N/(1+i)$, and the virulence only to the infected prey $B = Ni/(1+i)$. This gives equation (3.6). Finally, the differential equation for the ratio i of prey species (e.g. infecteds to susceptibles) requires a bit more care. The reason is that we have to use the quotient rule in order to get the time derivative. That is,

$$i' = \left(\frac{B}{A}\right)' = \frac{B'A - BA'}{A^2},$$

where the prime denotes differentiation with respect to time. We can replace B' and A' by the right-hand sides of (3.2) and (3.1), respectively. Then we are left with substituting A and B as before. Simplifying terms eventually gives equation (3.7).

This leads to the following model:

$$\frac{\mathrm{d}N}{\mathrm{d}t} = \underbrace{r(N,i) - n(i)}_{\text{total prey growth}} \quad \underbrace{-[V(N,i) - v(N,i)]}_{\text{transition to } i} \quad \underbrace{-F(N,P)}_{\text{consumption by } P}, \tag{3.6}$$

$$\frac{\mathrm{d}i}{\mathrm{d}t} = \left[\underbrace{v(N,i) + iV(N,i)}_{\text{increase of portion } i} \quad \underbrace{-ir(N,i)}_{\text{emergent loss}} \quad \underbrace{-n(i)}_{\text{natural mortality}} \right] \frac{1+i}{N}, \tag{3.7}$$

$$\frac{\mathrm{d}P}{\mathrm{d}t} = \underbrace{f(N,P)}_{\text{consumption of total prey}} \quad \underbrace{-m(P)}_{\text{natural mortality}}. \tag{3.8}$$

In this different but equivalent description of the general IGP scenario (3.1–3.3), the IG predator P appears as a consumer on the total prey population N. Note that (3.8) does not depend on i. The most important difference to model (3.1–3.3) is that the prey ratio i interacts only with the total prey N, i.e. (3.7) is independent of P. The emergent loss term in the rate of change (3.7) of the prey ratio is due to the differential growth of basal prey and IG prey and it reflects the lag with which basal prey growth is propagated through the trophic link to the IG prey. It will become clear in the next section that for biologically meaningful growth functions r, the prey ratio i can in fact be regarded as a consumer on N. This places the total prey biomass N at the bottom of the resulting community diagram, and we end up with two consumers P and i on a single resource N. This is the well-known structure of exploitative competition. A corresponding transfer diagram is shown in Figure 3.1.

3.3 An example from eco-epidemiology

We now apply the transformation described in the previous section for the general system to an example from eco-epidemiology (Hilker and Malchow, 2006). This model is of IGP type and describes a predator–prey community with an infection of the prey. The infectious disease splits the prey population into a susceptible portion A and an infected portion B. The predator is denoted by P and is assumed not to distinguish between sound and diseased prey, thereby fitting the abovementioned scenario of indiscriminate predation. The model equations are given in Table 3.1 ("IGP model").

The susceptibles are assumed to grow logistically with intrinsic growth rate r, while the infecteds do not reproduce anymore. However, they still do contribute to the common carrying capacity. The spread of the infection is assumed to follow a frequency-dependent incidence rate with transmissibility λ. Note, however, that the alternative assumption of density-dependent disease transmission yields qualitatively similar results. Predation is modelled by a Holling type II functional response for both susceptibles and infecteds, with equal predator attack rate a and half-saturation constant h. The conversion efficiency is given by ε lying between 0 and 1. The parameter m_P is the predator mortality rate and the infecteds suffer a disease-induced mortality μ.

We now apply the coordinate transformation with $N = A + B$ denoting the total prey population and $i = B/A$ the ratio of infecteds to susceptibles, to obtain the "transformed IGP model" shown in Table 3.1. While the equation of the IG predator remains essentially unchanged, the most interesting part is the interaction between prey ratio i and total prey N. Focusing on Eq. (T5), the prey ratio i can be viewed as a linear predator of Lotka–Volterra type on N. The associated functional response of the total prey N however is nonlinear, saturating for large prey ratios i. Nevertheless, it can be shown that this yields the same nullcline structure as for a linear predator (Turchin, 2003).

As a consequence, the prey ratio i and the IG predator P are consumers of the shared resource N. Besides this structural change, the growth rate of the total prey N has an additional factor $1/(1+i)$ reflecting that only susceptibles reproduce. In summary, the per-capita growth rates of P and i are functions only of the total prey population. The transformed IGP model thus describes two coupled consumer–resource systems. As suggested in the previous section, it thus corresponds to the community module of exploitative competition.

In fact, the transformed IGP model is very similar to a well-known model of exploitative competition (EC) proposed by Armstrong and McGehee (1980). It describes a linear predator B and a nonlinear predator P sharing a common prey species A. The equations

are given in Table 3.1 ("EC model"), where a_1 and a_2 are attack rates, ε_1 and ε_2 conversion efficiences, m_1 and m_2 per-capita mortalities. The remainder parameters are similar in their meaning to the eco-epidemiological model. There are only two structural differences between the two models, namely the reduced growth rate of the prey N in Eq. (T4) and the saturating functional response associated with the prey ratio i. The next section will show that, despite these differences, the overall structural similarity is reflected in a similar dynamical behavior, revealing a deep connection between the original eco-epidemiological IGP model and the ecological EC model.

3.4 IGP and exploitative competition: Similarity in structure and behavior

The eco-epidemiological IGP model predicts a switch in dominance from one consumer to another along an environmental gradient. For example, if the basal prey productivity (r) varies, the disease excludes the predators at low values of r, whereas the predators exclude the disease at high values of r. Coexistence of all three species is possible at intermediate productivities. In a general IGP model, the IG prey should be the better competitor for the shared basal prey, whereas the IG predator should primarily exploit the IG prey (Holt and Polis, 1997). These conditions for coexistence, however, are only necessary but not sufficient. Interestingly, coexistence in our transformed IGP model is only possible in form of non-equilibrium dynamics. This is also a very characteristic feature of EC models, cf. Koch (1974); Armstrong and McGehee (1980); Abrams et al. (2003), where cyclic oscillations allow two consumers to persist on a single resource; the heuristic principle of competitive exclusion (Hardin, 1960) does not hold in general for nonlinear EC models.

This similarity between the IGP and the EC model already gives a hint of the usefulness of the simple coordinate transformation. In the following, we will investigate the cyclic coexistence in more detail. Throughout this investigation, we will use a fruitful cross-fertilization between the EC and the IGP model: Well-known results from the EC model also hold for the IGP model, and new insights discovered in the IGP model apply to the EC model as well. A summary is given in Table 3.2.

One similarity in dynamical behavior that is already known for both models concerns extremely long transients before the cycling populations phase-lock to a regular oscillation. Abrams et al. (2003) illustrate this with an example of transient asynchronous cycles, while Hilker and Malchow (2006) refer to this phenomenon as "strange" periodic cycles.

model	equations				
IGP	$\frac{dA}{dt} =$	$\underbrace{r(1-(A+B))A}_{\text{susceptible growth}}$	$\underbrace{-\frac{\lambda AB}{A+B}}_{\text{infection}}$	$\underbrace{-\frac{aAP}{h+A+B}}_{\text{predation}},$	(T1)
	$\frac{dB}{dt} =$	$\underbrace{\frac{\lambda AB}{A+B}}_{\text{infection}}$	$\underbrace{-\frac{aBP}{h+A+B}}_{\text{predation}}$	$\underbrace{-\mu B}_{\text{virulence}},$	(T2)
	$\frac{dP}{dt} =$	$\underbrace{\varepsilon\frac{a(A+B)P}{h+A+B}}_{\text{predation of all prey}}$	$\underbrace{-m_P P}_{\text{natural mortality}}.$		(T3)
transformed IGP	$\frac{dN}{dt} =$	$\underbrace{\frac{r}{1+i}(1-N)N}_{\text{total prey growth}}$	$\underbrace{-\frac{\mu iN}{1+i}}_{\text{infection within prey}}$	$\underbrace{-\frac{aNP}{h+N}}_{\text{predation}},$	(T4)
	$\frac{di}{dt} =$	$\underbrace{riN}_{\text{linear infection increase}}$	$\underbrace{-(\mu+r-\lambda)i}_{\text{constant loss}},$		(T5)
	$\frac{dP}{dt} =$	$\underbrace{\varepsilon\frac{aNP}{h+N}}_{\text{total prey consumption}}$	$\underbrace{-m_P P}_{\text{natural mortality}}.$		(T6)
EC	$\frac{dA}{dt} =$	$\underbrace{r(1-A)A}_{\text{prey growth}}$	$\underbrace{-a_1 AB}_{\text{linear predator}}$	$\underbrace{-\frac{a_2 AP}{h+A}}_{\text{nonlinear predator}},$	(T7)
	$\frac{dB}{dt} =$	$\underbrace{\varepsilon_1 a_1 AB}_{\text{prey consumption}}$	$\underbrace{-m_1 B}_{\text{natural mortality}},$		(T8)
	$\frac{dP}{dt} =$	$\underbrace{\varepsilon_2\frac{a_2 AP}{h+A}}_{\text{prey consumption}}$	$\underbrace{-m_2 P}_{\text{natural mortality}},$		(T9)

Table 3.1: Model equations of the intraguild predation (IGP) and exploitative competition (EC) modules; see text for the meaning of variables

It is also Abrams et al. (2003) who present the first numerical evidence for even more complicated dynamics, namely chaos, in Armstrong and McGehee's EC model. This raises the question whether chaos may occur in the eco-epidemiological IGP model as well. And indeed, the population cycles undergo a cascade of period-doublings before eventually becoming chaotic. This is shown in the bifurcation diagrams for both the IGP and EC models

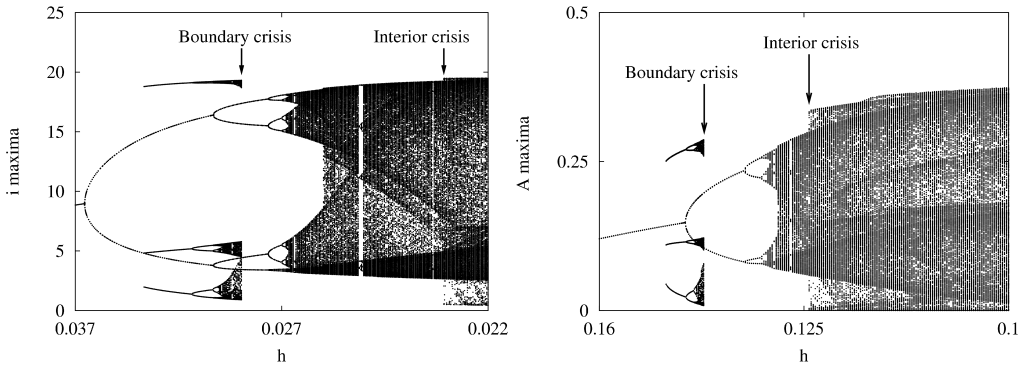

Figure 3.2: Dynamical behavior of the eco-epidemiological (transformed IGP) model (left) and the Armstrong–McGehee (exploitative competition) model (right). The bifurcation diagrams are qualitatively similar, suggesting an equivalence between the two community modules. Parameter values (top) $r = 1$, $\mu = 0.15$, $m_P = 0.8$, $\lambda = 0.8$, $a = 1$, $\varepsilon = 1$; (bottom) $r = 0.5$, $a_1 = 2.5$, $a_2 = 1$, $m_1 = 0.85$, $m_2 = 0.3$, $\varepsilon_1 = \varepsilon_2 = 1$. The half-saturation constant h is the control parameter, note the reversed axis.

in Figure 3.2.

Moreover, numerical experiments show that there exist at least two stable attractors in the IGP model for certain parameter ranges. Abrams et al. (2003) also briefly report on alternative attractors, which are periodic in all cases they observed. Here, we show in Figure 3.2 that one of the coexisting attractors can be chaotic.

In both models (Figure 3.2), one of the two attractors exists over the whole parameter range investigated. By contrast, the other attractor seems to exist only for a certain parameter range. Both attractors undergo a period-doubling cascade to chaos. At some point in the parameter space, this leads to the coexistence of a periodic and a chaotic attractor.

Consequently, fundamentally different dynamics can be observed depending on the initial conditions, or the 'history' of the ecological community. The alternative basins of attraction of the two attractors are arranged in an intricate way, which implies that the community dynamics are extremely fragile to perturbations. This raises the question how the basins of attraction of the two attractors are arranged in phase space. Here, the basin of attraction of an attractor denotes the set of all initial values for which the corresponding solution asymptotically approaches this particular attractor. Since we consider a three-dimensional model, a high resolution scan of the phase space would require an immense amount of computation time. Thus, we restrict the scan to a plane with $B = 0.5$ fixed in order to give an impression of the basins of attraction.

The result of the scan is shown in Figure 3.3. The parameter set is chosen such that one

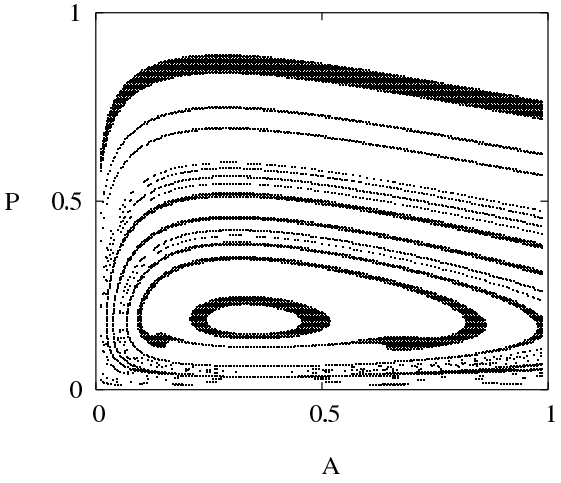

Figure 3.3: Basins of attraction for the exploitative competition (EC) model (T7)–(T9). Black indicates initial values for which the corresponding solution approaches the chaotic attractor. White indicates initial values for which the periodic attractor is approached. Parameters: $r = 1, a_1 = 5, a_2 = 1, h = 1/7, m_1 = 1.7, m_2 = 0.6, \varepsilon_1 = \varepsilon_2 = 1$.

attractor is periodic and the other one is chaotic. Even though only a two-dimensional transect has been explored and the resolution of the scan is not high enough to reproduce all details of the basin boundaries, the intricate structure of the basins of attraction is nevertheless visible. The basins of attraction seem to be made up of interleaved circular regions on the plane. This gives a hint of the three-dimensional structure of the basins, which might look like nested tubes.

Returning to the bifurcation scenario itself, a closer look reveals that there are some discontinuities in the attractors. Such sudden qualitative changes in the shape of a chaotic attractor as a parameter is varied are called attractor crises. Figure 3.2 suggests that there are two types of crises, namely a boundary crisis and an interior crisis. The former is associated with the destruction, or creation, of a chaotic attractor. The latter causes changes in the size of the attractor, for example the blow-up of an attractor, so that it suddenly occupies a larger region in phase space (Grebogi et al., 1983).

The consequences of attractor crises are illustrated in Figure 3.4. First, the sudden loss of a chaotic attractor due to a boundary crises is associated with transient chaotic dynamics. That is, time series starting from initial values formerly in the basin of attraction of the chaotic attractor show a chaotic transient before eventually approaching the remaining periodic attractor (Figure 3.4). Second, interior crises lead to irregular spikes of significantly higher population sizes. This can also be seen in the time series of population sizes (Figure 3.4). These spikes correspond to infrequent visits of the chaotic trajectory to regions of the phase space, which did not belong to the attractor before the crisis. These regions are sometimes called the halo of the attractor, and for decreasing half-saturation constant h the trajectory spends more and more time in the halo.

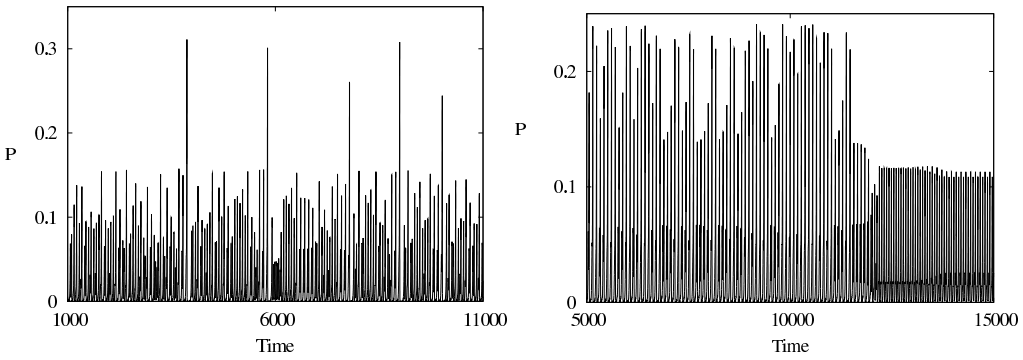

Figure 3.4: Sample time plots in the vicinity of the attractor crises of the eco-epidemiological IGP model. Left: Transient chaos close to the boundary crisis ($h = 0.0284$). The solution starts close to the formerly existing chaotic attractor but eventually settles on a periodic cycle. Right: Irregular spikes of unusually high population densities occur after the interior crisis of the chaotic attractor ($h = 0.0222$). These correspond to a blow-up of the attractor in phase space. Other parameter values as in Figure 3.2.

3.5 From intraguild predation to food chains

In the previous sections, we transformed a module of IGP into exploitative competition. This rested on the assumption that both the basal prey and IG prey are similar from the IG predator's point of view. In the case that the IG predator and the IG prey are similar from the basal prey's point of view, the IGP module may be transformed into a food chain. Here we give an example of this by using a special case of a model of intraguild predation suggested by Tanabe and Namba (2005) as our starting point. By transforming variables to total predator population and the ratio of IG predator to IG prey we arrive at a module structure corresponding to a food chain.

We start with the following IGP model studied by Tanabe and Namba (2005), where A, B, and P are the basal prey, IG prey and IG predator, respectively:

$$\frac{\mathrm{d}A}{\mathrm{d}t} = \underbrace{r(1-A)A}_{\text{logistic growth}} \quad \underbrace{-aAP}_{\text{predation by } P} \quad \underbrace{-aAB,}_{\text{predation by } B} \tag{3.9}$$

$$\frac{\mathrm{d}B}{\mathrm{d}t} = \underbrace{\varepsilon aAB}_{\text{consumption of } A} \quad \underbrace{-\lambda BP}_{\text{predation by } P} \quad \underbrace{-m_B B,}_{\text{natural mortality}} \tag{3.10}$$

$$\frac{\mathrm{d}P}{\mathrm{d}t} = \underbrace{\varepsilon aAP}_{\text{consumption of } A} \quad \underbrace{+\delta\lambda PB}_{\text{consumption of } B} \quad \underbrace{-m_P P.}_{\text{natural mortality}} \tag{3.11}$$

Note that the two predators have equal preferences for and attack rates of the basal prey. This

satisfies the condition of indiscriminate predation and yields a special case of the original Tanabe–Namba model ($a_{12} = a_{13}$ and $a_{21} = a_{31}$ in their formulation). Introducing the total predator population $C = P + B$ and the ratio $i = P/B$ of IG predator to IG prey leads to

$$\frac{\mathrm{d}A}{\mathrm{d}t} = \underbrace{r(1-A)A}_{\text{prey growth}} \quad \underbrace{-aCA,}_{\text{predation by C}} \tag{3.12}$$

$$\frac{\mathrm{d}C}{\mathrm{d}t} = \underbrace{\varepsilon aAC}_{\text{consumption of A}} \quad \underbrace{-\frac{(1-\delta)\lambda C + m_P}{1+i} Ci}_{\text{loss due to } i} \quad \underbrace{-\frac{m_B}{1+i} C,}_{\text{mortality}} \tag{3.13}$$

$$\frac{\mathrm{d}i}{\mathrm{d}t} = \underbrace{\frac{(\delta+i)}{1+i} iC}_{\text{gain from } C} \quad \underbrace{-(m_P - m_B)\, i.}_{\text{mortality}} \tag{3.14}$$

This is a food chain $A \to C \to i$. While C is a linear predator on A, the biomass flow from C to i is a bit more complicated. For $\delta = 1$ (perfect conversion efficiency), the "top-predator" i is linear in (3.14) and nonlinear in (3.13), yielding again a linear nullcline structure. This assumption would apply to the case of P and B being diseased and healthy predators, respectively.

In this model, coexistence of all three species is possible on a stable equilibrium. For some parameter ranges, we found numerical evidence of bistability (stable coexistence vs. extinction of one species and oscillations in the remainder two populations). However, we could not find chaotic dynamics that has been reported in Tanabe and Namba (2005) and is also known to occur in tri-trophic food chains with nonlinear predators (Hastings and Powell, 1991). This may be due to the fact that we are considering the special case of non-discriminating predators.

While this example originally stems from classical predator–prey ecology, it may also be interpreted as an eco-epidemiological model describing the spread of a vertically as well as horizontally transmitted disease in the predator population. In this interpretation the IG prey represents the susceptible predator subpopulation and the IG predator the infected subpopulation, with the attack rate of the IG predator corresponding to the transmissibility of the disease and assuming a perfect conversion efficiency. Underlying this interpretation is the assumption that the disease does not significantly alter the predation or consumption behavior of infected individuals, thus only manipulating the mortality rate of the infected subpopulation.

3.6 Discussion

Food webs and their basic modules are fundamental in our understanding of ecosystems and their stability (McCann, 2000). The results presented here suggest a new perspective on the structure and topology of foodwebs. Modules that were previously thought of as IGP may be equivalent to apparently simpler units. IGP could effectively be exploitative competition or a tri-trophic food chain "in disguise".

The equivalence of these modules depends critically on two assumptions that can be described shortly as indiscriminate predation. First, the consumer does not discriminate between its two resources. Second, the two resources are energetically equivalent for the consumer. In other words, even though one resource species predates the other one, they are quite similar—at least from the consumer's point of view. Note that this is not to be confused with a general similarity which would suggest to lump the species together. We actually need to keep track of their ratio because the two species function differently. Instead of the ratio, however, one can alternatively use the notion of prevalence, which is particularly apt in epizootic contexts.

Eco-epidemiological systems constitute prominent examples, since infection with a disease does not always alter predation preferences. For instance, this is believed to hold for the grazing of virally infected phytoplankton by zooplankton (Suttle, 2005; Hilker and Malchow, 2006). However, if parasites manipulate their host to induce discriminate predation (e.g. Lefèvre et al., 2009), then the transformation of food web modules presented here is not possible. Nevertheless, it should be noted that the results of this paper are not limited to non-manipulating parasites; the critical conditions are rather general and likely to apply to other IGP structures as well, which involve top-predators, parasitoids, hyper-infections, and size-structured cannibalism when large adult predators do not discriminate between small conspecifics and the shared basal prey.

When does an IGP module transform into exploitative competition and when into a food chain? In simple words, infection of the prey leads to exploitative competition, whereas infection of the predator leads to a tritrophic food chain. In the former case, we subsume the basal and IG prey. In the latter case, we subsume the IG prey and predator. There is one combination left, namely combining the IG predator and the basal prey. Doing so leaves the position of the IG prey in the food web essentially unchanged; it still retains its distinct feature of being both a resource (to the IG predator) and a consumer (of the basal prey). In particular, such a coordinate transformation does not lead to the module of apparent competition, the only trophic module that does not appear within these transformations.

behavior	biological meaning	EC model		IGP model
cyclic coexistence	community persistence regular oscillations	Armstrong and McGehee (1980)		Hilker and Malchow (2006)
asynchronous transients	asynchronous oscillations, which may prevail depending on initial conditions	Abrams et al. (2003)		Hilker and Malchow (2006)
chaos	irregular fluctuations long-term unpredictability	Abrams et al. (2003)	$\longrightarrow$	this paper
coexistence of periodic attractors	cycle amplitudes and frequency depend on initial conditions	Abrams et al. (2003)	$\longrightarrow$	this paper
coexistence with a chaotic attractor	oscillations may be regular or irregular depending on initial conditions	this paper	$\longleftarrow$	this paper
boundary crisis	sudden population crashes transient chaos	this paper	$\longleftarrow$	this paper
interior crisis	irregular spikes corresponding to population outbreaks	this paper	$\longleftarrow$	this paper

Table 3.2: Types of dynamical behavior in the exploitative competition (EC) and intraguild predation (IGP) modules. The arrows indicate the direction of cross-fertilization; i.e. the knowledge existing for one community module can be transferred to another community module.

This is noteworthy as many studies addressing parasites shared by multiple host species concern apparent competition phenomena (Hatcher et al., 2006; Lefèvre et al., 2009).

The equivalence of food web modules can be fruitfully utilized to find analogies in community dynamics and stability. We have transferred the knowledge stemming from a well-known and long-investigated exploitative competition (EC) model (Armstrong and McGehee, 1980; Abrams et al., 2003) to a recent eco-epidemiological model exhibiting IGP structure. Furthermore, we found a whole suite of dynamical behavior in the eco-epidemiological model that has, to our knowledge, not been reported before in any IGP structure (Table 3.2). We have also shown that all these types of behavior may arise in the classical EC model as well. The dynamics in both the IGP and EC are remarkably similar (cf. Figure 3.2).

For instance, both the IGP and EC model can be bistable and have coexisting attractors, one of them possibly being chaotic. The noise inherent in the environment and typical for nature can repeatedly trigger a population to jump from a low-abundance to a high-abundance state. Dwyer et al. (2004) find this mechanism to be instrumental in explaining episodic outbreaks of forest-defoliating insects such as the gypsy moth (*Lymantria dispar*) which occur at long, but irregular intervals. Interestingly, both pathogens and predators seem to be key in understanding these outbreaks.

Coexisting attractors and associated boundary crises have also been found in a stage-structured model of flour beetle (*Triboleum castaneum*) population dynamics (Cushing et al., 2003). McCann and Yodzis (1994) point out how boundary crises can be responsible for unexpected population crashes. The equivalence of food web strucure implies that IGP models are prone to such sudden extinctions of species as well—even though this may not be readily anticipated from the model formulation.

Parasitism is the most common consumer strategy (Price, 1980; de Meeûs and Renaud, 2002) and increasingly recognized to dominate food webs (Lafferty et al., 2006, 2008). The presence of parasites typically renders predator–prey interactions into intraguild predation modules (Borer et al., 2007). In this paper, we have shown that these seemingly more complicated modules can be equivalent to exploitative competition or food chains. That is, the omnivory link typical for IGP appears to be redundant when a pair of interacting species is relatively similar to their consumer or their shared resource.

This redundant link may well alter topological statistics of food webs. Parasites remain difficult to be incorporated into food web models, even though their importance is acknowledged in recent findings. Food webs can contain more host–parasite than predator–prey links (Lafferty et al., 2006) and parasite biomass can exceed that of top predators (Kuris et al., 2008). This ubiquity of parasites underlines the need of a holistic food web theory.

The results presented in this paper highlight the potential impact of parasites (and other consumers) and opens avenues to a better understanding of their dynamical behavior.

4 The impact of environmental fluctuations on travelling waves and chaos

4.1 Preliminaries: Reaction-diffusion equations

Mathematical models for spatially homogeneous processes with their potential steady-state multiplicity and complicated temporal dynamics are the cornerstone of ecological modelling. But only taking into account the spatial dimension of species growth, interaction, locomotion and transport yields the full diversity of population dynamics. The possible spatiotemporal dynamics include amongst others stationary and dynamic patchy patterns, regular and irregular oscillations, propagating fronts, target patterns and spiral waves.

Historically, the maybe best-known examples for spatiotemporal patterns come from physics and physical chemistry, cf. the Bénard convection cells (Bénard, 1900) and the waves in the Belousov-Zhabotinskii reaction (Belousov, 1958). Similar patterns have been found in biological and in particular population-dynamical systems, like the bioconvection of upswimming microorganisms (Hill and Pedley, 2005), travelling waves in cyclic populations (Sherratt and Smith, 2008), the wavy dynamics of amoeba (Gerisch, 1968) and striped vegetation patterns (White, 1971), cf. Figure 4.1.

Partial differential equations are one way to incorporate the spatial dimension in models of biological dynamics, and as such they are related to coupled map lattices and cellular automata. Often these equations have the form of reaction-diffusion models, especially if individuals are assumed to perform a random walk, similar to small particles in a fluid whose molecules are in constant thermal motion. These models can also be used to describe directed motion in the form of advection and even random environmental fluctuations. This section gives an overview of some basic models and the already interesting range of patterns they may generate, before turning to the question of how robust some of these spatiotemporal patterns are with respect to random environmental fluctuations.

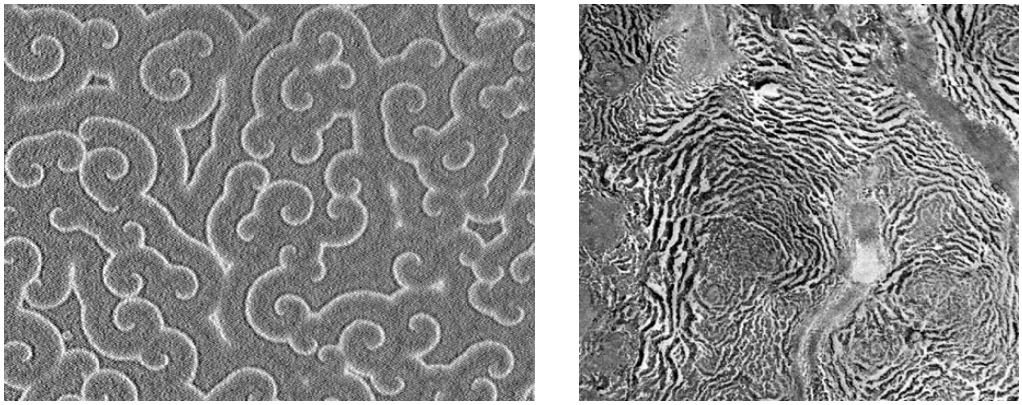

Figure 4.1: Left: Spirals in an amoeba population (*Dictyostelium discoideum*). The base line of the photo is about 28.9 mm. Courtesy of Christiane Hilgardt and Stefan C. Müller, University of Magdeburg. Right: Satellite image of tiger bush in Niger, the darker lines of woodland are on average about 20 to 40 m wide and 50 to 100 m apart. Courtesy of the U.S. Geological Survey.

4.1.1 Spatial dynamics of single-population models

The case of a population homogeneously distributed across its habitat has already been discussed in Chapter 1 and in this case the rate of change of the population density is given by the general ordinary differential equation (1.5).

Now, for a population that is inhomogeneously distributed across its habitat, the population density $u(t, \mathbf{x})$ changes not only over time t, but also with spatial location $\mathbf{x} \in D$. In biological scenarios, the domain or habitat D will usually be some bounded subset of three dimensional space. In this case, $\mathbf{x} = (x, y, z)$ usually denotes the cartesian coordinates of a point in that domain. For simplicitly, let us first consider only spatially one-dimensional domains.

If it is assumed that the motion of individuals on this domain D can be approximated by a random walk, the rate of change is described by the reaction-diffusion equation

$$\frac{\partial u}{\partial t} = f(u, x) + D \frac{\partial^2 u}{\partial x^2}. \tag{4.1}$$

As in the non-spatial case described in Chapter 1, the per-capita growth term f describes the species growth, which now additionally may depend on the spatial location x to reflect spatial heterogeneities of the environment. To shorten notation, the independent variable x is usually omitted in the following. The second term now describes the species dispersal, usu-

ally down its own spatial density gradient. The diffusion coefficient D reflects how motile the individuals of the population are. The fact that the population density now depends on two independent variables is reflected by the partial derivatives in (4.1), one with respect to time t and the other of second order with respect to the spatial variable x. A solution to this equation is a real-valued function u, whose partial derivatives satisfy (4.1) and which has a given initial population distribution $u(0,x) = u_0(x)$. If the spatial domain is bounded with boundary δ, the solution additionally needs to fulfill suitable boundary conditions. An important special case are the so called no-flux boundary conditions, given by

$$\frac{\partial u(t,x)}{\partial n} = 0$$

for all points $x \in \delta$. Here, the partial derivative is with respect to the outward pointing normal vector perpendicular to the boundary. This boundary condition simply reflects the assumption that no individual leaves or enters the domain through the boundary, i.e. because the population is physically confined to a certain habitat or the habitat is surrounded by hostile environment. Firstly we will now briefly describe which spatiotemporal patterns the basic growth models introduced in Chapter 1 may exhibit. Note, that we assume no-flux boundary conditions for all examples.

Recall that for exponential growth of a single population the per-capita growth term takes the form

$$f(u) = (b-d)\,u\,. \tag{4.2}$$

The intrinsic per capita growth rate $r = (b-d)$ is the only parameter. For $r > 0$, the population will grow explosively to arbitrary high values at every location x. If the initial population distribution is a localized patch this gives rise to a spatiotemporal wave moving outward from the initial patch. It has been proved by Luther (1906) that the speed v_F of this front of population spread is

$$v_F = 2\sqrt{rD}\,. \tag{4.3}$$

As has been pointed out in Chapter 1 unlimited growth as predicted by (4.2) is usually never observed in nature. However, the speed of the wave front obtained from this model is met again in the more realistic setting of logistic growth.

The introduction of a carrying capacity K yields a growth saturation at high population densities, effectively limiting the population to a maximal density at every point of the

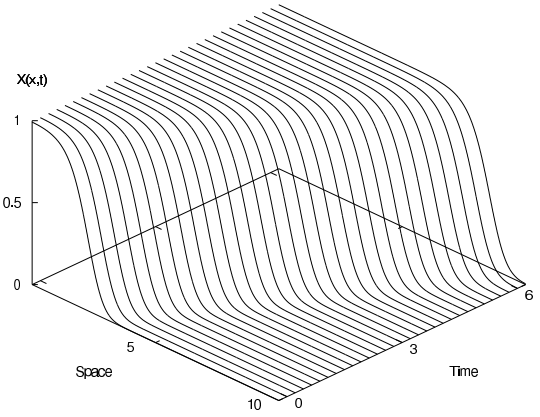

Figure 4.2: Spatial propagation of a logistically growing population for $r = 3$, $K = 1$, $D = 10^{-1}$, all parameters given in arbitrary units (a.u.), no-flux boundary conditions.

habitat. The logistic model in formulation (1.4) reads

$$f(u) = r\left(1 - \frac{u}{K}\right)u \tag{4.4}$$

and at carrying capacity the intrinsic growth rate locally vanishes, that is $f(K) = 0$, and this is the only stable steady state of the system. In combination with diffusion logistic growth has first been investigated by Fisher as a model for the spread of genes in a population (Fisher, 1937) and simultaneously by Kolmogorov (Kolmogorov et al., 1937). Any initial population distribution will after a transient phase form a wave front with a minimal front speed as given by (4.3), eventually filling the whole spatial domain with the population at its local carrying capacity. An illustration for a one-dimensional domain is shown in Figure 4.2.

In addition to the growth models already introduced in Chapter 1 we will have a brief look at the somewhat more interesting spatial dynamics of another important growth model. Allee (1931) found that population growth is optimal and highest at medium population densities. In his honour this phenomenon has been termed *Allee effect* and in its stronger formulation it implies the existence of a minimal viable population size (Courchamp et al., 2008). A population with a density below this value will die out, a population with a size above that value will grow to its capacity. A purely phenomenological growth model for the Allee effect reads

$$f(u) = r\left(1 - \frac{u}{K}\right)\left(\frac{u}{K_-} - 1\right)u\,, \tag{4.5}$$

where K_- is the minimal viable population density. The system is bistable, extinction as well as capacity are stable steady states. This changes the dynamics not only locally where the initial condition determines the final steady state, but with diffusion a given initial density distribution will not necessarily grow and propagate towards the carrying capacity K

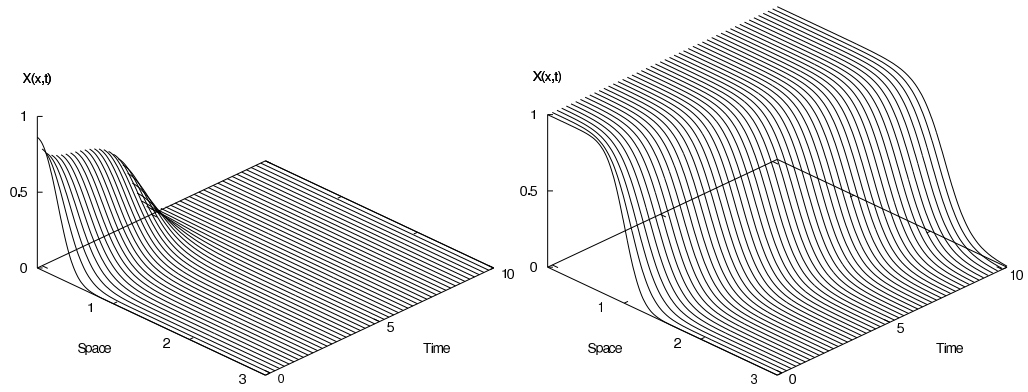

Figure 4.3: Spatial back (left) or forward (right) propagation of a population with Allee effect for an initial condition less or greater the critical radius. Parameters: $r = 3$, $K = 1$, $K_{-} = 0.4$, $D = 10^{-1}$ (a.u.), no-flux boundary conditions.

but can also break down. In this case the front moves back towards total extinction, i.e., until the population has died out everywhere. The two stable steady states introduce a critical size of the spatial extension of a population (Malchow and Schimansky-Geier, 1985). Population patches greater than the critical size will survive, while the others will go extinct. In spherically symmetric coordinates, the temporal dynamics of the radius R of a population patch is

$$\frac{dR}{dt} = 2D\left(\frac{1}{R_k} - \frac{1}{R}\right), \tag{4.6}$$

where R_k is the critical radius that has to be exceeded in order to survive even if the local density is greater than K_{-}. This is demonstrated in Figures 4.3.

The gist at this point is that one can find moving fronts in single-population systems, but in the long run the spatial population distribution on a finite domain will always be uniform.

4.1.2 Spatial dynamics of two-population models

As we have seen, growth and dispersal of a single population in a constant and homogeneous environment does not support spatial pattern formation, it merely balances out spatial differences in population density. However, spatial patterns can appear in models with at least two interacting and moving populations. Since these patterns are more striking in two spatial dimensions, we will also move on from one spatial dimension to a spatially two-dimensional model. The interaction and dispersal of both populations is then described by

the two equations

$$\frac{\partial u}{\partial t} = f_u(u,v) + D_u \nabla^2 u, \tag{4.7}$$

$$\frac{\partial v}{\partial t} = f_v(u,v) + D_v \nabla^2 v. \tag{4.8}$$

The basic structure of each equation is the same as for the single population model (4.1), but the respective growth terms $f_{u,v}$ now depend on the vector (u, v) of both populations. Also, dispersal of the populations is now possible in two dimensions, indicated by the two-dimensional Laplacian

$$\nabla^2 = \frac{\partial^2}{\partial x^2} + \frac{\partial^2}{\partial y^2},$$

which is simply the sum of the second order partial derivatives with respect to the spatial dimensions. The diffusivity or motility of the populations is given by D_1 and D_2, respectively.

A selection of stationary and dynamic patterns will be described below. All of these patterns arise from the following very important model of a prey species u, a predator v, and a constant top predator population P:

$$f_u(u,v) = r\left(1-\frac{u}{K}\right)u - \frac{a\,u}{1+b\,u}\,v, \tag{4.9}$$

$$f_v(u,v) = e\,\frac{a\,u}{1+b\,u}\,v - m\,v - \frac{g^2\,v^2}{1+h^2\,v^2}\,P. \tag{4.10}$$

Here, the prey grows logistically with growth rate r and carrying capacity K. The consumption of prey by the specialist predator v is modelled with the so-called Holling-type II functional response, which assumes a linear relation between prey density and prey consumption at low prey densities, but saturates if the prey becomes abundant. This takes into account, that there is maximum value of prey biomass that each predator can consume in a given time. This maximum value is given by a/b, the ratio of search rate a and prey handling time b. The parameter $e < 1$ is the predator's conversion efficiency and m its mortality. The constant top predator P is assumed to be a generalist, described by a Holling-type III functional response. This functional response saturates at g^2/h^2, but assumes a lower than linear consumption at low prey densities. This reflects, that the generalist predator P switches to a significant consumption of the specialist predator only when v becomes abundant.

In the case $P = 0$ where the top predator is absent model (4.9–4.10) reduces to the classical Rosenzweig-MacArthur predator-prey model (Rosenzweig and MacArthur, 1963),

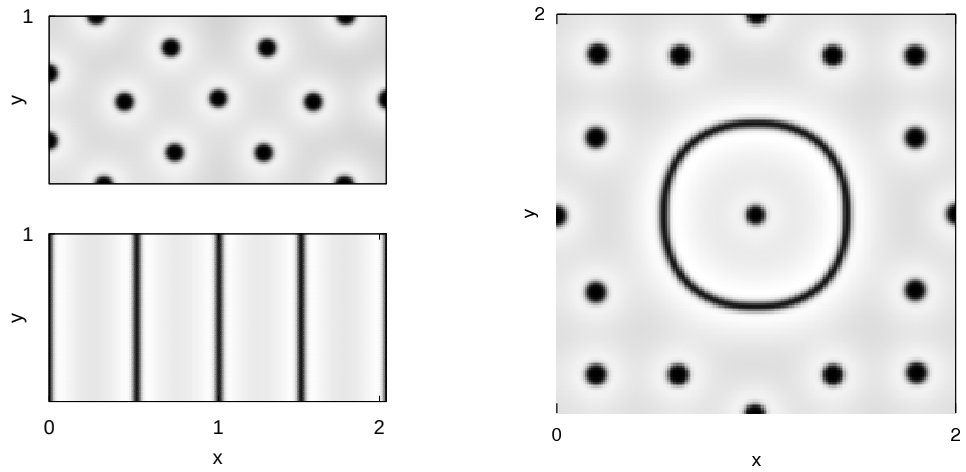

Figure 4.4: Formation of Turing patterns for different perturbations of the spatially uniform distribution of system (4.9–4.10). Parameters: $r = 5/14$, $K = 7/50$, $a = 2/3$, $b = 5/3$, $e = 3/5$, $m = 7/40$, $g^2 = 2/125$, $h^2 = 1/25$, $P = 1, D_u = 10^{-5}$, $D_v = 2 \cdot 10^{-3}$ (a.u.), no-flux boundary conditions.

which has featured prominently in the previous chapters. In this reduced model, the unique stationary point where both population densities are strictly positive can be stable or unstable. In the unstable case, the equilibrium is surrounded by a stable limit cycle, which corresponds to periodically varying population densities. As we will see, the form of the spatiotemporal patterns that can be observed in the full reaction-diffusion model greatly depends on whether the spatially homogeneous system given by (4.9–4.10) is in the parameter range of stationary or periodic dynamics.

The probably most famous spatial patterns arising from reaction-diffusion systems are the Turing patterns (Turing, 1952). These stationary patterns appear after diffusive instability of a stable spatially uniform population distribution. For them to arise the diffusion coefficients of the two species need to be sufficiently different, i.e. $D_v \gg D_u$, and the growth terms have to obey certain conditions. For two interacting species, these conditions are called activator–inhibitor Gierer and Meinhardt (1972) or destabilisator–stabilisator Segel and Jackson (1972) relations. Because of their often striking symmetry Turing had thought them as possible mechanism of forming physiological gradients in biomorphogenesis but also applications in population dynamics came early (Segel and Jackson, 1972). Three simulation results of system (4.9–4.10) for different initial conditions are shown in Figure 4.4.

In addition to stationary Turing patterns, system (4.9–4.10) also allows for dynamic spatiotemporal patterns. Therefore, assume that our sample system (4.9–4.10) is in the parameter region of limit cycle oscillations. In this case any local perturbation leads to the

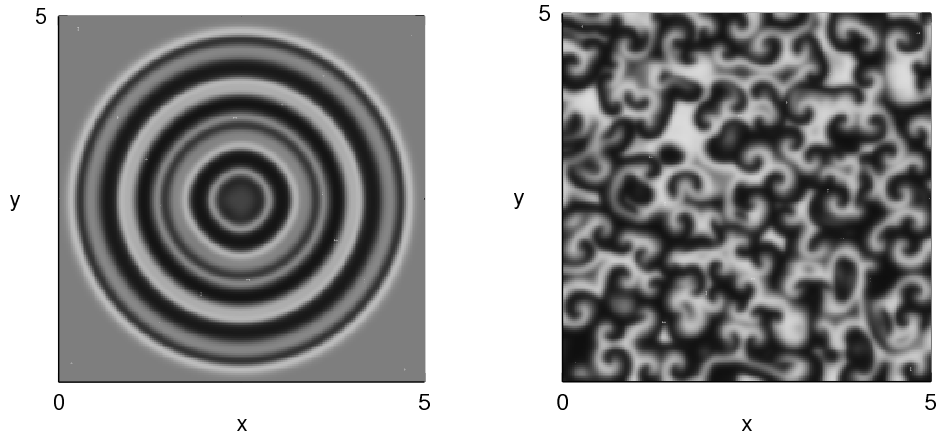

Figure 4.5: Generation of target patterns and spiral waves of system (4.9–4.10). Parameters: $r = K = 1,\ a_{=}b = 10/3,\ e = 2,\ m = 4/5,\ g = h = P = 0, D_u = D_v = 1$ (a.u.), no-flux boundary conditions.

formation of concentric waves, the so-called target patterns. A subsequent perturbation of the circular wave fronts, like a collision with an obstacle, the domain boundary or another wave, may cause the opening of these fronts and spiral waves can appear. The two corresponding patterns are shown in Figure 4.5. Closely related to this phenomenon are periodic and irregular travelling waves (see Sherratt and Smith (2008) for a review of theoretical results and field studies) and the so called "wave of chaos" (Malchow et al., 2008), which can be seen as the spatially one-dimensional analogon to the target pattern shown in Figure 4.5.

4.1.3 Heterogeneous environments

So far we have assumed that the environmental conditions relevant for species growth and interaction do not explicitly depend on the spatial position, i.e. the parameters are constant all over the spatial domain. However, it was already implied in equation (4.1) that the growth term f may explicitly depend on the spatial location $\mathbf{x}$. This allows to incorporate heterogeneous environmental conditions into the spatial model.

One effect of a heterogeneous environment in a spatially one-dimensional variant of model (4.9–4.10) has been presented by Pascual (1993), assuming a linear increase in the prey growth rate $r = r(x) = r_0 + cx$. Assuming that the system is in the oscillatory regime at all spatial locations, this leads to a line of infinitely many diffusively coupled non-identical oscillators. Following the temporal change of population density at fixed spatial locations indicates that the local dynamics undergo a transition from regular oscillations at high prey

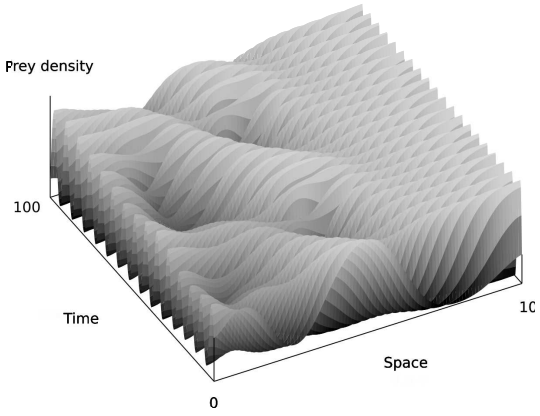

Figure 4.6: Diffusion-induced chaos in system (4.9–4.10) along a gradient in the prey growth rate. Parameters: $K = 1$, $a = b = 5$, $e = 1$, $m = 0.61$, $g = h = P = 0, D_u = D_v = 10^{-4}$ (a.u.), no-flux boundary conditions.

growth rate to quasiperiodic and finally chaotic oscillations at low prey growth rate. This is shown in Figure 4.6.

This last example shows nicely how the inclusion of space into population-dynamical models adds another level of complexity to population dynamics, namely the level of the environment, which sets the stage for all population-dynamical processes. However, although in this case the environment is assumed to be heterogeneous in space it is still fixed in time, i.e. there are no temporal changes in the local environmental conditions. The remainder of this chapter is devoted to investigate the impact of such environmental fluctuations on spatiotemporal patterns such as the waves shown in Figure 4.5.

4.2 Random environmental fluctuations

Noise is an important component in the modelling of population dynamics, since natural populations are inevitably subject to internal demographic and external environmental fluctuations. Thus, in order to be applicable to real world ecosystems the results obtained from reaction-diffusion systems must be robust with respect to noisy perturbations induced by the environment. In the context of ecological modelling, this environmental stochasticity subsumes all processes, that are not represented in the model, but for which an impact on the system dynamics can not be ruled out. This could be the case for processes, that are too poorly understood to allow for explicit description and/or for processes that are overly complex. Examples of such processes are rapidly changing atmospheric conditions such as temperature, humidity, precipitation or wind stress; other species that interact with the modeled species; the availibility of basic resources; the movement and salinity of the surrounding water column for aquatic species; intensity of light irradation for photosynthetic species; features of the habitat landscape.

Roughly speaking, there a three pathways over which such perturbations may influence a reaction-diffusion system. Firstly, there is purely spatial variation, reflecting a heterogeneous but fixed impact of landscape features on system dynamics. An example of this was described in Section 4.1.3. Secondly, there are purely temporal fluctuations. The most prominent of this type clearly is the periodic forcing imposed by the annual succession of the seasons. There are numerous models incorporating a periodic forcing of some kind to account for this type of large scale fluctuation, a specific example for oscillatory reaction-diffusion equations is the work by Webb and Sherratt (2003). However, especially on smaller scales there are many processes, that can not be represented by a periodic forcing and when many of such processes come together, one can truly speak of erratic fluctuations or noise forcing the system. The combination of the two mentioned pathways leads to spatiotemporal noise, that is, fluctuations both in time and space. It depends on the scale of the problem at hand to decide, which pathway may play a crucial role in the dynamics of the underlying system and which fluctuations may be neglected.

Among the more obvious effects of such random fluctuations in models of population dynamics is that noise blurs unrealistic distinct and symmetric spatial and spatiotemporal patterns, such as the concentric target patterns shown in Figure 4.5. In some cases, however, noise may induce transitions, sometimes catastrophic shifts, between different dynamical regimes of the model. Examples of such shifts include noise-triggered and -influenced transitions in bi- and multistable systems Ebeling and Schimansky-Geier (1979); Malchow and Schimansky-Geier (1985); Scheffer and Carpenter (2003); D'Odorico et al. (2005); Guttal and Jayaprakashh (2007); Serizawa et al. (2009), sustained oscillations in otherwise stationary systems, which may give rise to regular spatiotemporal patterns Aparicio and Solari (2001); Lindner et al. (2004); Sieber et al. (2007); Kuske et al. (2007) and the suppression of periodic travelling waves in oscillatory reaction–diffusion systems Sieber et al. (2010).

Now, there are several examples, where the introduction of noise into an ecological model via one of the abovementioned pathways may lead to a considerable shift in system dynamics, rather than just blurring the underlying deterministic dynamics. Examples of such shifts include noise-triggered and -influenced transitions between alternative stable states (Scheffer and Carpenter, 2003; van Nes and Scheffer, 2005; D'Odorico et al., 2005; Guttal and Jayaprakashh, 2007; Serizawa et al., 2009), sustained oscillations in an otherwise stationary system, which may give rise to regular spatiotemporal patterns (Aparicio and Solari, 2001; Sieber et al., 2007; Kuske et al., 2007), the survival of species that would go extinct in a deterministic environment (Malchow et al., 2005), and the persistence of periodic travelling waves in situations, where they would otherwise die out to spatially homogeneous

oscillations (Kay and Sherratt, 2000).

In the remainder of this chapter we will investigate the impact of purely temporal noise on the propagation of travelling waves and irregular oscillations in reaction-diffusion models. It will be demonstrated that periodic travelling waves are very susceptible to small erratic fluctuations and that they are replaced by spatially homogeneous oscillations in the presence of noise. Irregular spatiotemporal oscillations on the other hand prove to be more robust against the noise. We begin by introducing a general stochastic reaction-diffusion model in Section 4.3 and define some basic notation. In Section 4.4.1, we present numerical simulations for a particular predator-prey model, indicating, that a significant shift in spatiotemporal dynamics occurs under stochastic forcing. This example is used to motivate the use of a more generic oscillatory reaction-diffusion system in Section 4.4.2. Here, the effects are reproduced and investigated in more detail. The last section discusses the ecological and theoretical implications of the results.

4.3 Noise in reaction-diffusion systems

A general model for the interaction and dispersal of two species subject to noise is given by the two coupled stochastic reaction-diffusion equations

$$\frac{\partial u}{\partial t} = f_u(u,v) + g_u(u,v)\,\xi_t + D\,\frac{\partial^2 u}{\partial x^2}, \tag{4.11}$$

$$\frac{\partial v}{\partial t} = f_v(u,v) + g_v(u,v)\,\xi_t + D\,\frac{\partial^2 v}{\partial x^2}. \tag{4.12}$$

Here $u = u(t,x)$ and $v = v(t,x)$ denote the densities of the species at time t and spatial location $x \in [0,L]$ on a spatially one-dimensional domain of length L. The spatially homogeneous diffusion coefficient D is assumed to be the same for both species. The two-dimensional vectorfield $F(u,v) = (f_u(u,v), f_v(u,v))$, which is assumed not to depend on time nor space, forms the deterministic skeleton of the model. For our purpose, the skeleton will be required to contain a unique stable limit cycle, giving rise to oscillatory reaction kinetics. In the following, we will restrict our attention to Dirichlet boundary conditions $u = v = 0$ at $x = 0$ and $x = L$. In an ecological context, these boundary conditions reflect the assumption, that the regions $x < 0$ and $x > L$ are hostile. As has been pointed out in the introduction, this scenario is known to give rise to periodic travelling waves.

Noise is introduced into the model via the real-valued stochastic process ξ_t and the coupling functions $g_u(u,v)$ and $g_v(u,v)$. The stochastic process ξ_t is essentially a family of

real-valued random variables and for any fixed point in time, ξ_t is a usual random variable mapping elements of some sample space Ω to real numbers. The sample space Ω can be viewed as the product of state spaces of any intrinsic or environmental process, which is not explicitly modeled by the reaction kinetics. Examples of such processes have been given in the introduction. These processes can be assumed to possess long-term mean values, and the parameters in the deterministic skeleton will usually reflect this assumed mean value. However, to account for the inevitable fluctuations around this mean, we will assume, that the noise process ξ_t has a joint normal distribution with zero mean and unit variance, which does not change with time. Further, we require that the elements of this stationary noise process ξ_t at different times are uncorrelated. This gives rise to the autocorrelation function

$$C(h) = Cov(\xi_t, \xi_{t+h}) = \begin{cases} 0 & \text{if h} \neq 0 \\ \infty & \text{if h=0} \end{cases}$$

or alternatively $C(h) = \delta(h)$, where δ is the Dirac delta function. A stochastic process fulfilling these requirements is commonly known as Gaussian white noise. By introducing the white noise process ξ_t into the reaction-diffusion model (4.11–4.12), the solution to this model will also be a stochastic process. Due to the nature of the white noise ξ_t, equations (4.11–4.12) should merely be viewed as a more familiar abbrevation for the integral form of the underlying stochastic model (Walsh, 1986).

There are three assumptions underlying the specific form of the noise process, which may need some clarification. Firstly, most of the mentioned environmental processes subsumed in the noise process are continuous functions of time and thus, in fact, autocorrelated at least on very small time scales. However, white noise has been widely used as an approximation to such processes, if they can be assumed to fluctuate rapidly on time-scales, that are small compared to the time-scales of interaction and dispersal of the modeled species (Horsthemke and Lefever, 1984). The analysis of datasets of environmental variables indicates, that this assumption is acceptable for many terrestrial ecosystems (Steele, 1985; Vasseur and Yodzis, 2004). An implicit assumption reflected by the model is, that both species occupy the same habitat and thus experience the same noisy fluctuations. Consequently, the noise process ξ_t is the same for both species. Thirdly we assume, that the habitat is small enough, so that spatial variations of the fluctuations can be neglected. Thus, ξ_t does not depend on space, but rather is a purely temporal stochastic process. However, the length of the habitat will be chosen well above the intrinsic length of the particular system (Petrovskii et al., 2003). This ensures, that there is enough space for the spatial patterns to emerge, e.g., the

length of the habitat will be larger than several times the spatial wave length of the observed periodic travelling waves.

Before proceeding, the forms of the coupling functions $g_u(u,v)$ and $g_v(u,v)$ need to be specified. Since ultimately equations (4.11–4.12) are to describe the growth of populations, the coupling functions have to obey any conditions imposed by this modeling goal. For an isolated population surrounded by a hostile environment, which prevents immigration from outside into the habitat, a very general constraint is to require, that population growth inside of the habitat is zero if there is no population at all. For the deterministic reaction kinetics this corresponds to $f_u(0,v) = f_v(u,0) = 0$, and there is no reason to assume, that the introduction of noise renders void this postulate of parenthood (Hutchinson, 1978). Since ξ_t is almost surely non-zero for all t, this leads us to also require $g_u(0,v) = g_v(u,0) = 0$. This rules out the use of purely additive noise, where the coupling functions are essentially constants. However, the simplest coupling functions that fulfill the postulate of parenthood are homogeneous linear functions of the population densities, e.g. $g_u(u,v) = \eta\, u$ and $g_v(u,v) = \eta\, v$ with common noise strength η. This choice for the coupling functions leads to

$$\frac{\partial u}{\partial t} = f_u(u,v) + \eta\, u\, \xi_t + D\frac{\partial^2 u}{\partial x^2}, \tag{4.13}$$

$$\frac{\partial v}{\partial t} = f_v(u,v) + \eta\, v\, \xi_t + D\frac{\partial^2 v}{\partial x^2}. \tag{4.14}$$

This corresponds to multiplicative noise forcing the deterministic growth kinetics. In the next section, this general model will be used with specific oscillatory predator-prey growth kinetics.

4.4 The impact of noise on periodic travelling waves

There is growing evidence, that population densities of some species not only vary periodically over time (Turchin, 2003), but also in a specific spatial direction. In this case, the temporal and spatial oscillations may resemble a periodic travelling wave in population density (Ranta and Kaitala, 1997; Lambin et al., 1998; Bjørnstad et al., 2002; Tenow et al., 2007). While such empirical evidence for periodic travelling waves in population dynamics was lacking at that time, this form of pattern formation had already been theoretically established for oscillatory reaction-diffusion equations by Kopell and Howard (1973). Since then, mathematical models have been used to understand the mechanisms behind the generation of periodic travelling waves, at first with applications to chemical reactions

(Auchmuty and Nicolis, 1976; Kuramoto, 1984; Scott, 1994). Subsequently, periodic travelling waves gained considerable attention in theoretical population dynamics and they have been shown to exist in a variety of models. Examples are given by Shigesada et al. (1986) for a reaction-diffusion model with spatially varying diffusivity and population growth rate, Britton (1990) for an integro-differential reaction-diffusion model, Hassell et al. (1991) for a coupled map lattice and Sherratt (1996) for cellular automata.

For the case of oscillatory reaction-diffusion systems, at least two realistic ecological scenarios have been identified, which may lead to periodic travelling waves. The first one is the formation of periodic travelling waves in the wake of a predator population invading a homogeneously distributed prey species (Petrovskii et al., 1998; Petrovskii and Malchow, 2000; Sherratt, 2001). The second one is associated with suitable boundary conditions applied to the edges of the habitat, reflecting some degree of hostility of the adjacent space (Sherratt et al., 2002; Sherratt, 2003).

A key feature of periodic travelling waves in oscillatory reaction-diffusion systems is, that there is always a whole family of feasible solutions. Depending on system parameters and boundary conditions, a particular member of this solution family is selected, which can either be stable or unstable as a solution to the reaction-diffusion equations. The question of stability of periodic travelling waves has been solved only for a few special cases (Kopell and Howard, 1973; Maginu, 1981), but extensive numerical studies indicate, that whenever the selected solution is unstable, the long-term behavior of the system dynamics consists of irregular spatiotemporal oscillations (Sherratt, 1995; Petrovskii and Malchow, 1999; Petrovskii and Malchow, 2001). For a comprehensive review of periodic travelling waves in field studies and reaction-diffusion systems, see Sherratt and Smith (2008).

4.4.1 A predator-prey system

Predator-prey models in the form of ordinary differential equations have been studied extensively over a period of almost a century in order to explain cyclic population dynamics. A vast number of models possessing a stable limit cycle have been proposed and as a consequence, there are numerous choices for the reaction kinetics. In order to motivate the use of more general cyclic kinetics, in this section we will restrict our attention to the classic Rosenzweig-MacArthur model (Rosenzweig and MacArthur, 1963). Under very general conditions, this model possesses a unique stable limit cycle and it has been shown to generate travelling waves and spatiotemporal chaos when extended to a reaction-diffusion system (Petrovskii and Malchow, 2001; Sherratt and Smith, 2008). Using it as the deterministic

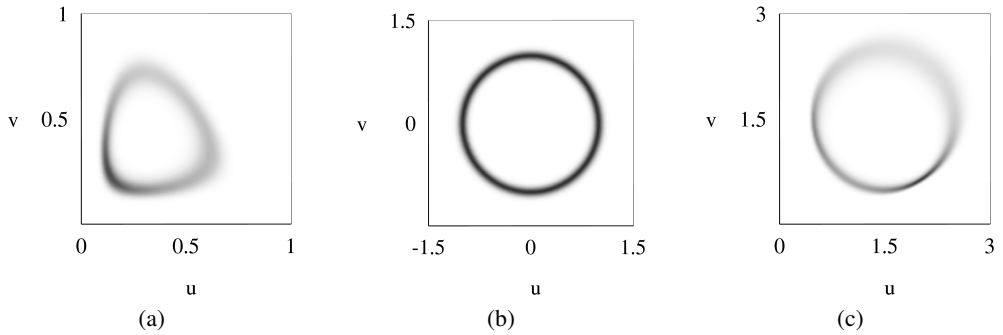

Figure 4.7: (a) Stationary probability distribution for the predator-prey system (4.15–4.16) with $\eta = 0.025$. Darker indicates higher probability. Stationary probability distribution for the $\lambda - \omega$ system (4.20–4.21) centered on the origin (b) and centered on $(1.5, 1.5)$ (c). Noise strength is $\eta = 0.1$ in both cases.

skeleton in equations (4.13–4.14) yields the full stochastic reaction-diffusion model

$$\frac{\partial u}{\partial t} = \left(r(1-u) - \frac{a\,v}{1+h\,u} + \eta\,\xi_t \right) u + D\,\frac{\partial^2 u}{\partial x^2}, \tag{4.15}$$

$$\frac{\partial v}{\partial t} = \left(\varepsilon\,\frac{a\,u}{1+h\,u} - m + \eta\,\xi_t \right) v + D\,\frac{\partial^2 v}{\partial x^2}. \tag{4.16}$$

Here, the prey population u grows logistically with intrinsic rate of growth r and a carrying capacity, which is scaled to unity in the above formulation. Predation follows a monod type functional response (Holling, 1959) with predation rate a and handling time h, which is characteristic for specialist predators preying on a single prey species. The numercial response of the predator v is scaled by the efficiency parameter ε and predators die with mortality rate m. The domain length will be fixed to $L = 20$ together with a diffusion coefficient of $D = 10^{-3}$. A typical parameter set yielding oscillatory behavior of the reaction-kinetics, which will be used from now on, is

$$r = 1, a = 10/3, h = 10/3, \varepsilon = 2, m = 1. \tag{4.17}$$

Note, that for this set of parameters and the chosen diffusion coefficient the intrinsic length of the system is about $\frac{\pi}{2}$ and the habitat length is chosen well above this value.

As has been mentioned in the previous section, the solution to the stochastic system (4.15–4.16) is a stochastic process. Starting from a given initial condition, a particular stochastic trajectory through phase space is realized and these sample paths or realizations of the solution process are amenable to numerical approximation. The numerical

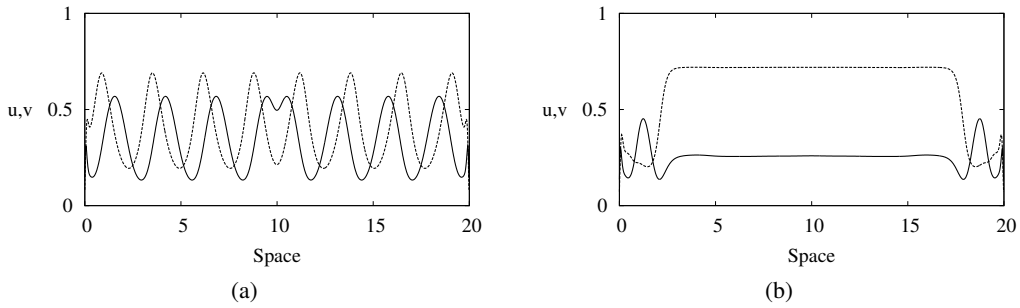

Figure 4.8: Snapshots of realizations of model (4.15–4.16), showing the spatial profile of prey u (solid) and predator v (dashed) densities. Periodic travelling waves for $\eta = 0$ at $t = 24500$ (a), which are suppressed to spatially homogeneous oscillations at $t = 28500$ (b), after noise intensity has been set to $\eta = 0.025$ at $t = 25000$. Note the disturbances at the boundaries, which are due to the Dirichlet boundary conditions.

data presented below is obtained by calculating particular realizations using the Euler-Maruyama method (Kloeden and Platen, 1999) for the stochastic reaction kinetics and a Crank-Nicolson scheme for diffusion. The temporal step size is $\Delta t = 10^{-3}$ and spatial step size is $\Delta x = 2 \cdot 10^{-2}$.

Before proceeding to the spatial dynamics, fig. 4.7a shows the stationary probability distribution for the reaction kinetics of equations (4.15–4.16) with parameters (4.17) and noise strength $\eta = 0.025$, obtained by averaging over many sample paths. The stable limit cycle appears smeared out in phase space, as would be expected for a system subject to stochastic forcing. However, the overall shape clearly resembles the deterministic orbit and in the following, care has been taken to ensure, that the noise strength η is low enough so that the oscillatory behavior of the local kinectics is qualitatively unaffected.

Turning to the full reaction-diffusion model, we start with a homogeneous distribution of the predator and prey populations and without stochastic forcing, that is $\eta = 0$. Without any perturbation, this homogeneous distribution would persist indefinitely. However, the fixed boundary conditions at both ends of the domain provide the necessary perturbations, from both of which a periodic travelling wave spreads across the entire domain. In fig. 4.8a a snapshot of the population densities is shown, after the periodic travelling wave occupies the whole domain. After this solution has settled, noisy perturbations are applied to the system by setting the noise strength η to some positive non-zero value. For very small values of η, the system dynamics does not change qualitatively. If the noise strength exceeds some critical value however, a significant shift in the system dynamics can be observed. Over the course of several time steps, the periodic travelling wave is gradually suppressed and

replaced by spatially homogeneous oscillations. A snapshot of the spatial profile after noise has been set to $\eta = 0.025$ is shown in fig. 4.8b. Disturbances of the otherwise spatially homogeneous profile are visible at the edges of the domain, which are due to the Dirichlet boundary conditions. For this noise strength the local dynamics is clearly still oscillatory as shown in fig. 4.7a and far away from the boundary the homogeneous oscillations correspond to the local limit cycle oscillations.

An example of the entire process of noise induced suppression of the periodic travelling wave is shown in fig. 4.9a for the same noise strength $\eta = 0.025$. When the noise is switched off again, the periodic travelling wave again starts to spread from the boundaries to eventually reoccupy the whole domain. In fact, even for non-zero noise intensities the local disturbances at the boundaries from time to time tend to spread from the edges before eventually being suppressed again by the noise. These intermittent break-ups of the spatially homogeneous oscillations are more frequent for lower noise intensities and their impact on regions far away from the boundaries is limited. This nevertheless shows, that the noise-induced suppression of the periodic travelling wave is an unstable system state, which crucially depends on the presence and the strength of the stochastic forcing.

The next section investigates this suppression of travelling waves in more detail and it will be shown, that it does not depend on the particular form of the oscillatory reaction kinetics, but rather may also be observed in a very generic setting.

4.4.2 A $\lambda - \omega$ system

Even the simplest reaction-diffusion systems of predator-prey interactions usually prove to be analytically intractable. Fortunately, in some cases one can revert to much simpler models which under certain conditions mimic the dynamical behavior of the more complicated one. In particular, there is a simpler counterpart to predator-prey models whose reaction kinetics generate population cycles via a super-critical Hopf bifurcation of an equilibrium. These are the so called $\lambda - \omega$ systems and reaction-diffusion equations based on these kinetics have the general form

$$\frac{\partial u}{\partial t} = \lambda(r)\,u - \omega(r)\,v + D\,\frac{\partial^2 u}{\partial x^2}, \tag{4.18}$$

$$\frac{\partial v}{\partial t} = \omega(r)\,u + \lambda(r)\,v + D\,\frac{\partial^2 v}{\partial x^2}, \tag{4.19}$$

with $r = \sqrt{u^2 + v^2}$. In fact, systems of $\lambda - \omega$ type arise as the normal form of any system whose reaction kinetics possess an equilibrium close to a Hopf bifurcation. Therefore, these

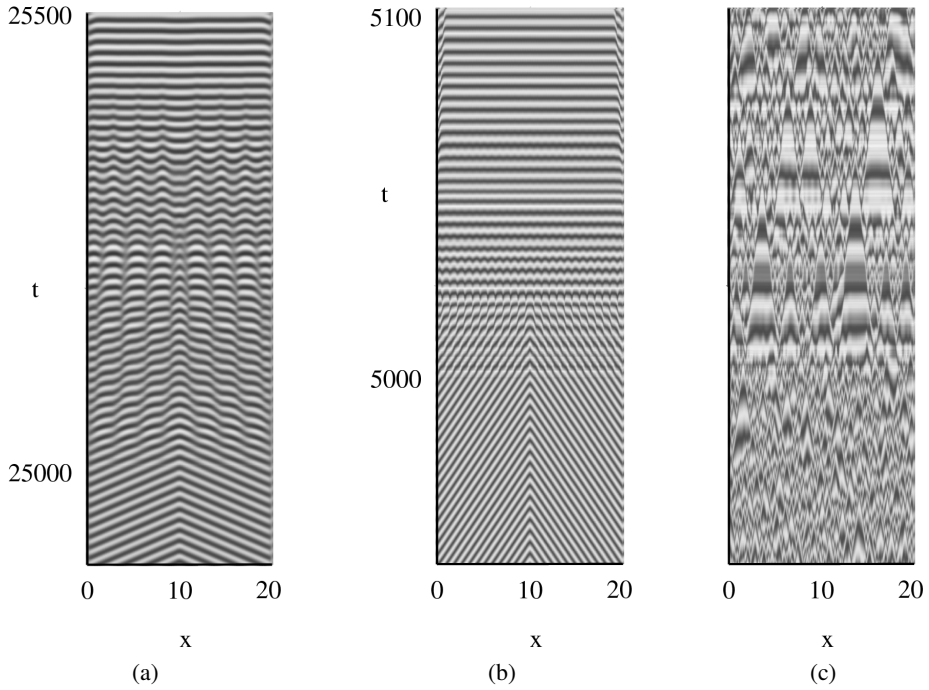

Figure 4.9: Suppression of travelling waves (a) in the predator-prey system (4.15–4.16). Noise strength is set to $\eta = 0.025$ at $t = 25000$. Suppression of travelling waves (b) and persistence of spatiotemporal chaos (c) in the $\lambda - \omega$ system (4.20–4.21). Here in both cases noise strength is set to $\eta = 0.1$ at $t = 5000$. Darker/lighter shades of gray indicate lower/higher population densities.

highly symmetric systems can be viewed as prototypical for more general oscillatory dynamics. Due to this fact and because they are amenable to analytical investigation, periodic travelling waves as solutions to equations of the form (4.18–4.19) have been studied intensively. One of the most interesting results is, that these periodic travelling waves can be stable or unstable as solutions to the reaction-diffusion equations and an analytical stability condition for the case of an infinite spatial domain has been derived by Kopell and Howard (1973). For a finite spatial domain subject to suitable boundary conditions, an equivalent stability condition is given by Sherratt (1995). In the same paper it is shown by numerical analysis, that when the periodic travelling wave is unstable, perturbations of the solution may lead to spatiotemporal chaos.

In the following, the effect of multiplicative noise on periodic travelling wave and chaotic solutions to a $\lambda - \omega$ system is investigated. We restrict our attention to a particular representative of the $\lambda - \omega$ class of reaction diffusion systems, whose stochastic equations on

the one-dimensional spatial domain $[0, L]$ read

$$\frac{\partial u}{\partial t} = (1-r^2)\,u - (3-b\,r^2)\,v + \eta\,u\,\xi_t + D\,\frac{\partial^2 u}{\partial x^2}, \tag{4.20}$$

$$\frac{\partial v}{\partial t} = (3-b\,r^2)\,u + (1-r^2)\,v + \eta\,v\,\xi_t + D\,\frac{\partial^2 v}{\partial x^2}. \tag{4.21}$$

The local kinetics of (4.20–4.21) possess a circular limit cycle with unit radius, centered at the unstable equilibrium located at the origin. This periodic solution of the reaction kinetics reads

$$u_p(t) = \cos((3-b)\,t),$$
$$v_p(t) = \sin((3-b)\,t).$$

The form of these local solutions indicates, that the parameter b determines the frequency of the local oscillation. In the deterministic reaction-diffusion system (4.20–4.21) on infinite and semi-infinite domains with $\eta = 0$, it depends on the parameter b, whether the corresponding travelling wave solution is stable or unstable (Sherratt, 1994). As will be shown below, also in the case of a finite domain subject to Dirichlet boundary conditions, b controls the observed spatiotemporal dynamics, e.g. whether the approached long-term behavior will be periodic travelling waves or spatiotemporal chaos.

Note, that we require $b \neq 3$, since otherwise the local kinetics reduce to

$$f_u(u,v) = (1-r^2)\,(u-3\,v),$$
$$f_v(u,v) = (1-r^2)\,(3\,u+v).$$

It is readily seen, that the unit circle is a continuum of non-hyperbolic equilibria, since in addition to the origin, the reaction functions then vanish at all points $r^2 = u^2 + v^2 = 1$. While spatiotemporally irregular solutions may still be observed in the reaction-diffusion system with $b = 3$ (Sherratt, 1995), the reaction kinetics in this case are clearly not oscillatory, e.g., they do not possess a limit cycle and thus, they do not mimic the oscillatory predator-prey system.

Proceeding to the stochastic dynamics, firstly we again have a look at the stationary probability distribution of the stochastic $\lambda - \omega$ kinetics. This is shown in fig. 4.7b for $b = 1$ and noise strength $\eta = 0.1$, where the distribution resembles the highly symmetric shape of the deterministic limit cycle.

For the oscillatory predator-prey system (4.15–4.16), a simple visual examination of the

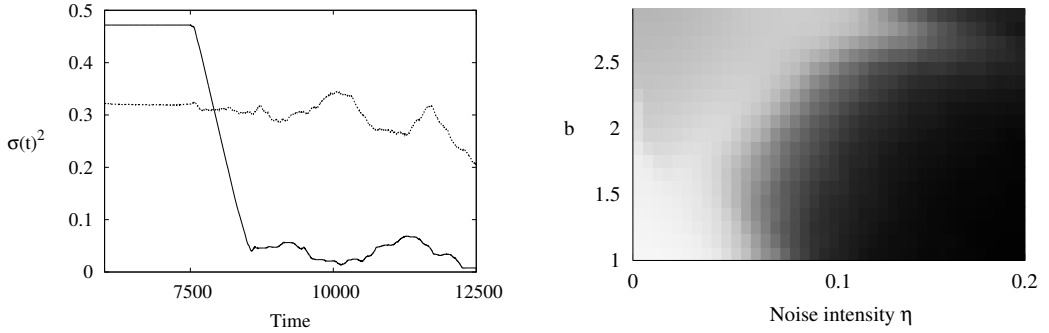

Figure 4.10: (a). Temporal evolution of the spatial variance shown for periodic travelling waves ($b = 1$, solid) and spatiotemporal chaos ($b = 2.5$, dashed), averaged over the preceding 1000 timesteps. In both cases, noise is set from zero to $\eta = 0.1$ at $t = 7500$. The sharp decline in the spatial variance in the case of travelling waves is clearly visible. In contrast, spatial variance of the chaotic solution varies around its deterministic value and does not decrease significantly. (b) Mean spatial variance of solutions for different noise strengths and different values of the parameter b averaged over 50000 timesteps. Darker means lower spatial variance, e.g. spatially more homogeneous oscillations. Note, that solutions for $b \geq 2.5$ are chaotic rather than periodic travelling waves.

solution plot has shown, that for a certain noise strength a fully developed periodic travelling wave is suppressed to spatially synchronized oscillations, except for small regions directly adjacent to the domain boundaries. To be able to quantify this effect of spatial synchronization at a fixed time t more exactly, in the following the current spatial mean value of a solution and the variation $\sigma(t)^2$ around this mean value with respect to the spatial position will be calculated. For periodic travelling waves with fixed amplitude the spatial variance is non-zero but constant over time, whereas $\sigma(t)^2 = 0$ corresponds to a perfectly homogeneous spatial distribution. Using a numerical realization, we calculate the empirical variation $\sigma(t)^2$ of all numerical mesh points on the subset $[x_0, L - x_0]$ of the domain. We will fix $x_0 = 1$ from now on, to avoid any influence of the fixed boundary conditions on the calculated spatial variance. Since there are $N = \frac{L-2x_0}{\Delta x}$ mesh points in the interval, the spatial variation of $u(t,x)$ at time t is given by

$$\sigma(t)^2 = \frac{\Delta x}{L - 2x_0 - \Delta x} \sum_{i=0}^{N-1} \left(u(t, x_0 + i\Delta x) - \overline{u(t)} \right)^2, \tag{4.22}$$

with $\overline{u(t)}$ being the current spatial mean value of u on that interval.

Now, to investigate the effect of noise on periodic travelling wave solutions, we start with

a small perturbation of the homogeneous distribution $u(0) = v(0) = 0$, and then numerically solve equations (4.20–4.21). As in the case of the predator-prey system, noise strength is kept at zero until the deterministic long-term behavior has fully developed. In the case of $b = 1$, travelling waves spread from the local perturbation until they cover the whole domain. Setting the noise strength to $\eta > 0$ at some time t shows, that this has no effect on the periodic travelling wave shape of the solution to the $\lambda - \omega$ system (4.20–4.21). Although the noisy perturbations lead to irregular temporal fluctuations of the amplitude of the waves, the qualitative form of the solution is not affected. This observation does not depend on the noise strength, as long as η is not too high and the limit cycle of the noisy local kinetics can still be clearly identified.

Apparently the stochastic shift in system dynamics observed in the predator-prey system can not be reproduced in the simpler $\lambda - \omega$ system (4.20–4.21). However, clearly there is a profound difference between the stochastic limit cycle of the $\lambda - \omega$ system and its predator-prey counterpart. The $\lambda - \omega$ system is radially symmetric around the origin and so are the multiplicative coupling functions. As a consequence, the effective noise strength of the stochastic forcing does not change along the limit cycle. Since the predator-prey system is neither radially symmetric around the non-trivial equilibrium nor centered at the origin, the situation is obviously not so simple in this system. Here the effective noise strength depends on the current position on the limit cycle, in general being higher further away from the origin and smaller when population densities are small.

Luckily, a similar situation can easily be mimicked in the $\lambda - \omega$ system by applying a simple coordinate transformation to the deterministic reaction kinetics. The linear transformation

$$u \mapsto u - u_s = u',$$
$$v \mapsto v - v_s = v',$$

moves the equilibrium away from the origin to (u_s, v_s). The surrounding limit cycle is then centered on this point rather than the origin. Note, that the deterministic local dynamics remains qualitatively unchanged by this coordinate transformation. However, the symmetry between the vectorfield (f_u, f_v) and the coupling functions (g_u, g_v) is broken for $(u_s, v_s) \neq (0,0)$. The effect of this broken symmetry is visible in the phase space diagram of the noisy system as shown in fig. 4.7c for $(u_s, v_s) = (1.5, 1.5)$. Clearly, the effective noise strength is now different at different locations of the limit cycle. As in the predator-prey system, the limit cycle is more distorted now at high values of u and v, where the linear coupling

functions attain higher values.

Fixing $(u_s, v_s) = (1.5, 1.5)$ and repeating the simulations as described above, the effect of noise that has been observed in the predator-prey system can then indeed be reproduced in the simpler $\lambda - \omega$ system. If the effective noise strength is high enough, the travelling waves observed for $b = 1$ are suppressed after a while and replaced by spatially homogeneous oscillations, as shown in fig. 4.9b. These synchronized oscillations persist as long as the noise is present in the system.

Figure 4.10a shows a time lapse of the spatial variance $\sigma(t)^2$ for this case, with $\sigma(t)^2$ being averaged over the previous 1000 time steps. Prior to noise being set to $\eta = 0.1$ at $t = 7500$, the periodic travelling wave yields a constant spatial variance as expected and the immediate decline in spatial variance thereafter is clearly visible.

In contrast to periodic travelling waves for $b = 1$, for $b = 2.5$ irregular oscillations can be observed in the deterministic system. As has been shown, noise may suppress the periodic travelling waves to spatially homogeneous oscillations when the limit cycle is centered at $(1.5, 1.5)$. A natural question to ask is now, what happens to spatiotemporally irregular solutions, if noise applied to them in the same fashion as to the periodic travelling waves.

Interestingly, the chaotic dynamics observed for $b = 2.5$ proves to be more robust to noisy perturbations with noise strength $\eta = 0.1$ as shown in fig 4.9c. While the spatial variance decreases slightly in response to the stochastic forcing, the overall chaotic pattern remains. The temporal evolution of the spatial variance as shown in fig. 4.10a reflects this observation. Note, that if the limit cycle is centered at the origin, the qualitative behavior of the chaotic solution is also not affected by the noise.

4.5 Interlude: Noise and transient system behaviour

The previous sections deal with noise-induced shifts that occur well after the system has settled on a particular long-term behavior. In this section we want to briefly discuss an effect of noise which is exclusively associated with the transient phase of solutions to the reaction–diffusion model (4.15–4.16) of predator–prey interaction. Here by transient phase we mean the period of time, during which the solution, starting from a particular initial condition, approaches an attractor of the system before eventually settling on that attractor. Depending on the initial condition, this transient phase can have considerable length and thus noise may have profound impacts.

As above we employ Neumann no-flux boundary conditions and the domain length will be fixed to $L = 1200$ together with a diffusion coefficient of $D = 1$. We also use the param-

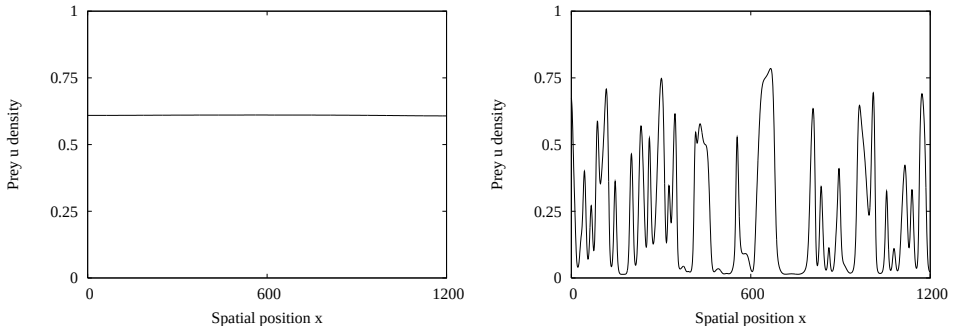

Figure 4.11: Starting from initial conditions (4.23), with stochasting forcing the two qualitatively different long term behaviors are approached with probability ϕ (homogeneous solution, left) and $1-\phi$ (irregular solution, right), respectively.

eter set (4.17) which yields oscillatory behavior.

It has been shown by Petrovskii and Malchow (2001) that depending on the initial spatial distribution of u and v the deterministic system (4.15–4.16) may approach two qualitatively different long term solution types. Either, spatially homogeneous oscillations emerge after a sometimes very long transient phase, or spatiotemporal irregular oscillations spread over the whole spatial domain which then persist indefinitely. This latter scenario has been termed "wave of chaos" by Petrovskii and Malchow (2001), due to the essentially chaotic dynamics at fixed spatial locations. The two possible scenarios are shown in Figure 4.11, the spatially homogeneous oscillations on the left and the persistent spatiotemporal irregular oscillations on the right. This phenomenon has also been investigated by Sherratt (1995) in the more generic setting of oscillatory reaction–diffusion systems of λ–ω-type. These irregular oscillations persist indefinitely and are not suppressed by low to moderate spatiotemporal fluctuations (Sieber et al., 2010).

In summary, in a deterministic setting with $\eta = 0$ the position of the initial condition with respect to the basins of attraction of the two possible attracting solution types completely determines the long term behavior of the corresponding particular solution to Eqns. (4.15–4.16). For noise intensities $\eta > 0$ however, the long term behavior of a solution can not be predicted with certainty, especially if the initial condition is close to the boundary of the two basins of attraction. In the following we will denote the basin of attraction of the spatially homogeneous oscillations as the *homogeneous basin* and the one of spatiotemporal irregular oscillations as the *irregular basin*.

Assume now that an initial condition is given that leads to spatiotemporal irregular behavior in the deterministic case $\eta = 0$, corresponding to an initial condition in the irregular

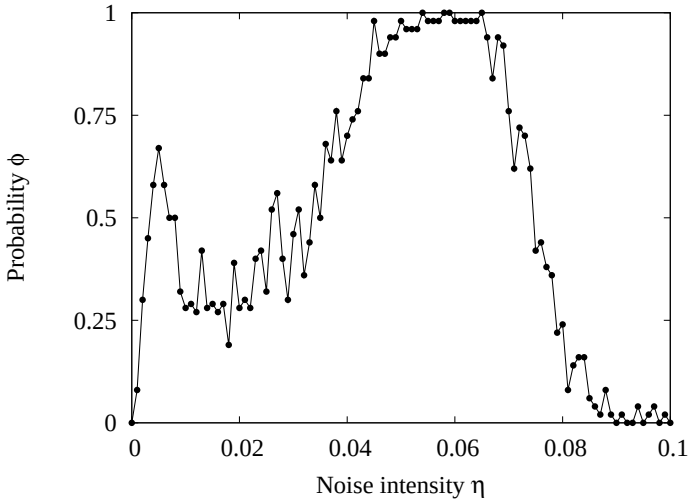

Figure 4.12: Probability ϕ vs. noise intensity.

basin. Let now ϕ denote the probability that spatially homogeneous oscillations arise instead of spatiotemporal irregular oscillations. This probability will in general depend on the strength of the stochastic forcing, that is $\phi = \phi(\eta)$, and we can expect $\phi(\eta) > 0$ for some $\eta > 0$ if the initial condition is close to the boundary with the homogeneous basin.

As an example, we consider the initial condition

$$\begin{aligned} u(0,x) &= u^*, \\ v(0,x) &= v^* + \alpha\,(x - x_0)\,, \end{aligned} \tag{4.23}$$

with $x_0 = L/2$ and $\alpha = 10^{-4}$, which is similar to the initial condition used in Petrovskii and Malchow (2001). This corresponds to a very slight linear spatial gradient in the initial predator distribution, while the prey is simply set to its equilibrium value across the entire domain. Note that the system's equilibrium value is attained at x_0. In a deterministic setting with $\eta = 0$, the solution starting at this particular initial condition eventually evolves into irregular spatiotemporal oscillations, as shown on the right in Figure 4.11. Thus, we have an initial condition for which $\phi(0) = 0$ holds.

Now we want to study how $\phi(\eta)$ behaves for rising noise intensity η. Therefore, we choose 100 noise intensities equally distributed over the interval $[0, 0.1]$ and then numerically integrate the system using the Euler-Maruyama method (Kloeden and Platen, 1999) for the stochastic reaction term combined with a Crank-Nicholson scheme for the diffusion term (LeVeque, 2002). For every noise intensity N independent simulations up to $t = t_{max}$

are performed and the numerical solutions are then classified according to the particular long-term behavior. Thus we obtain n_η spatially homogeneous oscillations and m_η spatiotemporally irregular oscillations with $n_\eta + m_\eta = N$ for each noise intensity and thus we can estimate $\phi(\eta)$ by

$$\phi(\eta) \approx \frac{n_\eta}{N}\,.$$

We choose $t_{max} = 25.000$, which is large enough even for the longest transient phases, and $N = 100$, which already gives a good approximation of the behavior of $\phi(\eta)$.

The results of the stochastic simulations are shown in Figure 4.9. Clearly, the probability ϕ that spatially homogeneous oscillations arise shows two distinct maxima, one at low noise intensity and one at intermediate noise intensity. The two maxima are seperated by a minimum where the spatiotemporal irregular solution is approached more often.

Intuitively one might expect a unimodal behavior of $\phi(\eta)$ with respect to noise intensity η, with ϕ strictly increasing at low noise intensity reflecting the increasing probability of an early shifting of the initial condition from the irregular basin to the homogeneous basin. After this initial increase the growing influence of the noisy forcing and its tendency to amplify spatial inhomogeneities can be expected to lead to a subsequent decline in ϕ, thus leading to a single maximum of ϕ at intermediate noise intensities.

The actual situation however appears to be more complicated, since the stochastic simulations indicate that there are two intervals of noise intensities which are optimal in terms of chaos prevention. It is not yet clear why ϕ shows the mentioned bimodal behavior, but repeated simulations with initial distributions other than those considered here and also incorporating stochastic terms other than multiplicative noise show at least a bimodal shape (Petrovskii et al., 2010). So this effect seems to be a quite robust feature of the stochastic model that has been considered here.

It is an interesting question for future work, how the observed probability distribution changes qualitatively with respect to changes in properties of the underlying stochastic reaction–diffusion system. Especially interesting is the question, how the form of the initial conditions relates to the probability to observe a particular long-term behavior in the stochastic system.

4.6 Discussion

Any model inherently is an idealization of the described natural processes. A plausible approach to account for processes, that have been blinded out by this idealization, is to treat

them as some sort of noise. This point of view has been adopted in this paper and it implies, that the stochastic reaction-diffusion models presented in the previous sections provide a more complete description of the problem at hand. In many cases, a stochastic forcing may simply blur the known deterministic dynamics, giving it a more realistic appearence without actually leading to qualitatively different behavior. However, of particular interest are results obtained from stochastic models, that indicate a significant noise-induced shift in system dynamics, that could not be anticipated from the deterministic skeleton.

This is the case for the results described above for a predator-prey model and a generic oscillatory reaction-diffusion system of $\lambda - \omega$ type. For the $\lambda - \omega$ system with the local limit cycle centered on $(1.5, 1.5)$, an overview of the growing spatial synchronization in response to increasing noise strength is shown in fig. 4.10b, displaying the mean spatial variance σ^2 for different values of the parameter b, averaged over a long time period after the noise has been switched on. Small noise below some critical noise strength has no significant effect, while suppression of travelling waves can be observed, if noise is above some critical value. With increasing b, higher noise levels are needed to suppress the travelling waves, which corresponds to the appearance of spatiotemporally irregular dynamics for these parameter values. For certain values of b, a small spatial variance is always present even for high noise intensities. Heuristically this robustness of the irregular oscillations seems plausbile, since they exhibit a higher spatiotemporal complexity than travelling waves, and as such are not so easily suppressed to spatially homogeneous oscillations. In the light of these results it is tempting to suggest, that in natural populations spatiotemporal irregular oscillations should be observed more frequently than periodic travelling waves.

In conclusion this indicates, that periodic travelling waves as solutions to oscillatory reaction-diffusion systems are very sensitive to stochastic forcing. In particular it has been shown, that a rapidly fluctuating, highly non-periodic forcing of low intensity is able to suppress such travelling waves. The resulting spatially homogeneous oscillations resemble the limit cycle dynamics of the local reaction kinetics. This corresponds to a significant noise-induced shift in system dynamics, which is insofar a rather surprising result, as there is no corresponding shift in the stochastic local dynamics. Sample paths of the stochastic reaction kinetics still closely follow the deterministic limit cycle, as reflected by the stationary probability distributions shown in fig. 4.7.

The apparent discrepancy between these results and the alleged travelling wave patterns in natural populations suggests at least two questions, that seem worth to be addressed in future research. The first question deals with the assumed properties of the noise process itself and the coupling functions used in the models above. This question is actually two-

fold, since the noise process may have a temporal as well as a spatial structure. Concerning the temporal properties, it has already been noted, that despite its useful mathematical properties, temporal white noise does not correspond to any real world process. This raises the question, whether periodic travelling waves persist under the forcing of temporally autocorrelated or colored noise. The second part of the question concerns the spatial properties of the environmental fluctuations. The assumption of spatially invariant fluctuations certainly becomes invalid when considering large distribution areas. Even for a habitat covering a mostly homogeneous landscape, weather conditions can be expected to be significantly different at different spatial locations, if the habitat is larger than a few dozen kilometers. This leads one to impose some spatial structure on the noise process via the use of spatially non-uniform perturbations. Similar to temporal white noise, one could use noise that is white in space, which is somewhat of the other extreme compared to spatially constant noise. Not surprisingly, this does not lead to spatially homogeneous oscillations, but the travelling wave pattern is nevertheless destroyed already for small noise intensities.

The second major question concerns the fact that as indicated in Section 4.2 periodic travelling waves have been observed in model types other than reaction-diffusion systems. It is now natural to ask, whether the travelling waves can be reproduced in appropriate stochastic variants of these models. If this is the case, this would give a hint towards which types of models may be more suitable than others to describe the travelling wave phenomenon observed in some natural populations.

Bibliography

Abrams, P. A. (2009). When does greater mortality increase population size? The long history and diverse mechanisms underlying the hydra effect. *Ecology Letters*, 12:462–474.

Abrams, P. A., Brassil, C. E., and Holt, R. D. (2003). Dynamics and responses to mortality rates of competing predators undergoing predator–prey cycles. *Theoretical Population Biology*, 64:163–176.

Abrams, P. A. and Ginzburg, L. R. (2000). The nature of predation: prey dependent, ratio dependent or neither? *Trends in Ecology & Evolution*, 15(8):337–341.

Abrams, P. A. and Matsuda, H. (2005). The effect of adaptive change in the prey on the dynamics of an exploited predator population. *Canadian Journal of Fisheries and Aquatic Sciences*, 62:758–766.

Allee, W. C. (1931). *Animal Aggregations: A Study in General Sociology*. University of Chicago Press, Chicago.

Anderson, R. M. and May, R. M. (1986). The invasion, persistence and spread of infectious diseases within animal and plant communities. *Phil. Trans. R. Soc. London B*, 314:533–570.

Aparicio, J. P. and Solari, H. G. (2001). Sustained oscillations in stochastic systems. *Mathematical Biosciences*, 169:15–25.

Arim, M. and Marquet, P. A. (2004). Intraguild predation: a widespread interaction related to species biology. *Ecology Letters*, 7:557–564.

Armstrong, R. A. and McGehee, R. (1980). Competitive exclusion. *The American Naturalist*, 115(2):151–170.

Auchmuty, J. F. G. and Nicolis, G. (1976). Bifurcation analysis of nonlinear reaction-diffusion equations. III. Chemical oscillations. *Bulletin of Mathematical Biology*, 38:325–350.

Bauer, F. (1979). Boundedness of solutions of predator-prey systems. *Theoretical Population Biology*, 15(2):268–273.

Bazykin, A. D. (1998). *Nonlinear dynamics of interacting populations*. World Scientific, Singapore.

Beddington, J. R. (1975). Mutual interference between parasites or predators and its effect on searching efficiency. *Journal of Animal Ecology*, 44:331–340.

Belousov, B. (1958). *Sbornik referatov po radiatsionnoi meditsine za 1958 g*. Medgiz, Moskau.

Bénard, H. (1900). Les tourbillons cellulaires dans une nappe liquide. *Rev. Gen. Sci. Pures Appl.*, 11:1261+1309.

Berryman, A. A., editor (2002). *Population cycles: the case for trophic interactions*. Oxford University Press, Oxford.

Bjørnstad, O. N., Peltonen, M., Liebhold, A. M., and Baltensweiler, W. (2002). Waves of larch budmoth outbreaks in the european alps. *Science*, 298:1020–1023.

Borer, E. T., Briggs, C. J., and Holt, R. D. (2007). Predators, parasitoids, and pathogens: A cross-cutting examination of intraguild predation theory. *Ecology*, 88:2681–2688.

Britton, N. F. (1990). Spatial structures and periodic travelling waves in an integro-differential reaction-diffusion population model. *SIAM J. Appl. Math.*, 50(6):1663–1688.

Conway, E. D. and Smoller, J. A. (1986). Global analysis of a system of predator-prey equations. *SIAM J. Appl. Math.*, 46(4):630–642.

Courchamp, F., Berec, L., and Gascoigne, J. (2008). *Allee Effects in Ecology and Conservation*. Oxford University Press, New York.

Cushing, J. M., Costantino, R., Dennis, B., Desharnais, R. A., and Henson, S. (2003). *Chaos in ecology. Experimental nonlinear dynamics*. Theoretical Ecology Series. Academic Press, Amsterdam.

de Feo, O. and Rinaldi, S. (1997). Yield and dynamics of tritrophic food chains. *American Naturalist*, 150:328–345.

de Meeûs, T. and Renaud, F. (2002). Parasites within the new phylogeny of eukaryotes. *Trends in Parasitology*, 18:247–251.

DeAngelis, D. L., Goldstein, R. A., and O'Neill, R. V. (1975). A model for trophic interaction. *Ecology*, 56:881–892.

Dercole, F., Ferrière, R., Gragnani, A., and Rinaldi, S. (2006). Coevolution of slow-fast populations: evolutionary sliding, evolutionary pseudo-equilibria and complex Red Queen dynamics. *Proceedings of the Royal Society B*, 273:983–990.

D'Odorico, P., Laio, F., and Ridolfi, L. (2005). Noise-induced stability in dryland plant

ecosystems. *Proceedings of the National Academy of Sciences of the United States of America*, 102(31):10819–10822.

Dwyer, G., Dushoff, J., and Yee, S. H. (2004). The combined effects of pathogens and predators on insect outbreaks. *Nature*, 430:341–345.

Ebeling, W. and Schimansky-Geier, L. (1979). Stochastic dynamics of a bistable reaction system. *Physica A*, 98:587–600.

Eckmann, J. P. and Ruelle, D. (1985). Ergodic theory of chaos and strange attractors. *Reviews of Modern Physics*, 57:617–656.

Elton, C. S. (1958). *Ecology of Invasions by Animals and Plants*. Chapman & Hall, London.

Fisher, R. A. (1937). The wave of advance of advantageous genes. *Annals of Eugenics*, 7:355–369.

Fulda, J. S. (1981). The Logistic Equation and Population Decline. *Journal of Theoretical Biology*, 91:255–259.

Gardner, M. R. and Ashby, W. R. (1970). Connectance of large dynamic (cybernetic) systems: critical values for stability. *Nature*, 228:784.

Gaunersdorfer, A. (1992). Time averages for heteroclinic attractors. *SIAM Journal on Applied Mathematics*, 52(5):1476–1489.

Gause, G. F. (1934). *The Struggle for Existence*. Williams and Wilkins, Baltimore.

Gerisch, G. (1968). Cell aggregation and differentiation in *Dictyostelium*. In Moscona, A. A. and Monroy, A., editors, *Current Topics in Developmental Biology*, volume 3, pages 157–197. Academic Press, New York.

Gierer, A. and Meinhardt, H. (1972). A theory of biological pattern formation. *Kybernetik*, 12:30–39.

Gragnani, A., de Feo, O., and Rinaldi, S. (1998). Food Chains in the Chemostat: Relationships Between Mean Yield and Complex Dynamics. *Bulletin of Mathematical Biology*, 60:703–719.

Grebogi, C., Ott, E., and Yorke, J. A. (1983). Crises, sudden changes in chaotic attractors, and transient chaos. *Physica D*, 7:181–200.

Guttal, V. and Jayaprakashh, C. (2007). Impact of noise on bistable ecological systems. *Ecological Modelling*, 201:420–428.

Hardin, G. (1960). The competitive exclusion principle. *Science*, 131:1292–1298.

Hassell, M., Comins, H., and May, R. M. (1991). Spatial structure and chaos in insect population dynamics. *Nature*, 353:255–258.

Hastings, A. and Powell, T. (1991). Chaos in a three-species food chain. *Ecology*, 72:896–903.

Hatcher, M. J., Dick, J. T. A., and Dunn, A. M. (2006). How parasites affect interactions between competitors and predators. *Ecology Letters*, 9:1253–1271.

Hilker, F. M. and Malchow, H. (2006). Strange periodic attractors in a prey-predator system with infected prey. *Mathematical Population Studies*, 13(3):119–134.

Hilker, F. M. and Westerhoff, F. H. (2006). Paradox of simple limiter control. *Physical Review E*, 73(5):052901.

Hill, N. A. and Pedley, T. J. (2005). Bioconvection. *Fluid Dynamics Research*, 37:1–20.

Hochberg, M. E., Hassell, M. P., and May, R. M. (1990). The dynamics of host-parasitoid-pathogen interactions. *American Naturalist*, 135:74–94.

Holling, C. S. (1959). The components of predation as revealed by a study of small mammal predation of the European pine sawfly. *The Canadian Entomologist*, 91(5):293–320.

Holt, R. D. (1997). Community modules. In Gange, A. C. and Brown, V. K., editors, *Multitrophic interactions in terrestrial ecosystems. 36th Symposium of the British Ecological Society*, pages 333–349. Blackwell Science, London.

Holt, R. D. and Dobson, A. P. (2006). Extending the principals of community ecology to address the epidemiology of host pathogen systems. In Collinge, S. K. and Ray, C., editors, *Disease ecology: community structure and pathogen dynamics*, pages 6–27. Oxford University Press, Oxford.

Holt, R. D. and Gomulkiewicz, R. (1997). How does immigration influence local adaptation? A reexamination of a familiar paradigm. *The American Naturalist*, 149:563–572.

Holt, R. D. and Hochberg, M. E. (1998). The coexistence of competing parasites. Part II—Hyperparasitism and food chain dynamics. *Journal of Theoretical Biology*, 193:485–495.

Holt, R. D. and Polis, G. A. (1997). A theoretical framework for intraguild predation. *American Naturalist*, 149:745–764.

Holt, R. D. and Roy, M. (2007). Predation can increase the prevalence of infectious disease. *American Naturalist*, 169:690–699.

Horsthemke, W. and Lefever, R. (1984). *Noise-induced transitions. Theory and applications in physics, chemistry, and biology*, volume 15 of *Springer Series in Synergetics*. Springer, Berlin.

Hutchinson, G. E. (1978). *An introduction to population ecology*. Yale University Press, New Haven.

Kay, A. L. and Sherratt, J. A. (2000). Spatial noise stabilizes periodic wave patterns in oscillatory systems on finite domains. *SIAM J. Appl. Math.*, 61:1013–1041.

Kendall, B. E., Briggs, C. J., Murdoch, W., Turchin, P., Ellner, S. P., McCauley, E., Nisbet, R. M., and Wood, S. N. (1999). Why Do Populations Cycle? A Synthesis Of Statistical And Mechanistic Modeling Approaches. *Ecology*, 80:1789–1805.

Kloeden, P. E. and Platen, E. (1999). *Numerical solution of stochastic differential equations*, volume 23 of *Applications of Mathematics*. Springer, Berlin.

Koch, A. L. (1974). Competitive coexistence of two predators utilizing the same prey under constant environmental conditions. *Journal of Theoretical Biology*, 44:387–395.

Kolmogorov, A., Petrovskii, I., and Piskunov, N. (1937). Étude de l'equation de la diffusion avec croissance de la quantité de matière et son application à un problème biologique. *Bulletin de l'Université de Moscou, Série Internationale, Section A*, 1:1–25.

Kopell, N. and Howard, L. N. (1973). Plane wave solutions to reaction-diffusion equations. *Studies in Appl. Math.*, 52:291–328.

Kuramoto, Y. (1984). *Chemical oscillations, waves, and turbulence*, volume 19 of *Springer Series in Synergetics*. Springer, Berlin.

Kuris, A. M., Hechinger, R. F., Shaw, J. C., Whitney, K. L., Aguirre-Macedo, L., Boch, C. A., Dobson, A. P., Dunham, E. J., Fredensborg, B. L., Huspeni, T. C., Lorda, J., Mababa, L., Mancini, F. T., Mora, A. B., Pickering, M., Talhouk, N. L., Torchin, M. E., and Lafferty, K. D. (2008). Ecosystem energetic implications of parasite and free-living biomass in three estuaries. *Nature*, 454:515–518.

Kuske, R., Gordillo, L. F., and Greenwood, P. (2007). Sustained oscillations via coherence resonance in SIR. *Journal of Theoretical Biology*, 245:459–469.

Kuznetsov, Y. A. (1995). *Elements of Applied Bifurcation Theory*, volume 112 of *Applied Mathematical Sciences*. Springer-Verlag, New York.

Lafferty, K. D., Allesina, S., Arim, M., Briggs, C. J., Leo, G. D., Dobson, A. P., Dunne, J. A., Johnson, P. T. J., Kuris, A. M., Marcogliese, D. J., Martinez, N. D., Memmott, J., Marquet, P. A., McLaughlin, J. P., Mordecai, E. A., Pascual, M., Poulin, R., and Thieltges, D. W. (2008). Parasites in food webs: the ultimate missing links. *Ecology Letters*, 11:533–546.

Lafferty, K. D., Dobson, A. P., and M.Kuris, A. (2006). Parasites dominate food web links. *Proceedings of the National Academy of Sciences*, 103:11211–11216.

Lambin, X., Elston, D. A., Petty, S. J., and MacKinnon, J. L. (1998). Spatial asynchrony

and periodic travelling waves in cyclic populations of field voles. *Proc. Biol. Sci. B*, 265:14911496.

Lefèvre, T., Lebarbenchon, C., Gauthier-Clerc, M., Missé, D., Poulin, R., and Thomas, F. (2009). The ecological significance of manipulative parasites. *Trends in Ecology & Evolution*, 24:41–48.

LeVeque, R. J. (2002). *Finite Volume Methods for Hyperbolic Problems*. Cambridge University Press, New York.

Levin, S. A. (1979). Non-uniform stable solutions to reaction-diffusion equations: Applications to ecological pattern formation. In Haken, H., editor, *Pattern formation and pattern recognition*, volume 5 of *Springer Series in Synergetics*, pages 210–222. Springer, Berlin.

Lindner, B., Garcia-Ojalvo, J., Neiman, A., and Schimansky-Geier, L. (2004). Effects of noise in excitable systems. *Physics Reports*, 392:321–424.

Liou, L. P. and Cheng, K. S. (1988). On the uniqueness of a limit cycle for a predator-prey system. *SIAM Journal on Mathematical Analysis*, 19:867–878.

Liu, Y. (2005). Geometric criteria for the nonexistence of cycles in Gause-type predator-prey systems. *Proceedings of the American Mathematical Society*, 133:3619–3626.

Liz, E. (2010). How to control chaotic behaviour and population size with proportional feedback. *Physics Letters A*, 374:725–728.

Lotka, A. J. (1925). *Elements of physical biology*. Williams and Wilkins, Baltimore.

Luther, R. (1906). Räumliche Ausbreitung chemischer Reaktionen. *Zeitschrift für Elektrochemie*, 12:596–600.

MacArthur, R. H. (1955). Fluctuations of animal populations and a measure of community stability. *Ecology*, 36:533–536.

Maginu, K. (1981). Stability of periodic traveling wave solutions with large spatial periods in reaction-diffusion systems. *J. Diff. Eqs*, 39:73–99.

Malchow, H., Hilker, F. M., Sarkar, R. R., and Brauer, K. (2005). Spatiotemporal patterns in an excitable plankton system with lysogenic viral infection. *Mathematical and Computer Modelling*, 42(9-10):1035–1048.

Malchow, H., Petrovskii, S. V., and Venturino, E. (2008). *Spatiotemporal patterns in ecology and epidemiology: Theory, models, simulations*. CRC Mathematical and Computational Biology Series. CRC Press, Boca Raton.

Malchow, H. and Schimansky-Geier, L. (1985). *Noise and diffusion in bistable nonequilibrium systems*, volume 5 of *Teubner-Texte zur Physik*. Teubner-Verlag, Leipzig.

Malthus, T. R. (1798). *An essay on the principle of population*. J. Johnson in St. Paul's Churchyard, London.

Matsuda, H. and Abrams, P. A. (2004). Effects of adaptive change and predator-prey cycles on sustainable yield. *Can. J. Fish. Aquat. Sci.*, 61:175–184.

May, R. M. (1973). *Stability and complexity in model ecosystems*, volume 6 of *Monographs in Population Biology*. Princeton University Press, Princeton.

May, R. M. (1976). *Theoretical ecology - Principles and applications*. Blackwell Sci. Publ., Oxford.

May, R. M. and Leonard, W. (1975). Nonlinear aspects of competition between three species. *SIAM Journal on Applied Mathematics*, 29:243–252.

McCann, K. (2000). The diversity–stability debate. *Nature*, 405:228–233.

McCann, K. and Yodzis, P. (1994). Nonlinear dynamics and population disappearances. *The American Naturalist*, 144:873–879.

McGehee, R. and Armstrong, R. A. (1977). Some mathematical problems concerning the ecological principle of competitive exclusion. *J. Diff. Equations*, 23:30–52.

Pascual, M. (1993). Diffusion-induced chaos in a spatial predator-prey system. *Proceedings of the Royal Society of London B*, 251:1–7.

Pearl, R. (1926). *The biology of population growth*. Williams and Norgate, London.

Pearl, R. and Reed, L. J. (1920). On the rate of growth of the population of the United States since 1870 and its mathematical representation. *Proceedings of the National Academy of Sciences*, 6:275–288.

Petrovskii, S. V. and Malchow, H. (1999). A minimal model of pattern formation in a prey-predator system. *Mathematical and Computer Modelling*, 29:49–63.

Petrovskii, S. V., Li, B.-L., and Malchow, H. (2003). Quantification of the spatial aspect of chaotic dynamics in biological and chemical systems. *Bulletin of Mathematical Biology*, 65(3):425–446.

Petrovskii, S. V. and Malchow, H. (2000). Critical phenomena in plankton communities: KISS model revisited. *Nonlinear Analysis: Real World Applications*, 1:37–51.

Petrovskii, S. V. and Malchow, H. (2001). Wave of chaos: new mechanism of pattern formation in spatio-temporal population dynamics. *Theoretical Population Biology*, 59(2):157–174.

Petrovskii, S. V., Morozov, A., Malchow, H., and Sieber, M. (2010). There and back again: Noise can prevent onset of chaos in spatiotemporal population dynamics. *European Phys-*

ical Journal B, 78:253–264.

Petrovskii, S. V., Vinogradov, M., and Morozov, A. (1998). Spatial-temporal dynamics of a localized populational burst in a distributed prey-predator system. *Oceanology*, 38:881–890.

Polis, G. A., Myers, C. A., and Holt, R. D. (1989). The ecology and evolution of intraguild predation: Potential competitors that eat each other. *Annual Review of Ecology and Systematics*, 20:297–330.

Price, P. W. (1980). *Evolutionary Biology of Parasites*. Princeton University Press, Princeton.

Raffel, T. R., Martin, L. B., and Rohr, J. R. (2008). Parasites as predators: unifying natural enemy ecology. *Trends in Ecology & Evolution*, 23:610–618.

Ranta, E. and Kaitala, V. (1997). Travelling waves in vole population dynamics. *Nature*, 390:456.

Ricker, W. E. (1954). Stock and recruitment. *J. Fish. Res. Board Can.*, 11:559–623.

Rosenzweig, M. L. and MacArthur, R. H. (1963). Graphical representation and stability conditions of predator-prey interactions. *The American Naturalist*, 97:209–223.

Rypstra, A. L. and Samu, F. (2005). Size dependent intraguild predation and cannibalism in coexisting wolf spiders (Araneae, Lycosidae). *The Journal of Arachnology*, 33:390–397.

Scheffer, M. and Carpenter, S. R. (2003). Catastrophic regime shifts in ecosystems: linking theory to observation. *Trends in Ecology & Evolution*, 18(12):648–656.

Schreiber, S. J. (2003). Allee effects, extinctions, and chaotic transients in simple population models. *Theoretical Population Biology*, 64:201–209.

Schreiber, S. J. and Rudolf, V. H. W. (2008). Crossing habitat boundaries: coupling dynamics of ecosystems through complex life cycles. *Ecology Letters*, 11:576–587.

Scott, S. K. (1994). *Oscillations, waves, and chaos in chemical kinetics*. Oxford University Press, Oxford.

Segel, L. A. and Jackson, J. L. (1972). Dissipative structure: an explanation and an ecological example. *Journal of Theoretical Biology*, 37:545–559.

Seno, H. (2008). A paradox in discrete single–species population dynamics with harvesting/thinning. *Math. Biosci.*, 214:63–69.

Serizawa, H., Amemiya, T., and Itoh, K. (2009). Noise-triggered regime shifts in a simple aquatic model. *Ecological Complexity*, 6:375–382.

Sherratt, J. A. (1994). On the evolution of periodic plane waves in reaction-diffusion equa-

tions of lambda-omega type. *SIAM J. Appl. Math.*, 54:1374–1385.

Sherratt, J. A. (1995). Unstable wavetrains and chaotic wakes in reaction-diffusion systems of $\lambda - \omega$ type. *Physica D*, 82:165–179.

Sherratt, J. A. (1996). Periodic travelling waves in a family of deterministic cellular automata. *Physica D*, 95:319–335.

Sherratt, J. A. (2001). Periodic travelling waves in cyclic predator-prey systems. *Ecology Letters*, 4(1):30–37.

Sherratt, J. A. (2003). Periodic travelling wave selection by dirichlet boundary conditions in oscillatory reaction-diffusion systems. *SIAM J. Appl. Math.*, 63:1520–1538.

Sherratt, J. A., Lambin, X., Thomas, C. J., and Sherratt, T. N. (2002). Generation of periodic waves by landscape features in cyclic predator-prey systems. *Proc. R. Soc. Lond. B*, 269:327–334.

Sherratt, J. A. and Smith, M. J. (2008). Periodic travelling waves in cyclic populations: field studies and reaction-diffusion models. *J. R. Soc. Interface*, 5:483–505.

Shigesada, N., Kawasaki, K., and Teramoto, E. (1986). Traveling periodic waves in heterogeneous environments. *Theoretical Population Biology*, 30:143–160.

Sieber, M. and Hilker, F. M. (2011a). The hydra effect in predator-prey models. *Journal of Mathematical Biology*. doi: 10.1007/s00285-011-0416-6.

Sieber, M. and Hilker, F. M. (2011b). Prey, predators, parasites: intraguild predation or simpler community modules in disguise? *Journal of Animal Ecology*, 80:414–421.

Sieber, M. and Malchow, H. (2010). Oscillations vs. chaotic waves: Attractor selection in bistable stochastic reaction-diffusion systems. *European Physical Journal Special Topics*, 187:95–99.

Sieber, M. and Malchow, H. (2011). Partial differential equations. In Jopp, F., Reuter, H., and Breckling, B., editors, *Modelling complex ecological dynamics*, pages 93–103. Springer-Verlag, Berlin, Heidelberg.

Sieber, M., Malchow, H., and Petrovskii, S. V. (2010). Noise-induced suppression of periodic travelling waves in oscillatory reaction-diffusion systems. *Proceedings of the Royal Society A*, 466:1903–1917.

Sieber, M., Malchow, H., and Schimansky-Geier, L. (2007). Constructive effects of environmental noise in an excitable prey–predator plankton system with infected prey. *Ecological Complexity*, 4(4):223–233.

Sinha, S. and Parthasarathy, S. (1996). Unusual dynamics of extinction in a simple ecolog-

ical model. *Proceedings of the National Academy of Sciences*, 93:1504–1508.

Slobodkin, L. B. (2001). The good, the bad and the reified. *Evolutionary Ecology Research*, 3:1–13.

Smith, T. M. and Smith, R. L. (2006). *Elements of Ecology*. Pearson Education, San Francisco.

Steele, J. H. (1985). A comparison of terrestrial and marine ecological systems. *Nature*, 313:355–358.

Suttle, C. A. (2005). Viruses in the sea. *Nature*, 437:356–361.

Tanabe, K. and Namba, T. (2005). Omnivory creates chaos in simple food webs models. *Ecology*, 86(12):3411–3414.

Tenow, O., Nilssen, A. C., Bylund, H., and Hogstad, O. (2007). Waves and synchrony in *Epirrita autumnata/Operophtera brumata* outbreaks. I. Lagged synchrony: regionally, locally and among species. *J. Anim. Ecol.*, 76:258–268.

Terry, A. J. and Gourley, S. A. (2010). Perverse Consequences of Infrequently Culling a Pest. *Bulletin of Mathematical Biology*, 72:1666–1695.

Turchin, P. (2003). *Complex Population Dynamics: A Theoretical/Empirical Synthesis*. Princeton University Press, Princeton and Oxford.

Turing, A. M. (1952). On the chemical basis of morphogenesis. *Philosophical Transactions of the Royal Society of London B*, 237:37–72.

van Nes, E. H. and Scheffer, M. (2005). Implications of spatial heterogeneity for catastrophic regime shifts in ecosystems. *Ecology*, 86(7):1797–1807.

van Voorn, G. A. K., Hemerik, L., Boer, M. P., and Kooi, B. W. (2007). Heteroclinic orbits indicate overexploitation in predator-prey systems with a strong Allee effect. *Mathematical Biosciences*, 209:451–469.

Vasseur, D. A. and Yodzis, P. (2004). The color of environmental noise. *Ecology*, 85(4):1146–1152.

Verhulst, P. F. (1838). Notice sur la loi que la population suit dans son accroissement. *Correspondance Mathématique et Physique Publiée par A. Quételet*, 10:113–121.

Volterra, V. (1926). Fluctuations in the abundance of a species considered mathematically. *Nature*, 118:558–560.

Volterra, V. (1931). *Leçons sur la théorie mathématique de la lutte pour la vie*. Gauthier - Villars, Paris.

Walsh, J. B. (1986). An introduction to stochastic partial differential equations. In Carmona,

R., Kesten, H., and Walsh, J. B., editors, *École d'été de probabilités de Saint-Flour XIV -1984*, volume 1180 of *Lecture Notes in Mathematics*, pages 265–437. Springer, Berlin.

Wang, J., Shi, J., and Wei, J. (2011). Predator–prey system with strong Allee effect in prey. *Journal of Mathematical Biology*, 62:291–331.

Webb, S. D. and Sherratt, J. A. (2003). Oscillatory reaction-diffusion equations with temporally varying parameters. *Math. Comp. Modelling*, 39:45–60.

White, L. P. (1971). Vegetation stripes on sheet wash surfaces. *Journal of Ecology*, 59:615–622.

Yodzis, P. (1989). *Introduction to Theoretical Ecology*. Harper & Row, New York.

Zicarelli, J. (1975). *Mathematical analysis of a population model with several predators on a single prey*. Ph.d. thesis, University of Minnesota.

Zipkin, E. F., Kraft, C. E., Cooch, E. G., and Sullivan, P. J. (2009). When can efforts to control nuisance and invasive species backfire? *Ecological Applications*, 19:1585–1595.